January 2016

COMPLEX FORMATION BY ALPHA-LACTALBUMIN AND POLYSACCHARIDE COPOLYMERS

Juan Du
Purdue University

Graduate School Form
30 Updated 12/26/2015

PURDUE UNIVERSITY
GRADUATE SCHOOL
Thesis/Dissertation Acceptance

This is to certify that the thesis/dissertation prepared

By Juan Du

Entitled
COMPLEX FORMATION BY ALPHA-LACTALBUMIN AND POLYSACCHARIDE COPOLYMERS

For the degree of Doctor of Philosophy

Is approved by the final examining committee:

Dr. Owen Jones
Chair

Dr. Ganesan Narsimhan

Dr. Bradley L. Reuhs

Dr. Osvaldo Campanella

To the best of my knowledge and as understood by the student in the Thesis/Dissertation Agreement, Publication Delay, and Certification Disclaimer (Graduate School Form 32), this thesis/dissertation adheres to the provisions of Purdue University's "Policy of Integrity in Research" and the use of copyright material.

Approved by Major Professor(s): Dr. Owen Jones

Approved by: Arun K. Bhunia 10/13/2016

Head of the Departmental Graduate Program Date

COMPLEX FORMATION BY ALPHA-LACTALBUMIN AND POLYSACCHARIDE COPOLYMERS

A Dissertation

Submitted to the Faculty

of

Purdue University

by

Juan Du

In Partial Fulfillment of the

Requirements for the Degree

of

Doctor of Philosophy

December 2016

Purdue University

West Lafayette, Indiana

To my family

ACKNOWLEDGMENTS

First and foremost, I would like to give my sincere respect and greatest gratitude to Dr. Owen G. Jones. As a respectable, responsible and resourceful scholar, he has enlightened me not only in my graduate study with his experienced learning and his insightful ideas of my research area, but also in my future career with his responsible attitude towards my lab work. I truly appreciate his impressive patience and kindness with me. It is my great fortune to be his student, and it is my great fortune to have his continuous guidance and support throughout my PhD study at Purdue.

Secondly, I would like to express my heartfelt gratitude to my PhD advisory committee members: Dr. Ganesan Narsimhan, Dr. Bradley L. Reuhs, and Dr. Osvaldo Campanella. Their constructive and valuable comments have greatly helped to my research and study. My gratitude also goes to all the food science department staffs at Purdue, especially Mitzi Barnett as the Graduate Program Coordinator. My deep thanks to her help with operating and assisting throughout my years of PhD study. I am thankful to my labmates: Ryan Murphy, Jay Gilbert, Chris Cheng, and et al., who created a great atmosphere by exchanging their ideas, giving valuable suggestions and comments from all the group members.

Finally, I would like to give my special thanks to my family members, my father Chongde Du, my mother Lianrong Zhu, my brother Peng Du, my grandfather Zhongyou Du, and my grandmother Shuyan Xu for their thoughtfulness and encouragement all along from the very beginning of my school years.Especially, I am so blessed to have many dear ones from Christian Student at Purdue club, and have my love Feng Zhu as a companion of mine during the years at Purdue.

TABLE OF CONTENTS

Page

Page

LIST OF TABLES

LIST OF FIGURES

ABSTRACT

Du, Juan PhD, Purdue University, December 2016. Complex Formation by Alpha-Lactalbumin and Polysaccharide Copolymers. Major Professor: Owen Jones.

Colloidal delivery systems, such as surfactant micelles, emulsions, liposomes, and nanoparticles, are widely used in food and pharmaceuticals to improve the dispersion of poorly-soluble ingredients or modify their bioaccessibility within the body. As a delivery system for medical- and health-relevant bioactive components, surfactant micelles are used for delivery of poorly water-soluble compounds. Many commercial surfactants are block copolymer assemblies of hydrophilic and hydrophobic polymeric blocks, or polymer segments, where the hydrophobic segments form the internal core of the micelle. However, studies show that surfactant micelles have potential toxicity due to the disruption of cell membranes and interference with cell membrane transporters. [1]

Complexes formed among proteins and polysaccharides, as renewable biopolymers, are drawing attention for their potential application in the food, pharmaceutical, and cosmetic industries due to their non-toxicity and higher potential for rapid biodegradation. Complex coacervate core micelles (C3M) are nano-assemblies of interacting polyelectrolytes and copolymers with a physical structure resembling surfactant micelles, which are increasingly disfavored because of their potential irritation of biological tissues.

In our studies, carboxymethyl-dextran-block-poly(ethylene glycol) (CMD-b-PEG) and chitosan-graft-poly(ethylene glycol) (CH-PEG) were successfully prepared from dextran or chitosan (CH) by covalently attaching a poly(ethylene glycol) chain, which was confirmed by nuclear magnetic resonance spectroscopy and chromatography.

[1] taken with permission from [62].

Complex formation between polysaccharides and the globular dairy protein alpha-lactalbumin was investigated following acid or base titration, where complexes with unmodified chitosan (CH) or carboxymethyl-dextran (CMD) were used as controls. The successful assembling of complexes between alpha-lactalbumin and polysaccharides at different mixing ratios was confirmed through turbidity, light scattering, colloidal charge, and electron microscopy. Covalent attachment of the PEG chains to either polysaccharide was found to decrease the turbidity of complexes, while size of the formed complexes was reduced only in specific protein-to-polysaccharide ratios or polysaccharides of certain molecular weights. Diameter of spherical complexes formed with CMD-b-PEG and CH-g-PEG was found to be less than 100 nm, and assemblies of 200-500 nm were formed from apparent bridging interactions between spherical complexes. Heat treatment of the complexes, shown in prior studies with unmodified polysaccharides to lead to the formation of protein-rich spherical aggregates, was also studied to determine the influence of the attached PEG chain on the structure of heat-induced aggregates. Similar to the unheated complexes, the covalently-attached PEG chain had minimal influence on the size of formed spherical aggregates, yet the turbidity of the suspensions was reduced. These results demonstrate that non-interactive components of ionic polysaccharides have a significant impact on the formation of complexes with alpha-lactalbumin, which could translate to novel designs of vehicles for the controlled-delivery of active molecules.

1. LITERATURE REVIEW

1.1 Introduction

Colloidal delivery systems, such as surfactant micelles, emulsions, liposomes, and nanoparticles, are widely used in food and pharmaceuticals to improve the dispersion of poorly-soluble ingredients or modify their bioaccessibility within the body. As a delivery system for medical- and health-relevant bioactive components, surfactant micelles are used for delivery of poorly water-soluble compounds. Many commercial surfactants are block copolymer assemblies of hydrophilic and hydrophobic polymeric blocks, or polymer segments, where the hydrophobic segments form the internal core of the micelle. However, studies show that surfactant micelles have potential toxicity due to the disruption of cell membranes and interference with cell membrane transporters. [1]

Complexes formed among proteins and polysaccharides, as renewable biopolymers, are drawing attention for their potential application in the food, pharmaceutical, and cosmetic industries due to their non-toxicity and higher potential for rapid biodegradation. Complex coacervate core micelles (C3M) are nano-assemblies of interacting polyelectrolytes and copolymers with a physical structure resembling surfactant micelles, which are increasingly disfavored because of their potential irritation of biological tissues.

1.2 Complex Coacervation

The potential applications for complexes formed by proteins and polysaccharides, as renewable biopolymers, are drawing attention in the food, pharmaceutical, and cos-

[1] taken with permission from [62].

metic industries due to their properties such as non-toxicity and being environment friendly (Jones & McClements, 2011). Complex coacervation between proteins and polysaccharides was first discovered by Tiebackx (1911). By definition, coacervation means the separation of one homogeneous liquid solution into two liquid phases in the colloidal system where the portion with more concentrated solution is defined as coacervates (IUPAC, 1997; de Kruif et al., 2004). To distinguish from single polymer coacervation, Bungenberg de Jong and Krupt (1926) came up with the term complex coacervation which was caused by interaction of two oppositely charged colloids. By Bohidar (2008), coacervation is further defined as a phenomenon that a homogenous aqueous solution with charged macromolecules goes through liquid-liquid phase separation due to the associative interactions of charged macromolecules, resulting in one phase more concentrated in polyelectrolyte. The other phase, which appeared as supernatant is still in equilibrium with the coacervates phase rich in polyeleytrolytes, but it is immiscible and therefore incompatible to the other phase (Bungenberg de Jong and Krupt, 1935; Bohidar, 2008). In comparison to precipitation, which also has the phenomenon of phase separation, complex coacervation is a liquid-liquid phase separation, which means that in both phases polyelectrolytes remain soluble. Precipitation is a separation process caused by the insolubility of solutes, and it is a liquid-solid phase separation.

From a thermodynamic aspect of phase separation, it was stated that tThe driving forces for complex coacervates to form are the electrostatic solute-solvent interactions that causes the decreases of Gibbs free energy, which results can be further differentiated by in the increase of configurational entropythe driving force of either attractive (associate) or repulsive (segregative) interactions between biopolymers, and the dense coacervate phase has randomly arranged mixture of polyelectrolytes (de Kruif & Tuinier, 2001 and Jones & McClements, 2010): the segregative interaction is thermodynamic incompatible event, and in this system phasing separation will not happen unless concentrations of biopolymers reach to certain point with decreases of Gibbs free energy. Thermodynamic incompatible systems, which can be formed

by electrostatic interactions, hydrophobic interactions, single biopolymer association, hydrogen bonds and et al.

During the last century, the studies of complex coacervation was much expended. The study of complex coacervates formation by biopolymers have been increased dramatically due to many benefits of natural sourced biopolymers, such as biodegradable, low cost, renewable and non-toxicity compared to the synthesized polymers. As a review study, de Kruif and et al. (2004) investigated a long list of previous studies on complex coacervation of protein and polysaccharide, and summarized a few characteristics of protein and polysaccharides formed complexes (Table 1). These characteristic features include: 1. The mobility of both protein and polysaccharide is observed in the coacervates phase. 2. At the maximal coacervation formation ratio of protein to polysaccharides, the charges carried by complexes are neutral. 3. If one of the polyelectrolytes is too strong, such as sulfated carrageenan, precipitation will happen instead of forming complex coacervates, while the physiochemical condition for forming complexes is narrowed 4. The concentration of salts in both supernatant and coacervates phases are almost the same. While the addition of salt is increasing the dissociating the complexes. 5. The complexes remain modestly charged, even with excess amount of one of the polyelectrolytes. Other reviews also The details of the mechanism of these characteristics will be explained in 1.2.2.

The preparation of forming complex coacervates is typically achieved by mixing two solutions in a certain ratio (volumetric mass, or molar). Then titrate the mixture with base or acid standard solutions while stirring. The changes The turbidity and scattering intensity of the solution is monitored at the same time to determine the critical pH values at which complex formation and phase separation take place. A few important pH regions were well illustrated by Jones & McClements (2010) as is follows:

Suppose we are conducting an acid titration of a protein and polysaccharide solution starting from high pH of the solution of mixture, in the initial stage, when both polyelectrolytes were carrying strong negative charges, that the pH is far above

pI, no complexation happens, once the pH is reduced enough that even though the charges of both biopolymers are negative, but a weak association happened due to the electrostatic interactions between the anionic polysaccharide and some locations of the positively charged protein portion. In the pH region, soluble complexes can be detected by light scattering and the pH that scattering intensity started to rise up is defined as the complexation pH (pHC). Coacervates will not be formed until a further reduction of pH, which leads to stronger electrostatic interactions, that complexes increase in size largely, that the intensity from light scattering largely increased, even an increase of turbidity in solution, with a peaking up of the signals detected by a visual light spectrometer. The formation of coacervates is accompanied with phase separation, and the pH is defined as the critical pH value that coacervation starts to happen. If the electrostatic interaction between two highly oppositely charged biopolymers are too strong, then precipitation will happen rather than coacervation since the the polymers are binding closely, that they became insoluble in the solution. Once the pH was reduced too low, far below the pKa of anionic polysaccharide, that no further interaction between biopolymers will happen, that there might be no complexation. Some other literature also defined the coacervation pH as pHϕ1, while pHϕ2 as the critical value that the solution starts to exhibit a loss in turbidity, and phase due to the suppressed phase separation separation (Weinbreck et al., 2002). These critical pH values are determined in the figures as is follows:

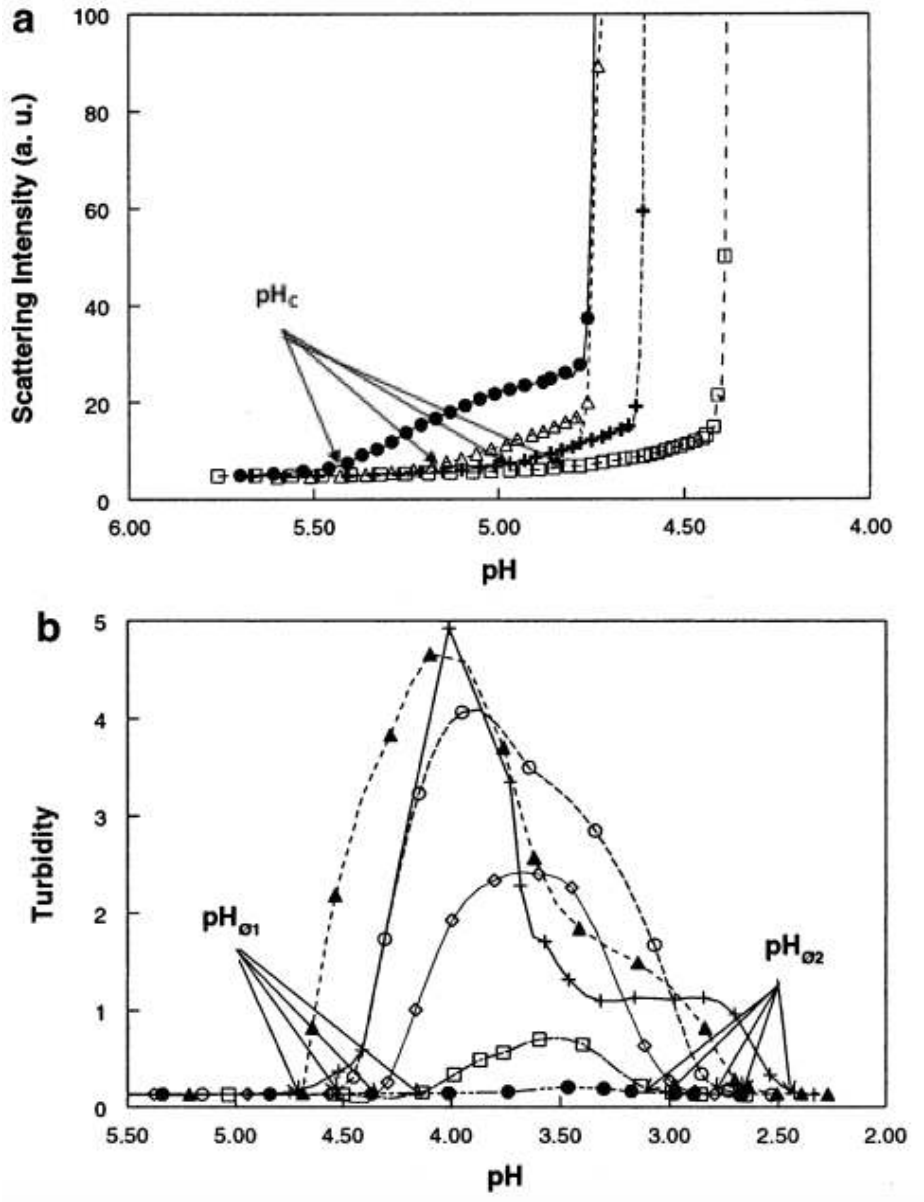

Fig. 1.1. (a) Scattering intensity as a function pH of mixture of whey protein/gum arabic for pHC determination (b) Turbidity as a function of pH for pHϕ1and pHϕ2 determination. (Figures adopted with permisson from Weinbreck et al., 2003) Copyright (2003), American Chemical Society.

Table 1.1.
Overview of the biopolymer complexes according to the nature of the polysaccharide (Tables adopted with permission from de Kruif and et al., (2004)) Copyright (2004) Elsevier

Strong/weak polyelectrolytes	Polysaccharide/protein	References	Coacervation or precipitation
Weak (carboxylated) PE/gelatin	Gum arabic/gelatin	Burgess & Carless, 1984	Coacervation
Weak (carboxylated) PE/globular protein	Gum arabic/albumin	Burgess et al., 1991; 1993	Coacervation
Weak (carboxylated) PE/gelatin	Carbopol/gelatin	Elgindy & Elegakey, 1981	Coacervation
Weak (carboxylated) PE/gelatin	Low methoxy pectin/gelatin	Gilsenan et al., 2003	Coacervation
Weak (carboxylated) PE/gelatin	Xanthan gum/gelatin	Lii et al., 2002	Coacervation
Weak (carboxylated) PE/gelatin	Gum arabic/gelatin	Peters et al., 1992	Coacervation
Weak (carboxylated) PE/gelatin	Sodium carboxymethyl guar gum/gelatin	Thimma & Tammishetti, 2003	Coacervation
Weak (carboxylated) PE/globular protein	Low and high methylated pectin/h-lactoglobulin	Girard et al., 2002-2004	Coacervation
Weak (carboxylated) PE/globular protein	High-methoxyl pectin/-lactoglobulin	Kazmiersi et al., 2003	Precipitation
Weak (carboxylated) PE/globular protein	Xanthan gum/whey protein	Laneuville et al., 2000	Coacervation
Weak (carboxylated) PE/globular protein	Gum arabic/h-lactoglobulin	Sanchez et al., 2001;2002	Coacervation
Weak (carboxylated) PE/globular protein	Gum arabic/h-lactoglobulin	Schmitt et al., 1999; 2000; 2001	Coacervation
Weak (carboxylated) PE/plant protein	Carboxy methyl cellulose/potato proteins	Vikelouda & Kiosseoglou, 2004	Precipitation
Weak (carboxylated) PE/globular protein	Gum arabic/whey proteins	Weinbreck et al., 2003-2004	Coacervation
Cationic polysaccharide/plant protein	Chitosan/faba bean legumin	Plashchina et al., 2001	Precipitation
Two polysaccharides (weak PE/chitosan)	Alginate/chitosan	Yan et al. 2000; 2001	Coacervation
Two polysaccharides (strong PE/chitosan)	Carrageenan/chitosan	Shumilina & Shchipunov, 2002	Precipitation
Strong (sulfated) PE/gelatin	n-carrageenan/gelatin	Antonov and Gonc, 1999	Precipitation
Strong (sulfated) PE/globular protein	L- or n-carrageenan or dextran sulfate/bovine serum albumin	Galazka et al., 1999	Precipitation
Strong (sulfated) PE/globular protein	L-carrageenan/poly(l-lysine)	Girod et al., 2004	Coacervation
Strong (sulfated) PE/globular protein	Dextran sulfate/sodium caseinate or soybean protein	Gurov et al., 1988	Precipitation
Strong (sulfated) PE/gelatin	n-carrageenan/gelatin	Haug et al., 2003	Coacervation
Strong (sulfated) PE/globular protein	Carrageenan/whey protein	Weinbreck et al., 2004	Precipitation
Strong (phosphated) PE/gelatin	Sodium hexametaphosphate/gelatin	Fogle & Hfrger, 1972	Coacervation
Strong (phosphated) PE/globular protein	Exopolysaccharide B40/whey proteins	Weinbreck et al., 2003	Precipitation

1.2.1 Factors Influencing the Formation of Complex Coacervatesn

Since complex coacervates are formed by electrostatic interactions, their formation may be influenced by many factors, such as pH, ionic strength, polymer concentration, or polycation to polyion ratios.

Changes of pH are typically used to promote the association between proteins and polyscahharides, since the pH can alter the charges of polymers and therefore favors the electrostatic interactions between biopolymers (Jones and McClements, 2010).

Since complex coacervate formation is driven by the electrostatic interaction between polymers, ionic strength of the polymer surrounding environment will also influence the surface charge density of the complexes, thereby affecting complex formation. The addition of high concentration of salts has screening effects on the surface charges of polyelectrolytes, since the ions in solution can neutralize the charges carried by polyelectrolytes, as a result, preventing the association (Schmitt et al., 1998). With very ow concentration of salts added into the solution, the influence of salt might increase the tendency for association when compared to nearly ion-free solutions since it reduces longer-range repulsions among charged bodies.

Ratio between different polymers can also influence the complex coacervation. Since complex coacervation is formed by electrostatic interaction, an optimal ratio with neutral charges of the system can create a maximum coacervation with controlled concentration of total polymers. In a system that does not have optimal ratio, the extra polyion will form non-neutral charged complexes, their extra charges will function as repulsive force that prevent the coacervates to form, as well as a reduction in turbidity of the sample. Due to these reasons, the optimal ratio between polyions is an important factor that has been studied by many researchers. For example, Schmitt et al., (1998) reported that at total solid concentration of 1%, the optimal beta-lactoglobulin and acacia gum ratio was determined to be 4:1.

Molecular conformations of biopolymers can also influence the shape, size, and physicochemical properties of complexes. Polysaccharide typically have structures of

random coil or helix. The random coil polysaccharide favors the linear structure due to the glycosidic bond rotation and limited chain flexibility, while helical polysaccharides, such as carrageenan and agar, are structured with inter-polymeric hydrogen bonds that are reversible upon heating (Jones and McClements 2010).

Charge density of polyelectrolytes, as an important physicochemical parameter of biopolymers, is another important factor influencing the complex coacervation. Weak polyelectrolyte charge is mainly determined by the solution pH. By definition, charge density is the number of charges that presented on a certain biopolymer length. An example of the influence of charge density was that during acid titration complex preparation, pHC is above the pI of both biopolymers when both of the polymers were both negatively charged, weak complex start to form, which is due to the increase of positive charge density of the higher pI biopolymer (Schmitt et al., 1998)

1.2.2 Complex Coacervate Core Micelle

[2]Complex coacervate core micelles (C3M), a type of block ionomer complex or interpolyelectrolyte complex, are novel nano-assemblies formed by electrostatic interactions between ionic segments of hydrophilic block copolymers (i.e. block ionomers) and oppositely charged polyelectrolytes (Pergushov, Mller, & Schacher, 2012; Voets, de Keizer, & Cohen Stuart, 2009). In such complexes the ionic segments of both the block copolymer and the polyelectrolyte form a neutralized complex that separates from bulk solution to form a core region, whereas the hydrophilic segments of the block copolymer remain as a solubilized outer shell (Pergushov, Mller, & Schacher, 2012) . The chief difference between C3Ms and surfactant micelles is that hydrophobic interactions do not drive C3M assembly, and, therefore, the C3Ms are not potentially toxic to cellular life, in vivo. The length of the nonionic block on copolymers has been found to have a significant influence on the physical stability of formed C3Ms, with a minimum nonionic block length required to interact with the aqueous sol-

[2]Section 1.2.2 is taken with permission from [62].

vent (Novoa-Carballal, Pergushov, & Mller, 2013; Novoa-Carballal, Pfaff, & Mller, 2013). Length of the nonionic block has also been correlated with the size of resulting C3Ms, as demonstrated for C3Ms formed between polystyrene and dextran/poly(2-(dimethylamino)ethyl methacrylate) with increasing dextran size (Novoa-Carballal, Pfaff, & Mller, 2013).

Although C3M formation has been well established for synthetic polyelectrolytes and corresponding block-copolymers, there is a need to develop delivery systems using biologically-derived polymers, such as proteins and polysaccharides. Food-grade proteins and polysaccharides are biodegradable and have low toxicity concerns. Many proteins and polysaccharides possess dominant positive or negative charges and are capable of interacting to form the core of a C3M structure. Such electrostatic interactions between proteins and oppositely-charged polyelectrolytes are well studied in the literature (Schmitt & Turgeon, 2011). Initial electrostatic interactions between proteins and charged polysaccharides leads to the formation of soluble complexes, which can be recognized by an increase in the scattering of incident light (Hirt & Jones, 2014). Further electrostatic interactions eventually leads to the neutralization of the complexes, where the quantity of positive and negative-charges are approximately equivalent, and the resultant complexes separate from the aqueous phase to form a hydrated complex coacervate that is recognized by a significant increase in solution turbidity (Hirt & Jones, 2014).

C3Ms have been formed among numerous block-copolymers and polyelectrolytes of synthetic origin, but very few studies have investigated the formation of C3Ms among modified polyelectrolytes of biological origin, such as proteins and polysaccharides. An early study demonstrated the formation of C3Ms with diameter 50 nm by the interaction of hen egg white lysozyme with a PEG-block-poly(aspartic acid) copolymer (Harada & Kataoka, 1998). More recently, C3Ms were assembled from synthetic polyelectrolytes and block copolymers containing either dextran or hyaluronic acid, demonstrating the feasibility of including a polysaccharide within the C3M structure (Novoa-Carballal, Pergushov, & Mller, 2013; Novoa-Carballal,

Pfaff, & Mller, 2013). Charged polysaccharide-containing copolymers may also be formed by Maillard reactions, with the resulting charged copolymers possessing affinity for oppositely-charged bioactive molecules (Zhou, Sun, Zhang, Zhang, Li, & Liu, 2012). Maillard conjugates of whey protein and dextran were recently assembled into C3M-like structures with chondroitin sulfate, yet only the heat-treated aggregates were characterized (Dai, Zhu, Abbas, Karangwa, Zhang, Xia, et al., 2015).

1.3 Biopolymer structures

Polysaccharides are polymeric carbohydrates that formed by repeating units joined by glycoside linkage with various degrees of branching. They have common properties such as non-toxic, biocompatible, low cost, and available from renewable resources with diverse applications (Kalia et al., 2013). Since C3M is formed by electrostatic interaction between biopolymers, the biopolymers properties, such as molecular weight, composition, surface charge density, and structural characteristics, can largely influence the coacervates complex shape, particle size, and internal structures. Besides, biopolymer type, concentration, and the location of functional groups within the biopolymer will also influence the physicochemical properties of complex, including reflective index, density, complex integrity, and enzyme digestibility (Jones & McClements, 2010). Therefore, the properties of biopolymers will further influence the functionality of the complex, such as the stability overtime, optical properties, and in vivo digestibility.

1.3.1 Chitosan

Chitosan has been widely studied and used as a polymer due to its low toxic, biodegradable, antibacterial property on a range of bacteria, and many other characteristics (Park and et al., 2002). As a natural cationic polymer derived from chitin, which is abundant in crab and shrimp cells, chitosan is much cheaper than synthesized polymers (Dutta, et al., 2004). The properties of chitosan, such as positive charge at

lower pH, gel-forming ability, and ability to form complexes with many low molecular weight compounds (Ilium, 1998). However, due to the rigid crystalline structure and hydrogen bonding partly taken by primary amino groups of chitosan, the insolubility of chitosan limits its application (Nishimura et al., 1991). There are many publications concerning grafting poly(ethylene glycol) (PEG) onto chitosan through the use of amination, since hydrophilic PEG can be used as solubilizing aids and surface conditioners (Janciauskaite et al., 2008). By utilizing the functional groups of C2-amino, synthesis of chitosan-grafted-poly(ethylene glycol) can be achieved through covalent binding to monocarboxyl-poly(ethylene glycol) molecules with coupling agents, and is can form hydrogels with α-cyclodextrin (Huh, 2004).

1.3.2 Dextran

Similar to the concept of chitosan-graft-PEG, dextran as a natural hydrophilic polysaccharide also can be used as grafting material onto chitosan with ability to enhance solubility of chitosan (Janciauskaite et al., 2008). Dextran is a non-ionic bacterial homo-polysaccharide composed of 1,6-linked -D-glucopyranosyl units that is frequently used in food and pharmaceutical systems due to its excellent solubility and simple structure (Waldherr & Vogel, 2009). Synthesis of carboxymethyl-dextran-block-poly(ethylene glycol) (CMD-*b*-PEG) from dextran has been established in recent literature (Hernandez et al., 2007 and Zhang & Marchant, 1994), which modified dextran polymers with ionic charges that may interact with polyelectrolyte like α-lac protein and tehrefore to form complex coacervates. Due to the charges of carboxymethyl groups, CMD is able to form complexes as nanoparticles with proteins and then to form hydrogels that can be alternated through ionic strength (Zhang et al., 2005).[3]

[3]taken with permission from [62].

1.3.3 α-Lactalbumin

As one of the major whey protein, α-lactalbumin (a-lac) is a globular protein with molecular weight of about 14.2 kDa and an isoelectric point of 4.2-4.8 (Bramaud et al., 1995 and Hernndez-Hernndez et al., 2008). The structure of small globular -lac protein contains 4 disulfide bridges, and it is a regulating protein of lactose synthesis in mammary grind (Fox & McSweeney, 2003). Previous studies by researches indicates that the removal of calcium can cause conformational changes of α-lac, causes α-lac to be able to of bind retinol and palmitic acid hydrophobic molecules (Barbana et al, 2006), which shows the potential of using α-lac for encapsulation of hydrophobic compounds. Complex formation between chitosan and α-lac was previous studies by Lee and Hong (2009), with strong prove of complex coacervates formation at pH 5.0 at concentrations of 0.1% chitosan and 0.5% α-lac and scanning electron microscopy images indicating unevenly associated clusters. However, complex coacervates formed by α-lac and CH-PEG, which will be a main portion of our study.

1.3.4 Poly(ethylene glycol)

Poly(ethylene glycol) (PEG) is an FDA-approved hydrophilic polymer with partial solubility in organic solvents, and it is frequently attached covalently to polymers or colloids to increase dispersibility in water (Harris & Chess, 2003; Otsuka, Nagasaki, & Kataoka, 2012). Attachment of PEG blocks onto the terminal end of a hydrophobic polymer creates block-copolymer surfactants, such as Tweens and Pluronics, that are extensively utilized as emulsion stabilizers or as components of micellar delivery vehicles (Tadros, 2005). Due to excellent hydrophilicity, low toxicity, rapid clearance in vivo, and potential to reduce allergenicity of peptides, PEG groups have been utilized in protein-based pharmaceuticals and delivery vehicles (Roberts, Bentley, & Harris, 2012). PEG has been popularly used also for its long-circulating properties due

to its shielding effect that prevents uptake of nano-particles from reticuloendothelium system (RES) (Abgoustakis, 2004; Lin & Hsu, 2014).[4]

1.4 Micelle Structure as Delivery Vehicles

Colloidal delivery systems, such as surfactant micelles, emulsions, liposomes, and nanoparticles, are widely used in food and pharmaceuticals to improve the dispersion of poorly-soluble ingredients or modify their bioaccessibility within the body (Patel & Velikov, 2011). As a delivery system for medical- and health-relevant bioactive components, surfactant micelles are used for delivery of poorly water-soluble compounds. Many commercial surfactants are block copolymer assemblies of hydrophilic and hydrophobic polymeric blocks, or polymer segments, where the hydrophobic segments form the internal core of the micelle. However, studies show that surfactant micelles have potential toxicity due to the disruption of cell membranes and interference with cell membrane transporters (Rege, Kao, & Polli, 2002; Swenson & Curatolo, 1992). [5]

[4]taken with permission from [62].
[5]taken with permission from [62].

2. INFLUENCE OF PEGYLATION ON THE ABILITY OF CARBOXYMETHYL-DEXTRAN TO FORM COMPLEXES WITH α-LACTALBUMIN

[1]

2.1 Abstract

Electrostatic interactions between α-lactalbumin (α-lac) and carboxymethyldextran (CMD) in acidic solutions lead to phase-separated complexes. By adding a non-ionic poly(ethylene glycol) (PEG) chain onto the reducing end of CMD, forming carboxymethyl-dextran-block-poly(ethylene glycol) (CMD-*b*-PEG), the PEG block was hypothesized to reduce interactions with α-lac and promote formation of a micelle-like complex structure. Formation of complexes between α-lac and CMD-*b*-PEG or α-lac and CMD was determined following acidification by light scattering and electrophoretic mobility. Phase separation, size, and structure of α-lac/CMD-*b*-PEG complexes were characterized by turbidimetry, dynamic light scattering, and electron microscopy, respectively. Complexes of α-lac/CMD-*b*-PEG formed at pH values near pH 6, while α-lac/CMD complexes formed at pH 5.5. Both CMD and CMD-*b*-PEG decreased the charge of α-lac below pH 5.5 and led to phase separation below pH 5. Shift in charge and the critical pH of phase separation were both sensitive to the α-lac to CMD ratio, while the relative amount of CMD-*b*-PEG did not significantly influence either. Hydrodynamic radii of α-lac/CMD-*b*-PEG complexes was between 11 and 20 nm, which increased with increasing α-lac to CMD-*b*-PEG ratio and with decreasing pH. Spheroidal structures of 10 nm were also observed in micrographs that were attributed to α-lac/CMD-*b*-PEG complexes.

[1]This chapter is taken with permission from [62].

2.2 Objectives

The objective of this research was to determine the influence of covalently-attached PEG on (i) the ability of CMD to form complexes with α-lactalbumin (α-lac) and (ii) the colloidal properties of the resulting complexes. α-Lac is a globular protein obtained from dairy whey, a byproduct of cheese manufacturing, with an approximate molecular weight of 14.2 kDa and an isoelectric point of $\sim$4.24.8 (Bramaud et al., 1995 and Hernndez-Hernndez et al., 2008). Dextran is a non-ionic bacterial homo-polysaccharide composed of 1,6-linked α-D-glucopyranosyl units that is frequently used in food and pharmaceutical systems due to its excellent solubility and simple structure (Waldherr & Vogel, 2009). Synthesis of carboxymethyl-dextran-block-poly(ethylene glycol) (CMD-*b*-PEG) from dextran has been established in recent literature (Hernandez et al., 2007 and Zhang and Marchant, 1994). To the authors' knowledge, no studies have yet investigated the pH conditions and polymer ratios necessary for the formation of complexes between a polysaccharide-containing copolymer and a protein.

2.3 Materials

Dextran with a reported average molecular weight (MW) of 20 kDa was purchased from Alfa Aesar Specialty & Intermediates (Ward Hill, MA). O-(2-aminoethyl)-PEG (MW = 5 kDa), 3-ethylcarbodiimide hydrochloride, N-hydroxysuccinimide, and monochloroacetic acid were purchased from SigmaAldrich (St. Louis, MO). α-Lactalbumin (α-lac) was kindly donated by Davisco Food International (Le Sueur, MN). Protein was further purified to remove minerals by dialysis (molecular weight cutoff of 3.5 kDa) against ultrapure water ($\sigma \geq$18 mΩ-cm; Barnstead E-pure, Thermo Scientific, Waltham, MA). Protein was then lyophilized and kept at 4 °C as a dry solid until use. Deuterium oxide (D_2O), sodium hydroxide, and hydrochloric acid were purchased from SigmaAldrich (St. Louis, MO).

2.3.1 CMD and CMD-*b*-PEG synthesis and characterization

Dextran was oxidized by iodine in basic solution and purified in a cation exchange resin to obtain dextran aldonic acid (Zhang & Marchant, 1994). O-(2-Aminoethyl)-PEG was then coupled to the terminal aldonate/lactone, as described in literature (Hernandez et al., 2007). Samples were dialyzed (MWCO = 1214 kDa) to remove non-bonded O-(2-aminoethyl)-PEG, and then lyophilized to obtain dextran-block-PEG. Formation of dextran-lactone and dextran-block-PEG was verified by 1H NMR spectroscopy (Fig. 2.1).

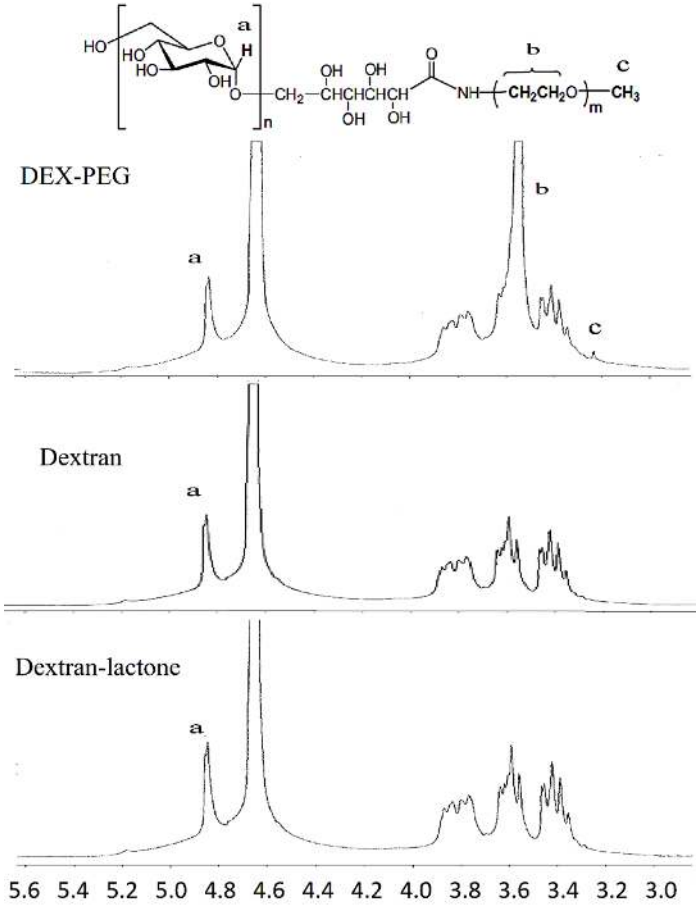

Fig. 2.1. ^{1}H NMR spectra of dextran-block-PEG, Dextran, and Dextran-lactone in D_2O at room temperature

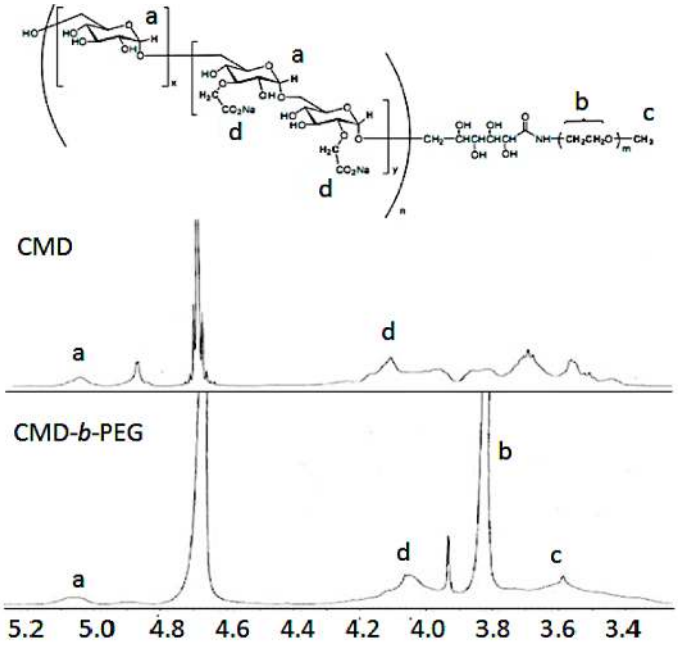

Fig. 2.2. ^{1}H NMR spectra of CMD, and CMD-*b*-PEG in D_2O at room temperature

Both carboxymethyl-dextran (CMD) and CMD-*b*-PEG were prepared by dissolving dextran and dextran-block-PEG, respectively, in 85/15 v/v isopropanol/water mixture and treated with aqueous NaOH (9.0 M) at 60 °C with monochloroacetic acid to produce CMD-*b*-PEG. The final product was washed by methanol and purified by ultrafiltration (Huynh, Chaubet, & Jozefonvicz, 1998). Retentate was then lyophilized to obtain a dry powder, which was stored at 20 °C until further use. Successful incorporation of carboxylate groups onto dextran or dextran-block-PEG, forming CMD and CMD-*b*-PEG, respectively, was verified by 1H NMR spectroscopy (Fig. 2.2).

The 1D proton Nuclear Magnetic Resonance (NMR) spectra of dextran-lactone, dextran-PEG, CMD, and CMD-*b*-PEG samples dissolved in D_2O were acquired in order to characterize the successful incorporation of carboxylate groups and PEG groups onto the dextran block. All the samples were prepared for NMR by three cycles

of dispersion within D_2O and lyophilization to a solid in order to reduce interference from water. Samples were diluted in D_2O before measurements to a concentration of 1.0 mg/mL. 64 scans of each sample were performed using an INOVA 300 MHz NMR with a 5mm quadrupole-nucleus probe.

2.3.2 Solution Preparation

Solutions of protein (purified α-lac) and polysaccharide (CMD or CMD-*b*-PEG) were prepared by dissolving lyophilized powders in 3 mM acetate buffer for a minimum of 2 h. Solutions were mixed for at least 30 min at pH 6.5 at different volumetric ratios to obtain mixtures with α-lac to CMD or α-lac to CMD-*b*-PEG ratios (r) of between 2 and 8. The total biopolymer concentration, including both α-lac and CMD or CMD-*b*-PEG, in each mixture was fixed at a constant of 0.032% (w/w). Mixtures were then acidified using 0.1 N HCl solution. Aliquots were collected every 0.1 pH units for light scattering and turbidity measurements and every 0.5 pH units for ζ-potential measurement. All samples were vortexed prior to colloidal characterization to ensure even dispersion.

2.3.3 Colloidal Sample Characterization

ζ-Potential of α-lac, CMD, CMD-*b*-PEG, and mixtures were determined at different pH values by electrophoretic mobility measurements (Malvern Zetasizer Nano ZS, Malvern Instruments, Worcestershire, UK) at a scattering angle of 173°.

Turbidity of pure solutions and mixtures as a function of pH was measured in polystyrene cuvettes using a PerkinElmer UV/vis Spectrometer Lambda 25 at a wavelength of 450 nm, as previously described for proteinpolysaccharide complex formation (Hirt & Jones, 2014). Turbidity was presented as 100 %T, where T is the light transmitted through the sample and cuvette, in order to accentuate the increase in light scattering during colloidal interactions within dilute solution. Pure acetate buffer was utilized as a reference blank.

Critical pH values for the formation of soluble complexes (pH_c) and phase separated structures ($pH\phi$) between α-lac and dextran derivatives were determined based on the method described by Mattison et al. (1995). Briefly, turbidity and light scattering intensity values from aliquots of mixtures at different pH values were utilized to create pH-dependent plots. Critical pH values pH_c and $pH\phi$ were then determined from significant increases in the slope of scattering intensity or turbidity, respectively, as a function of pH. An example of these procedures was mentioned in Chapter 1.2.

Hydrodynamic radii of constituents present in the mixtures were determined by dynamic light scattering using an ALV-CGS3 light scattering goniometer (ALV, Langen, Germany). Scattered light from a HeNe laser with a wavelength of 632.8 nm was detected by ALV High Q.E. avalanche photodiode (APD) dual detectors in pseudo cross correlation mode.Z-average diffusion coefficients (D_z) of dextran, CMD, and CMD-*b*-PEG samples were obtained from measurements of the first cumulant (Γ) at scattering vectors (q) between 0.008 and 0.017 nm^{-1}, which were extrapolated to zero-q based on Expression (2.1):

$$\lim_{q^2 \to 0} \Gamma / q^2 = D_z \tag{2.1}$$

This expression accounts for angle-dependent scattering effects on the apparent diffusion coefficient with the condition that the radius of gyration is significantly less than the inverse of q, which was adequately satisfied for all samples tested (Burchard, 1983). Hydrodynamic radii reported in the figures were calculated from the z-average diffusion coefficients using the StokesEinstein equation. Hydrodynamic radii of mixed α-lac/CMD-*b*-PEG solutions were determined using the CONTIN algorithm within the instrument software (ALV, Langen, Germany). All samples were diluted in buffer until concentration dependence was no longer observed in order to eliminate multiple scattering effects.

Transmission electron microscopy (TEM) images of dried samples (α-lac, CMD-*b*-PEG, and representative α-lac CMD-*b*-PEG complexes) were obtained using a FEI/Philips CM-100 TEM (FEI Company, Hillsboro, Oregon, USA). Selected sam-

ple mixtures were placed on a copper grid coated with a continuous carbon support film, then being stained with 0.5% uranyl acetate in distilled water and air-dried at room temperature. Representative images shown were selected from approximate 1015 images from each sample.

2.3.4 Statistical Treatment

All samples were prepared in at least triplicate, unless otherwise specified. Statistical significance between determined critical pH values was established by means of the student's t-test. Significance of linear relation between r value and both turbidity and hydrodynamic size was established by means of linear regression analysis. In all figures, displayed error bars represent the standard deviation from independent sample measurements.

2.4 Results and Discussion

2.4.1 Influence of pH on protein polysaccharide complex formation

Fig. 2.3 demonstrates the influence of pH during acid titration from pH 5.5 to 3.5 on the surface charge (ζ-potential) of α-lac, CMD, CMD-*b*-PEG, or mixtures of α-lac with either CMD or CMD-*b*-PEG. Fig. 2.3a showed the charge of the individual polymers as a function of pH, indicating their potential for complex formation at different pH values. In Fig. 2.3b and c, the shift in surface charge among mixtures showed the interactivity between the components at different pH values.

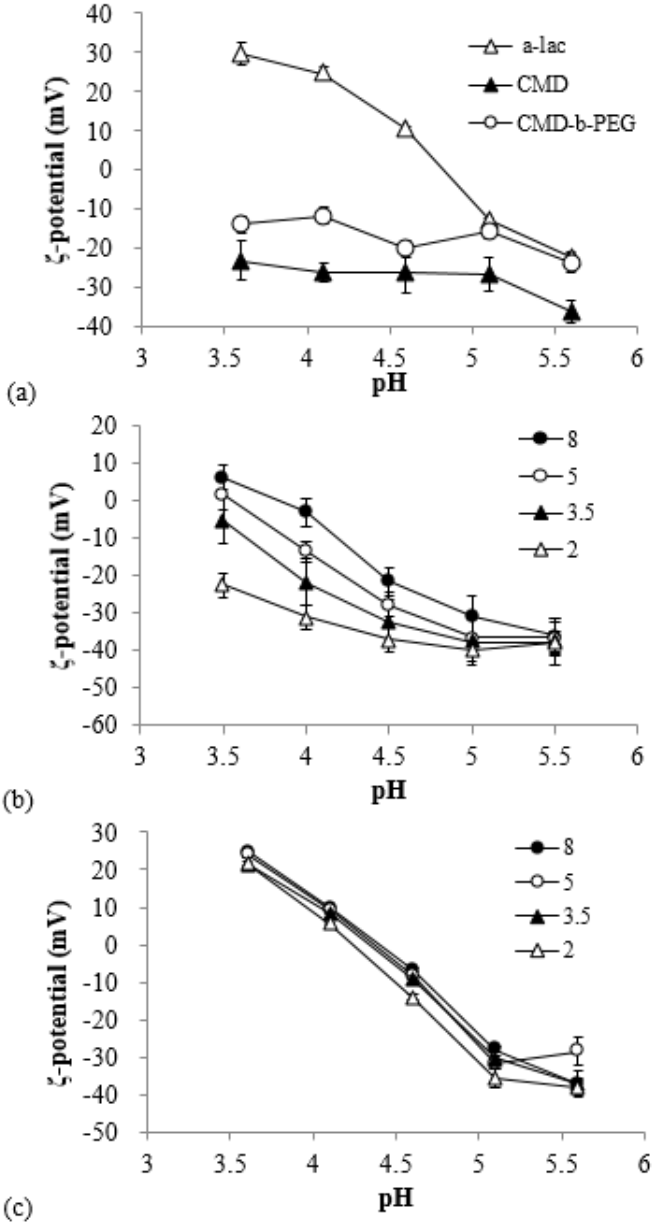

Fig. 2.3. ζ-potential as a function of solution pH of (a) α-lac (0.028 wt%), CMD (0.012 wt%), or CMD-*b*-PEG (0.012 wt%) alone, (b) complexes formed by α-lac and CMD of different r values (shown in legend), or (c) complexes formed by α-lac and CMD-*b*-PEG of different r values (shown in legend)

The ζ-potential of α-lac was negative at neutral pH values then became positive between pH 4.5 and 5.2 (Fig. 2.3a), implying an isoelectric point of α-lac within this pH range. An isoelectric point between pH 4.5 and 5.2 is in agreement with literature values that have indicated experimentally determined isoelectric points up to pH 4.6 (Bramaud et al., 1995). ζ-Potential values of CMD and CMD-*b*-PEG were both negative at all studied pH values, with CMD-*b*-PEG less negatively charged than CMD. Since PEG is present as a terminal-block on the CMD-*b*-PEG polymer, PEGylation would not have reduced the number of potential charges on the CMD block. Rather, the reduced electrophoretic mobility of CMD-*b*-PEG relative to CMD could have been due to an increase in hydrodynamic size following covalent attachment of PEG or to a shielding of the CMD charge if the PEG-block had folded back upon the CMD-block.

ζ-Potential values of mixtures between α-lac and CMD (Fig.2.3b) were reduced compared to pure α-lac and greater than pure CMD at the same pH values (except at pH 4.5 for $r = 2$ and 3.5), which indicated the formation of complexes. At $r = 8$, ζ-potential values of the mixtures were less than that of pure α-lac, particularly at pH values near α-lac's isoelectric point. As r decreased, the ζ-potential of α-lac/CMD complexes further decreased at pH values of 5 and below, indicating greater interaction between the positively-charged sites on the protein and negatively-charged CMD when more CMD was present. This concentration-dependent correlation between the molar ratio of anionic polysaccharide and decrease in ζ-potential was indicative of complex formation, as has been observed for -lactoglobulin/pectin or -lactoglobulin/carrageenan complexes (Jones, Lesmes, Dubin, & McClements, 2010).

For α-lac/CMD-*b*-PEG mixtures, the ζ-potential values were again decreased compared to that of pure protein at pH 5 (Fig. 2.3c). Only one peak was observed in the ζ-potential distribution of the mixtures, implying that α-lac and CMD-*b*-PEG were electrostatically interacting rather than present as two separate entities. Observed ζ-potential values were insensitive to r for all studied pH values. These results suggested that CMD-*b*-PEG interacted electrostatically with α-lac in solution, while the uncharged PEG chains may have remained exposed to the aqueous environment

on the outer portions of the complex and led to a generally observed reduced surface charge relative to the α-lac/CMD complexes (Fig. 2.3b). Alternatively, the structure of the resultant complex or the presence of PEG on the exterior regions of the complex may have limited the number of CMD-*b*-PEG chains interacting with α-lac. Although there were no additional peaks in the ζ-potential distribution that would indicate the presence of excess, non-interacting CMD-*b*-PEG chains, the scattering signal from these individual chains would be relatively weak compared to the larger complexes and thus it is plausible that they were not observed within the distribution.

Critical pH values of α-lac/CMD or α-lac/CMD-*b*-PEG complexes, describing the relative tendency of the components to electrostatically interact and form separate phases using light scattering and turbidity measurements, are shown in Table 2.1. Comparable concentrations of pure α-lac, CMD, and CMD-*b*-PEG contributed negligibly to light scattering and turbidity over the same pH ranges, verifying that the critical pH values were indicative of inter-polymer interactions (not shown). Critical pH values for complex formation (pH_c) between α-lac and CMD were significantly lower than pH_c values of α-lac and CMD-*b*-PEG for all r values. For both α-lac/CMD and α-lac/CMD-*b*-PEG, the value ofr had no influence on pH_c, which is in agreement with previous findings for proteinpolyelectrolyte complexes (Hirt and Jones, 2014 and Mattison et al., 1995). The critical pH values for phase separation ($pH\phi$) of complexes between α-lac and CMD were between pH 4.3 and 5, while those for α-lac and CMD-*b*-PEG were at pH 5 for all r.

Table 2.1.
pH_c and $pH\phi$ values for mixed solutions of α-lac and CMD or α-lac and CMD-*b*-PEG of different r values

r value[3]	pH_c[1]		$pH\phi$[2]	
	α-lac and CMD	α-lac and CMD-*b*-PEG	α-lac and CMD	α-lac and CMD-*b*-PEG
8	5.47±0.03	5.84±0.12	4.97±0.07	5.03±0.03
5	5.54±0.13	5.94±0.13	4.91±0.07	5.03±0.12
3.5	5.56±0.05	5.79±0.16	4.79±0.03	4.98±0.05
2	5.46±0.05	5.95±0.11	4.30±0.01	4.95±0.04

1: pH_c is the critical pH of complex formation, as determined by light scattering measurements as a function of pH

2: $pH\phi$ is the critical pH of phase separation, as determined by turbidimetry measurements as a function of pH

3: r is the protein-to-polysaccharide (or modified polysaccharide) ratio on a weight basis

As expected, $pH\phi$ values of α-lac/CMD complexes decreased with decreasing r, which is in agreement with trends observed for other polyelectrolyte complexes (Mattison et al., 1998 and Mattison et al., 1995). This responsiveness of $pH\phi$ to r has been attributed to the re-balancing of total charges in the proteinpolyelectrolyte system, so that a relative increase in the polyelectrolyte concentration necessitates an increase in the protein charge to reach zero net-charge, which is facilitated by further reduction of solution pH. Interestingly, $pH\phi$ values of α-lac/CMD-*b*-PEG complexes did not decrease with decreasing r. Normally, a decrease in r would increase the number of negatively-charged components in the complex and shift $pH\phi$ to lower values, as observed for the complex with CMD. The lack of reduction in $pH\phi$ with CMD-*b*-PEG implied that the covalently attached PEG chain reduced the contribution of negative charges to the protein complex, possibly by limiting the number of protein molecules that could interact with CMD-*b*-PEG. This was supported by ζ-potential measurements, which showed that increasing relative quantities of CMD-*b*-PEG (lower r) had little effect on reducing the net-charge of the complex (Fig. 2.3).

As the pH_c for α-lac and CMD mixtures were significantly lower than those for α-lac and CMD-*b*-PEG and $pH\phi$ values were either the same or lower, it was proved that the PEGylation of CMD favored both complex formation with α-lac and the

subsequent phase separation of complexes. This was not expected, as PEG in isolation has been utilized as a means to obtain isolated α-lac from solution because it is incompatible with α-lac at neutral pH values (Rodrigues, Venncio, & Teixeira, 2001). PEG has also been shown to reduce protein adhesion to nanoparticle surfaces by increasing the hydrophilicity (Zhang, Desai, & Ferrari, 1998). Thus, it was expected that addition of PEG to CMD would have decreased both pH_c and $pH\phi$, with the PEG group reducing the ability of α-lac to associate with the charged CMD. However, observance of higher or equal pH_c and $pH\phi$ values for α-lac/CMD-*b*-PEG indicated that PEG increased the favorability of polymeric interactions. Significant interactivity between α-lac and the PEG chain was not considered likely. Thus, it is proposed that α-lac and CMD-*b*-PEG formed a C3M with a coreshell structure, and the formation of such a coreshell structure was energetically favorable in a manner akin to the formation of surfactant micelles, driving interactions between α-lac and CMD-*b*-PEG at higher pH values. Such a model could also be utilized to explain the insensitivity of $pH\phi$ values for α-lac/CMD-*b*-PEG complexes with changing r, as formation of a coreshell C3M structure has a limited dimension that may not be able to accommodate additional CMD-*b*-PEG chains. This hypothetical energetic explanation of C3M formation causing increased pH_c and $pH\phi$ values could be resolved by detailed isothermal titration calorimetry experiments in future studies.

2.4.2 Effect of PEG on Complex Stability

Turbidity of α-lac/CMD or α-lac/CMD-*b*-PEG suspensions was measured at pH 3.8 (below $pH\phi$) in order to distinguish the relative size and quantity of the phase-separated structures in suspensions (Fig. 2.4). In general, the turbidity values of α-lac/CMD complexes were significantly higher than those of α-lac/CMD-*b*-PEG. For both complexes, there was a significantly negative linear relation between turbidity at pH 3.8 and r value.

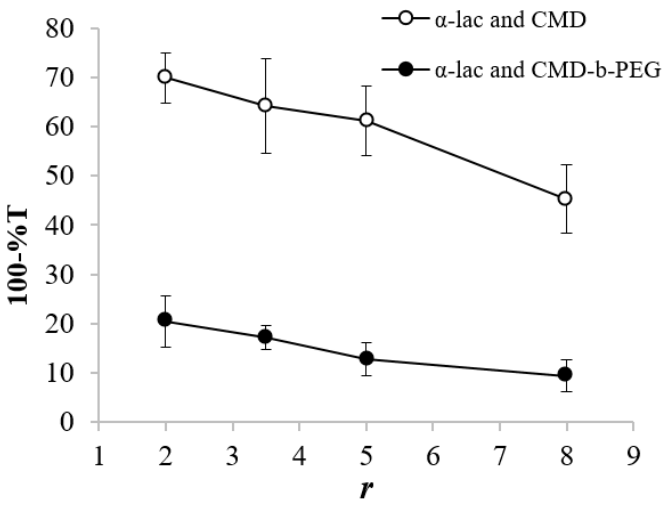

Fig. 2.4. Turbidity of α-lac with CMD or CMD-*b*-PEG at pH 3.8 as a function of r

Based upon colloidal charge measurements and critical pH values with decreasing pH and r (Fig. 2.3 and Fig. 2.4), it was proposed that α-lac/CMD complexes formed coacervate structures. Thus, at these acidic pH values the turbidity of α-lac/CMD suspensions was due to a large and gradually separating coacervate phase dispersed within a α-lac- and CMD-depleted aqueous phase. Increased turbidity in samples with smaller r was attributed to the increased relative quantity of CMD that became available for interaction with the positively-charged α-lac, forming more of the turbid coacervate phase. Suspensions of α-lac/CMD-*b*-PEG, however, were much less turbid at the same concentrations and r-values. Low turbidity values even at pH values well below the pHϕ indicated that α-lac/CMD-*b*-PEG formed a phase-separated structure with a smaller size, reduced quantity, or both. The difference in turbidity values between the two mixtures of similar composition suggested that the structure formed in mixtures with CMD-*b*-PEG were of a different nature than the typical complex coacervate structures that were formed in mixtures with CMD.

At higher pH, dynamic light scattering was utilized to investigate the hydrodynamic size of soluble complexes formed between α-lac and CMD-*b*-PEG near their

critical pH values of interaction. The experimentally determined hydrodynamic radii of α-lac/CMD-*b*-PEG mixtures within the pH range of 6.55 are shown in Fig. 2.5. Two major diffusive colloidal modes were identified in this pH range: one that was relatively fast-moving and one slower-moving. The fast-moving mode was detected at all tested pH values, possessing an average hydrodynamic radius of 15 nm that was consistent for all r and pH values (Fig. 2.5a). This average hydrodynamic radius could be attributed to individual α-lac molecules, which is in agreement with literature values for α-lac (2.0 and 2.2 nm for native and denatured α-lac, respectively) (Redfield, Schulman, Milhollen, Kim, & Dobson, 1999). Larger components within this population distribution could have also included individual CMD-*b*-PEG chains, as well as small fractions of unconverted CMD and dextran precursors. CMD-*b*-PEG, CMD, and dextran chains were independently characterized at pH 6 to have hydrodynamic radii of 11.5, 8.0, and 6.3 nm, respectively, which is in line with the size of a similarly structured CMD-*b*-PEG of relatively smaller molecular weight (MW 16.7 kDa; RH = 35 nm) (Hernandez et al., 2007). This same group had found a second, larger population of aggregates with hydrodynamic radius of 50 nm at pH 3 and 6 that was not observed in our samples.

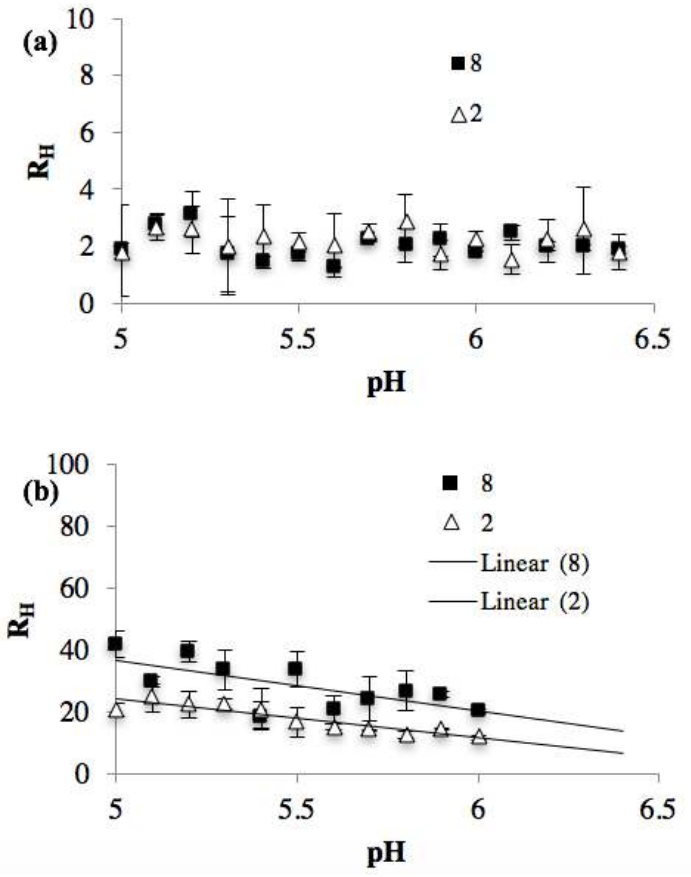

Fig. 2.5. Hydrodynamic radii (RH) of α-lac/CMD-*b*-PEG complexes (r = 2 or 8) as a function of pH and r-value between pH_c and $pH\phi$ for (a) the fast mode and (b) the slow mode.

When the mixtures were acidified to pH 6 and below, particles with a slower diffusive profile were detected by dynamic light scattering. Fig. 2.5b shows the size of these slower detected particles in suspension for samples containing the most and the least α-lac (r = 8 and 2, respectively). These slower particles possessed average hydrodynamic radii of 1120 nm at pH 6, which generally increased to 2042 nm at pH 5. The pH at which these slower particles appear was the same as the experimentally determined pH_c of α-lac/CMD-*b*-PEG (Table 1), and these detected particles were attributed to soluble complexes. The comparable size of the smaller complexes to the determined hydrodynamic radius of CMD-*b*-PEG by itself at pH

6 (11.5 nm) implied that the relatively smaller α-lac molecules interacted along the length of chain, increasing the density of the complex but not its hydrodynamic size, as previously found for whey protein/gum Arabic complexes (Weinbreck, de Vries, Schrooyen, & de Kruif, 2003). At greater r, the average hydrodynamic radius of the complex was significantly larger than that of CMD-*b*-PEG, so the greater amount of interacting α-lac must have been sufficient to increase the hydrodynamic size of the chain. Further information on the complex structure can be resolved using X-ray or neutron scattering in future studies.

Average hydrodynamic radii of the complexes (slower diffusive mode) were typically larger for α-lac/CMD-*b*-PEG complexes as r increased and pH decreased. Fig. 2.6 demonstrates the effect of increasing r on average hydrodynamic radius of α-lac/CMD-*b*-PEG complexes at pH values of 5.8, 5.5, and 5.0. As in Fig. 2.5, the size of the complexes were larger at the more acidic pH values. For each tested pH value, the increase in complex size with increasing r was similar, indicating that the relative quantity of α-lac in the mixture consistently controlled the size of the complex structure. As α-lac was the sole source of positively-charged sites for interaction with the CMD-*b*-PEG, the relative quantity of α-lac (r) and ionization of α-lac (pH) were critical in the size of formed complexes. Thus, the largest complexes were formed at $r = 8$ and at lower pH values.

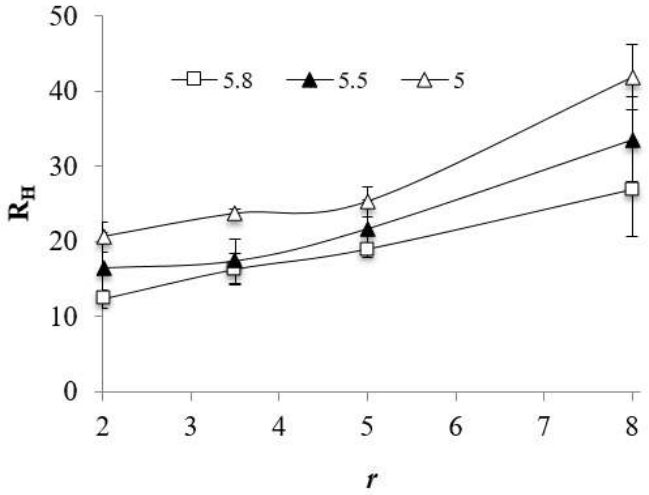

Fig. 2.6. Hydrodynamic radii (RH) of α-lac/CMD-*b*-PEG complexes (slow diffusive mode from dynamic light scattering) as a function of r-value at select pH values.

Below pH 5, the complexes underwent phase separation (Table 2.1), and the resulting particle diffusion at these low pH values, as determined by dynamic light scattering, significantly decreased for all samples (not shown). This implied that α-lac/CMD-*b*-PEG complexes were not stable to colloidal aggregation and formed large phase-separated domains. Reduced turbidity of α-lac/CMD-*b*-PEG complexes at low pH (Fig. 2.4) then indicated that the domains were of smaller number or of reduced scattering contrast when compared to the complex coacervate domains of α-lac/CMD. It was hypothesized that the PEG chains were not of sufficient length to prevent flocculation of the α-lac/CMD-*b*-PEG complexes. Based upon Table 2.1 and Fig. 2.3, both phase separation (pHϕ) and ζ-potential values were not significantly influenced by r. In light of these facts, the larger size of complexes with increasing r (Fig. 2.6) indicated that the balance between protein and CMD-*b*-PEG in the complexes only changed the relative amount of components within the structure but not the surface charge of the complexes or the phase stability.

2.4.3 Visual Characterization of Complexes

In order to identify whether a C3M structure formed at pH values between the pH_c and $pH\phi$, pure α-lac and mixed α-lac/CMD-*b*-PEG samples at pH 5.2 were characterized by transmission electron microscopy (Fig. 2.7). Pure α-lac at pH 5.2 was found as a spherical agglomerate of 1020 nm in diameter (Fig. 2.7a). There was no evidence of these spherical agglomerates in light scattering measurements of pure α-lac at pH 5.2, and the observed agglomerates were attributed to aggregated protein that resulted from drying when samples were prepared for imaging. Electron micrographs of pure CMD-*b*-PEG at pH 5.2 showed spherical structures with diameter of 60 nm against a rough background (Fig. 2.7b). Since the 60 nm agglomerates were not evidenced by dilute-solution scattering measurements, these spherical structures were attributed to the agglomeration of CMD-*b*-PEG that formed during sample drying prior to imaging, which agrees with previous reports of 50 nm CMD-*b*-PEG aggregates in neutral pH solutions (Hernandez et al., 2007). Images taken of mixed α-lac and CMD-*b*-PEG ($r = 3.5$) at pH 5.2 show both larger spherical structures and smaller, irregularly-shaped aggregates with diameters of approximately 60 and 10 nm, respectively (Fig. 2.7c). The smaller aggregates could be attributed either to aggregates of pure α-lac that formed during drying (Fig. 2.7a) or to smaller complexes of α-lac and CMD-*b*-PEG, which possessed average diameters as low as 30 nm in these conditions (Fig. 2.7b). A case for the latter scenario is strengthened by the fact that the small aggregates in Fig. 2.7c were not as spherical in shape when compared to the pure α-lac aggregates (Fig. 2.7a). The larger spherical aggregates in Fig. 2.7c could either be attributed to the formation of larger agglomerates of α-lac/CMD-*b*-PEG complexes or to CMD-*b*-PEG, itself, during the drying step. There were no ropy structures evident in mixed α-lac/CMD-*b*-PEG solution, indicating that the presence of α-lac prevented their formation during drying. Structural formations of CMD-*b*-PEG at higher concentrations, as experienced during drying, needs to be investigated in future studies in order to verify these suppositions.

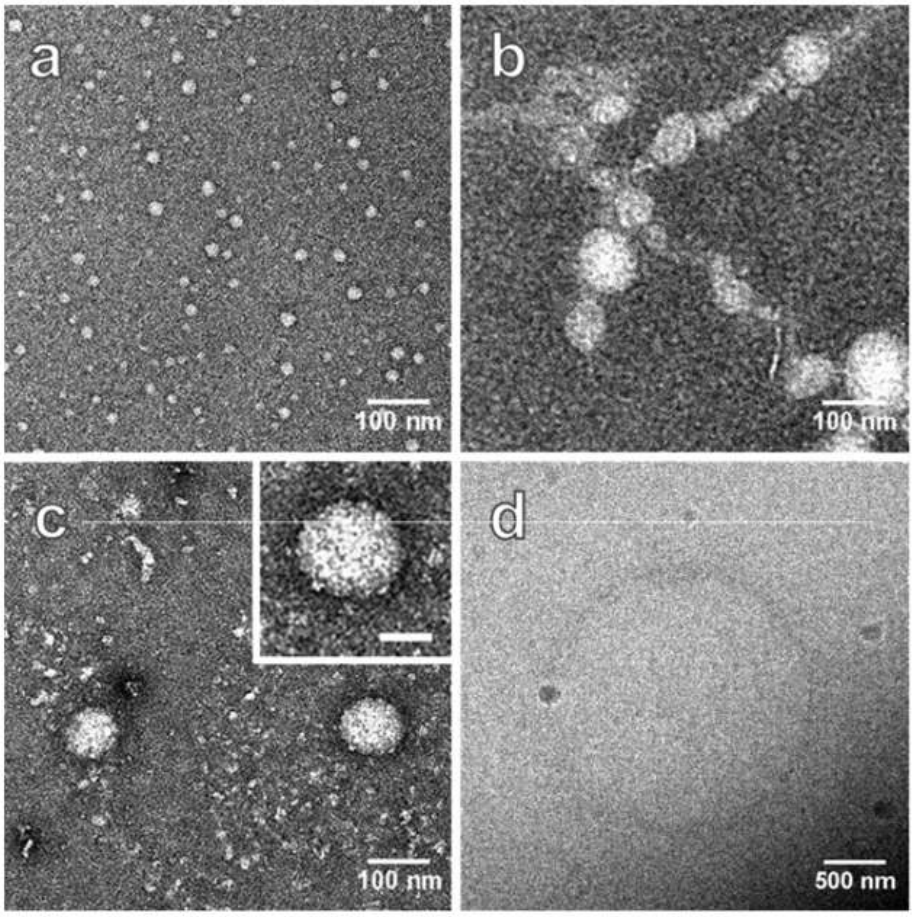

Fig. 2.7. Transmission electron micrographs of (a) α-lac at pH 5.2, (b) CMD-*b*-PEG at pH 5.2, (c) α-lac/CMD-*b*-PEG mixtures with $r = 3.5$ at pH 5.2, and higher-magnification image of sample in (c). scale bars = 100 nm, (d) cryo-TEM images of α-lac/CMD-*b*-PEG mixtures with $r = 3.5$ at pH 5.2

2.5 Conclusions

Interactions between α-lac and CMD-*b*-PEG were verified by a negative-shift in the electrophoretic mobility when compared to pure α-lac, as well as significant increases in light scattering and turbidity at pH 5.9 and 5, respectively. Neither complex formation at pH 5.9 nor phase separation at pH 5 was influenced by the α-lac to CMD-*b*-PEG ratio (r). Complex formation also occurred at a higher pH value be-

tween α-lac/CMD-*b*-PEG when compared to α-lac/CMD. This insensitivity of phase separation to r and the increased pH of complex formation implied that addition of the PEG chain to CMD increased the favorability of forming complexes with α-lac in a manner that was insensitive to the quantity of added CMD-*b*-PEG, at least in the concentration regimes tested here. It was proposed that α-lac/CMD-*b*-PEG formed a C3M structure that was energetically favored at pH 5.9, and that at pH 5 the C3M, surrounded by the non-ionic PEG chains, flocculated and separated from the continuous phase. However, the internal structure of the complex needs to be further characterized to verify this hypothesis, which may be done by small angle scattering in future studies. Also, further studies are also needed to understand if greater lengths of the PEG chain will confer increased stability of the complexes to lower pH values.

3. INTERACTION AND STRUCTURE FORMATION BETWEEN α-LACTALBUMIN AND CHITOSAN GRAFTED WITH POLY (ETHYLENE GLYCOL) CHAINS

3.1 Abstract

Hypothesis

Assemblies are formed in solution between chitosan (CH), a polysaccharide composed of D-glucosamine residues, and the whey protein α-lactalbumin (α-lac) above pH 5 due to strong electrostatic interactions, yet the process is poorly controlled and large phase-separated domains result. The incorporation of a non-ionic poly(ethylene glycol) (PEG) chain will encourage the formation of a micelle-like structure with α-lac, which will limit the phase-separation process. The micelle like structure formed with α-lac will also be affected by the sizes of CH, including high, medium, and low molecular weight CH (HMWCH, MMWCH, LMWCH, respectively) after PEGylation.

Experiments

SEC chromatography determined the peak molecular weight distribution of CH samples. NMR analysis verified successful grafting of PEG onto HMWCH, MMWCH, and LMWCH. NMR was also used to estimate the degree of deacetylation (DDA), degree of substitution (DS) of PEG onto each chitosan sample. Formation and structure of α-lac/CH-PEG or α-lac/CH complexes was determined as the solution pH was increased from pH 3 to 7 at varied ratios using light scattering, electrophoretic mobility, turbidimetry, and cryo-electron microscopy.

Findings

Complex formation for α-lac/CH and α-lac/LMWCH-PEG occurred at pH values of 4.1-4.2, while α-lac/HMWCH-PEG and α-lac/MMWCH-PEG occurs at approximately pH 3.8. Above pH 5.0, turbidity significantly increased for both complexes, indicating a phase-separation at a similar pH range. Turbidity values of α-lac/CH-PEG samples above pH 5 were significantly less than α-lac/CH samples, although the determined hydrodynamic radii of the different complexes was not significantly different, possessing small complexes and larger assemblies with diameter of 20-80 nanometers and 200-400 nanometers, respectively. The critical pH value of phase separation was significantly influenced by the molar ratios of lac to CH but not by the molar ratios between α-lac and CH-PEG.

3.2 Introduction

Polysaccharides are polymeric carbohydrates that are formed by repeating units joined by glycoside linkage with various degrees of branching. Most polysaccharides possess desirable properties for commercial application, such as minimal toxicity, high biocompatibility, low cost, and sourcing from renewable materials (Kalia et al., 2013). Chitosan has been widely studied and used in the production of biopolymer-based copolymers because of its positive charge at acidic pH, gel-forming ability, and capacity to form complexes with many low molecular weight compounds (Ilium, 1998). However, due to the rigid crystalline structure and tendency for inter-polymeric hydrogen-bonding between primary amino groups of chitosan, the insolubility of chitosan limits its application (Nishimura et al., 1991). Previous research has demonstrated that grafting hydrophilic poly(ethylene glycol) (PEG) onto chitosan through amination increases its solubility and provides functionality as a surface conditioner (Janciauskaite et al., 2008).

3.3 Materials and Methods

3.3.1 Materials

High purity chitosan with molecular weight ranges from 60,000 to 120,000 Da, which was directly used as high molecular weight chitosan (HMWCH), Monocarboxylated poly(ethylene glycol) (MPEG) with molecular weight of 5000 Da, 1-ethyl-3-(3-dimethylaminopropyl)carbodiimide (EDC), and N-Hydroxysuccinimide (NHS) were purchased from Sigma-Aldrich (St. Louis, MO). α-Lactobumin (α-lac) was kindly donated by Davisco Food International from Le Sueur, MN. α-Lac was further purified by dialysis against ultrapure water ($\sigma \geq$18mΩ-cm, Thermo Scientific, Waltham, MA) for removal of minerals. The dialysis membrane has molecular weight cut off of 3500 Da. After dialysis, protein solution was lyophilized and kept at 4 °C as dry power before use. Chemicals including acetic acid, sodium hydroxide, sodium nitrite, sodium chloride, sodium acetate, imidazole, hydrochloride acid, and deuterium chloride were purchased from Sigma-Aldrich (St. Louis, MO). Deuterium oxide were purchased from Cambridge Isotope Laboratories, INC. (Andover, MA).

3.3.2 Different Molecular Weight of Chitosan Preparation and Characterization

Part of the chitosan purchased from Sigma-Aldrich (St. Louis, MO) was depolymerized to achieve medium molecular weight chitosan (MMWCH), and low molecular weight chitosan (LMWCH), by oxidative degradation with 0.1 M sodium nitrite. Chitosan depolymerization method was adopted from Mao et al. (2004). In brief, 1% (w/w) chitosan was dissolved in 1% acetic acid with stirring on for overnight, then a predestinated amount of 0.1N $NaNO_2$ was added by droplet for 30 mins at ambient temperature. The reaction continued to another 30min before neutralization with 1N NaOH. The precipitated chitosan was collected by centrifugation, and washing by deionized water, and finally lyophilization. Characterization of the molecular weight

of chitosan samples before and after oxidative degradation was performed through Size Exclusion Chromatography (SEC). The measurement was done on an Agilent 1260 high performance liquid chromatography system equipped with a Sephadex 200/30 combination column, an Agilent 1260 ISO pump, and an Agilent 1260 Refractive Index Detector (Agilent Co., USA). Chitosan samples were dissolved at 1mg/mL overnight in a pH 4.5 solution of 100mM NaCl and 20mM acetate and passed through a 0.45 m pore size syringe filter (Berth & Dautzenberg, 2002).

3.3.3 Chitosan-graft-Poly(ethylene glycol) Synthesis and Characterization

The synthesis of chitosan-graft-poly(ethylene glycol) (CH-PEG) was performed with chitosan of different molecular weight (HMWCH, MMWCH, and LMWCH) based on the method of Huh et al. (2004). Briefly, chitosan samples with different size were dissolved at a concentration of 10mg/mL in 1% acetic acid solution and then diluted with the same volume of methanol. The coupling reactions between chitosan and MPEG were achieved by using EDC and NHS as coupling agents with predetermined amount: for each 1g chitosan powder, 0.5 g of MPEG, 0.096 g of EDC and 0.05g of NHS were added. After adding each reagent, solution was allowed to react at ambient temperature for 24 hours, and terminated by dialysis against ultrapure water for 3 days to remove coupling agents and unreacted MPEG. The successful grafting of PEG onto chitosan were verified by 1 D proton Proton Nuclear Magnetic Resonance (NMR), as indicated in Fig. 3.1. The PEGylated chitosan samples were lyophilized and labeled as high molecular weight, medium molecular weight, and low molecular weight CH-PEG (HMWCH-PEG, MMWCH-PEG, LMWCH-PEG) based on the starting molecular weight of each sample.

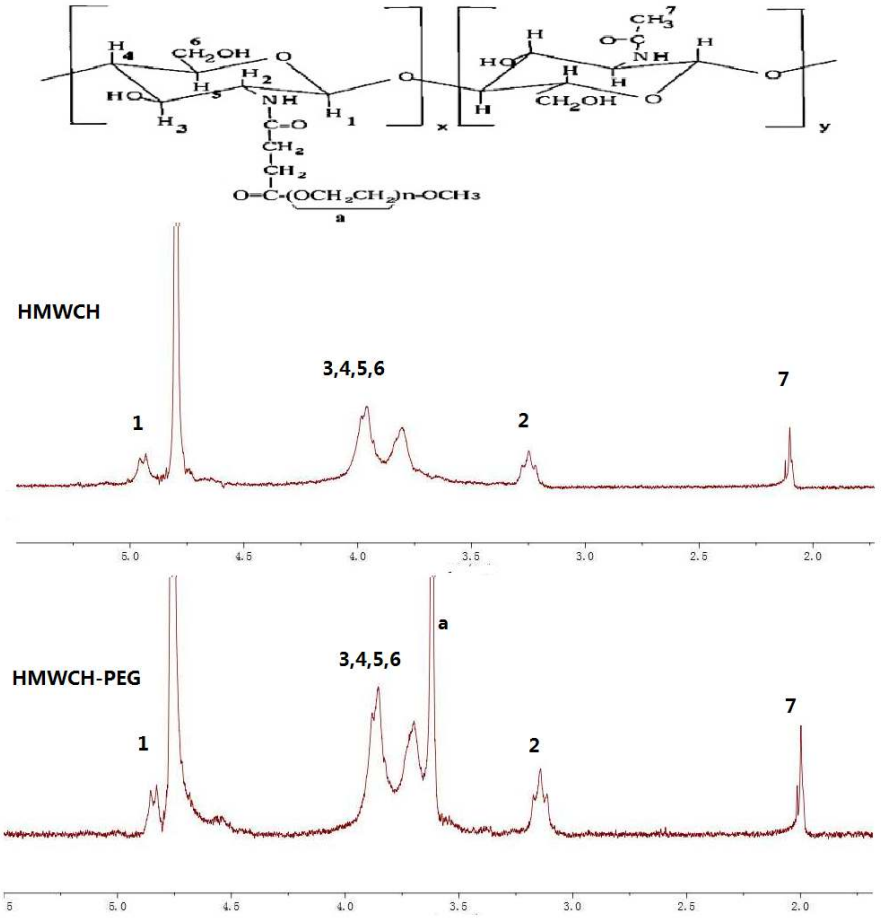

Fig. 3.1. ^{1}H NMR spectra of HMWCH and HMWCH-PEG in 2% DCl in D_2O at 45 °C

The degree of deacetylation (DDA) of chitosan and the degree of substitution (DS) of PEG (HMWCH, MMWCH, and LMWCH) were determined through 1D Proton Nuclear Magnetic Resonance (NMR) spectra by using a 300MHz NMR (Varian, Inova 300) with a 5mm quadrupole-nucleus probe. All samples were dissolved by using 2% wt DCl/D2O and then heated to 70o C and cooled to room temperature right before the measurement. An example of the spectra for each molecular weight of chitosan is provided for non-PEGylated and PEGylated samples in Figures 3.2 and 3.3, respectively. Calculation of DDA was adopted from Hirai et al. (1991) and

Lavertu et al. (2003), that the sum of integral intensity, H26(chemical shifted at 4.87, 3.18, 3.0, 3.81, 3.78, 3.74 ppm), and integral of peak of acetyl group (Hac) (5.4 ppm) were used for DDA calculation, based on equation 3.1:

$$DDA(\%) = (1 - (\frac{1}{3}Hac\frac{1}{6}H26))100 \tag{3.1}$$

The determination method of DS of PEG grafted onto chitosan was adopted from Huh et al. (2004), by comparing the integral of peak of the methylene units of PEG (3.19ppm), and the H1 of chitosan monosaccharides residues (2.92ppm) in NMR spectrum.

Table 3.1.
Physical data of chitosan and PEGylated-chitosan samples in this study

	Average Molecular Weight (Da)	Degree of Deacytylation DDA ± Stdev (%)	Degree of PEG substitution DS ±Stdev (%)	Average Molecular Weight after PEGylation (Da)
HMWCH	113K	77.46±0.59	6.78±0.94	337K
MMWCH	76K	83.37±0.44	8.14±1.41	259K
LMWCH	8.9K	77.20±2.54	9.94±1.58	26K

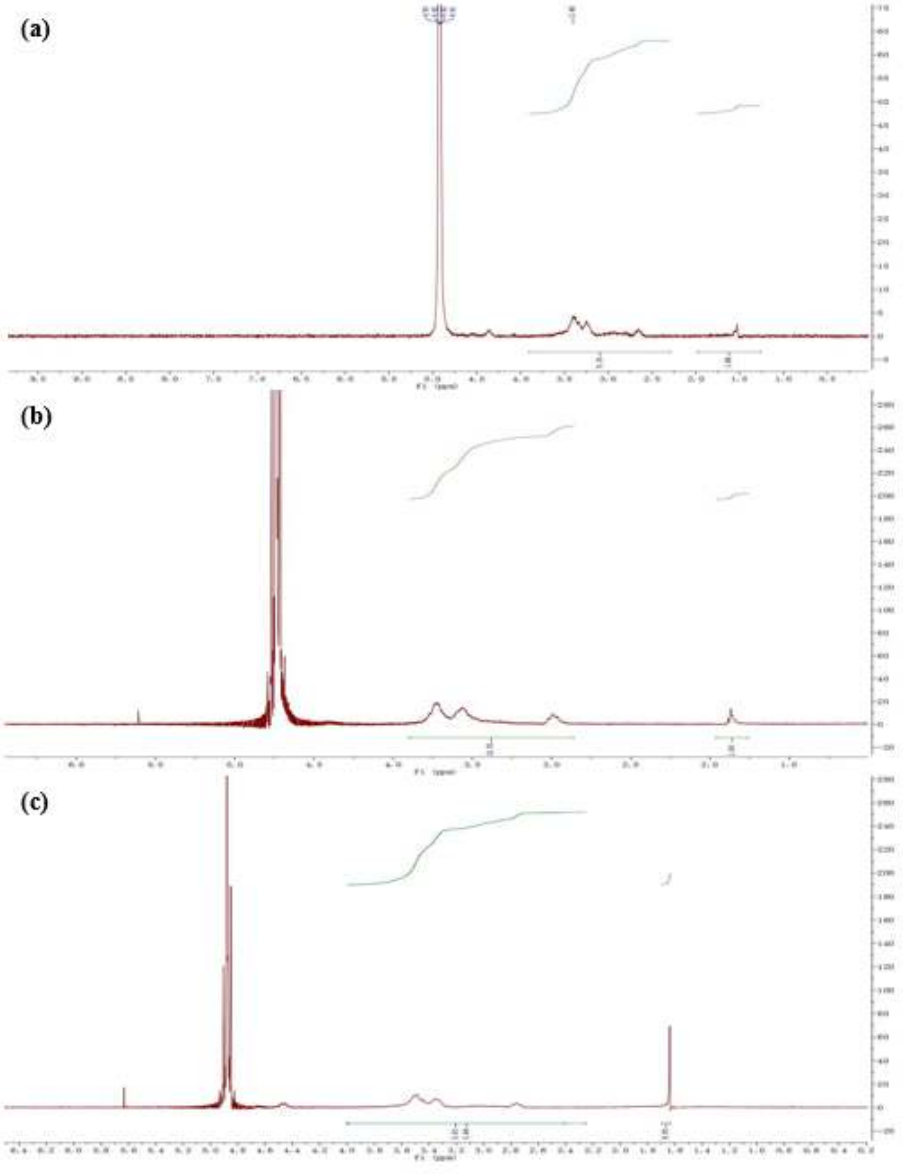

Fig. 3.2. ^{1}H NMR spectra of (a)HMWCH, (b)MMWCH, and (c)LMWCH after heating to 70°C then cooled to room temperature

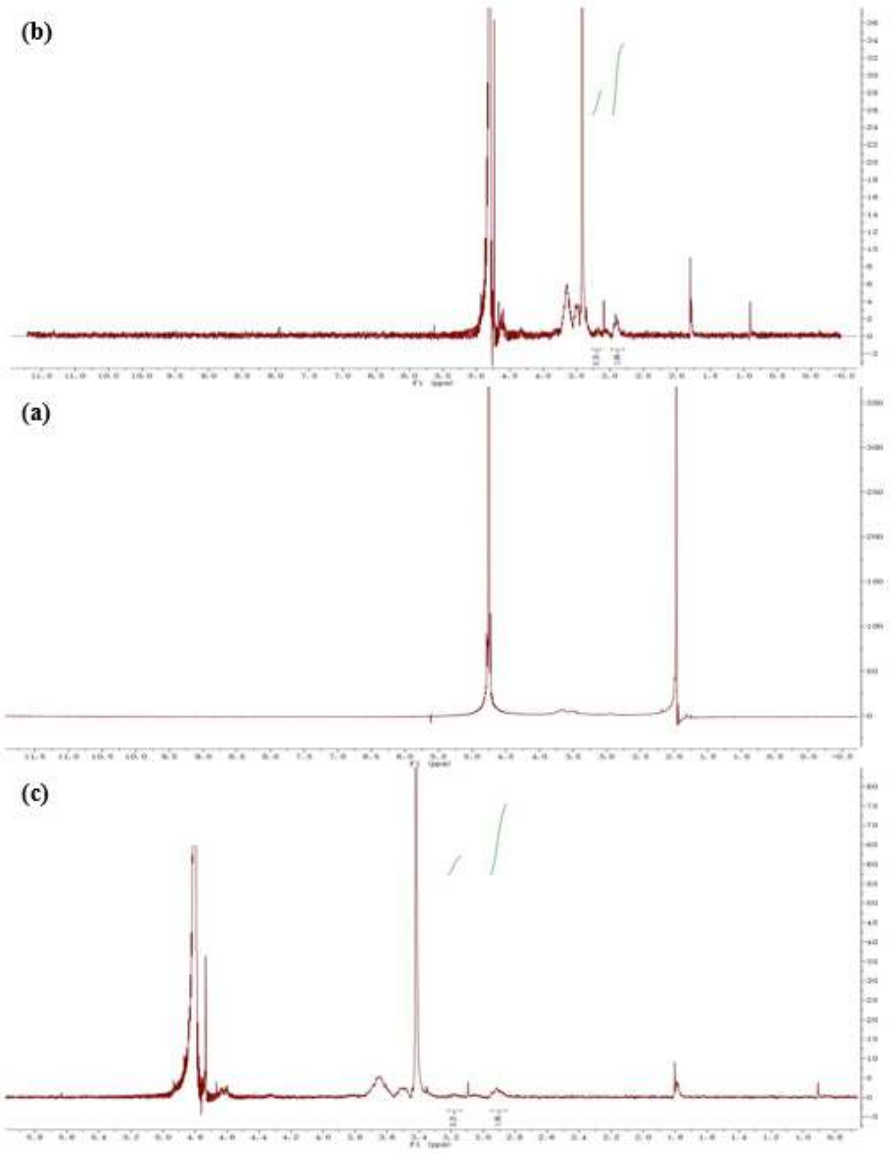

Fig. 3.3. ^{1}H NMR spectra of HMWCH-PEG, MMWCH-PEG, LMWCH-PEG after heating to 70°C then cooled to room temperature

3.3.4 Solution Preparation

Solution of α-lac was prepared by dissolving lyophilized protein powder in 6mM acetate, 3mM imidazole buffer at pH 3.5 for 4 hours at ambient temperature. Solutions of chitosan or CH-PEG samples were prepared by dissolving lyophilized powder

in 6mM acetate, 3mM imidazole buffer at pH 3.5 for 12 hours at ambient temperature before use. Solutions of protein and chitosan/CH-PEG were prepared from the stock protein and polysaccharide solutions by mixing at the desired proportions with 6mM acetate 3mM imidazole buffer (pH 3.5) for 2 hours. The total solid concentration of α-lac and chitosan (HMWCH, MMWCH, or LMWCH) in the final solutions was 0.036% (w/w). As addition of PEG to chitosan samples approximately tripled the molecular weight of HMWCH, MMWCH, and LMWCH (Table 3.1), mixed solutions were prepared with the same concentrations of α-lac but triple the concentration of polysaccharide. While this increased the total biopolymer concentration in solution, this maintained a consistent quantity of protein and chitosan in solution while simultaneously maintaining a consistent molar ratio between protein and the chitosan component, as it is indicated in Table 3.2. Final ratios, by weight-basis, between α-lac and the chitosan component (r value) were 10, 5, and 2.

Table 3.2.
Total solids content ratios in α-lac and copolymer mixtures in comparison of chitosan and PEGylated-chitosan with varying MW in this study

sample	r value	Total Solid Content w/w	sample	r value	Total Solid Content w/w
	10	0.036%		10	0.042%
α-lac and HMWCH	5	0.036%	α-lac and HMWCH-PEG	5	0.043%
	2	0.036%		2	0.056%
	10	0.036%		10	0.044%
α-lac and MMWCH	5	0.036%	α-lac and MMWCH-PEG	5	0.045%
	2	0.036%		2	0.061%
	10	0.036%		10	0.042%
α-lac and LMWCH	5	0.036%	α-lac and LMWCH-PEG	5	0.043%
	2	0.036%		2	0.055%

3.3.5 Colloidal Sample Characterization

ζ-Potential of α-lac, CH (HMWCH, MMWCH, LMWCH), CH-PEG (HMWCH-PEG, MMWCH-PEG, LMWCH-PEG), or solutions of protein and polysaccharide

complexes were determined from their electrophoretic mobility at ambient temperature (Malvern Zetasizer Nano ZS, Malvern Instruments, Worcestershire, U.K.).

Turbidity of α-lac and mixtures as a function of pH was also measured by a UV-Vis spectrophotometer (DU 730 Beckman Coulter, CA) at wavelength of 450 nm (Hirt et al., 2014; Du et al., 2016). The results of turbidity were presented as 100-T%, where T is the light transmitted through the sample in cuvette. Buffer of 6mM acetate, 3mM imidazole was used as blank reference.

Complex formation pH (pHc) of mixtures were used to detect the pH that soluble complexes started to form based on the method used by Mattison et al., 1995. These critical pH values were determined by the significant increase in the slope of light scattering intensity as a function of pH (ALV, Langen, Germany) as a functions of pH. The details of the methods are illustrated by Du et al., 2016.

Hydrodynamic radii of complexes formed by protein and polysaccharide mixture were determined by dynamic light scattering with a ALV-CGS3 goniometer (ALV, Langen, Germany) at an angle of 90 degrees. Hydrodynamic radii reported in the figures were calculated from the z-average diffusion coefficients using the StokesEinstein equation. Hydrodynamic radii of mixed α-lac/CH-PEG solutions were determined using the CONTIN algorithm within the instrument software (ALV, Langen, Germany). All samples were diluted in buffer until concentration dependence was no longer observed in order to eliminate multiple scattering effects. The details of this method was published by our previous study (Burchard, 1983; Du et al., 2016).

Cryo-Transmission electron microscopy (TEM) experiments were conducted to study the morphology of complexes formed by α-lac and MMWCH-PEG. The complex samples were diluted 1:1 by volume with buffer (6mM acetate, 3mM imidazole). About 3-4 L of diluted sample was deposed onto copper grids (400 mesh, Electron Microscopy Sciences). Then the sample was vitrified with liquid ethane. A Titan Krios cryo-electron microscope (FEI, Eindhoven, The Netherlands) was used with operation at 300 kV. A K2 Summit camera (Gatan) was installed with the microscope. Additional information can be found by Badwalk et al. (2016) and Gary et al. (2011).

Representative images shown were selected from approximate 1015 images from each sample.

3.3.6 Statistical Treatment

The results were presented as the average of duplicate or triplicate. Statistical significance was conducted by means of the students t-test. Displayed error bars represent the standard deviation from independent sample measurements.

3.4 Results and Discussion

3.4.1 Influence of pH on protein polysaccharide complex formation

Fig. 3.4 demonstrates pHc as a function of r of complexes formed with different MW of co-polymer before and after PEGylation. For co-polymers with higher MW (HMWCH-PEG and MMWCH-PEG), pHc values were significantly lower than the non-PEGylated complexes, which indicated that PEGylation favored complex formation at lower, less favorable pH values. This result is also in agreement with our previous study of complexes formed by α-lac and CMD-b-PEG, where the covalently-attached PEG induced complex formation at less favorable (i.e., higher) pH values (Du et al., 2016). However, for lower MW copolymer, the difference before and after PEGylation was not significant, which might due to the smaller size of co-polymer reducing the favorability of interaction prompted by the addition of PEG.

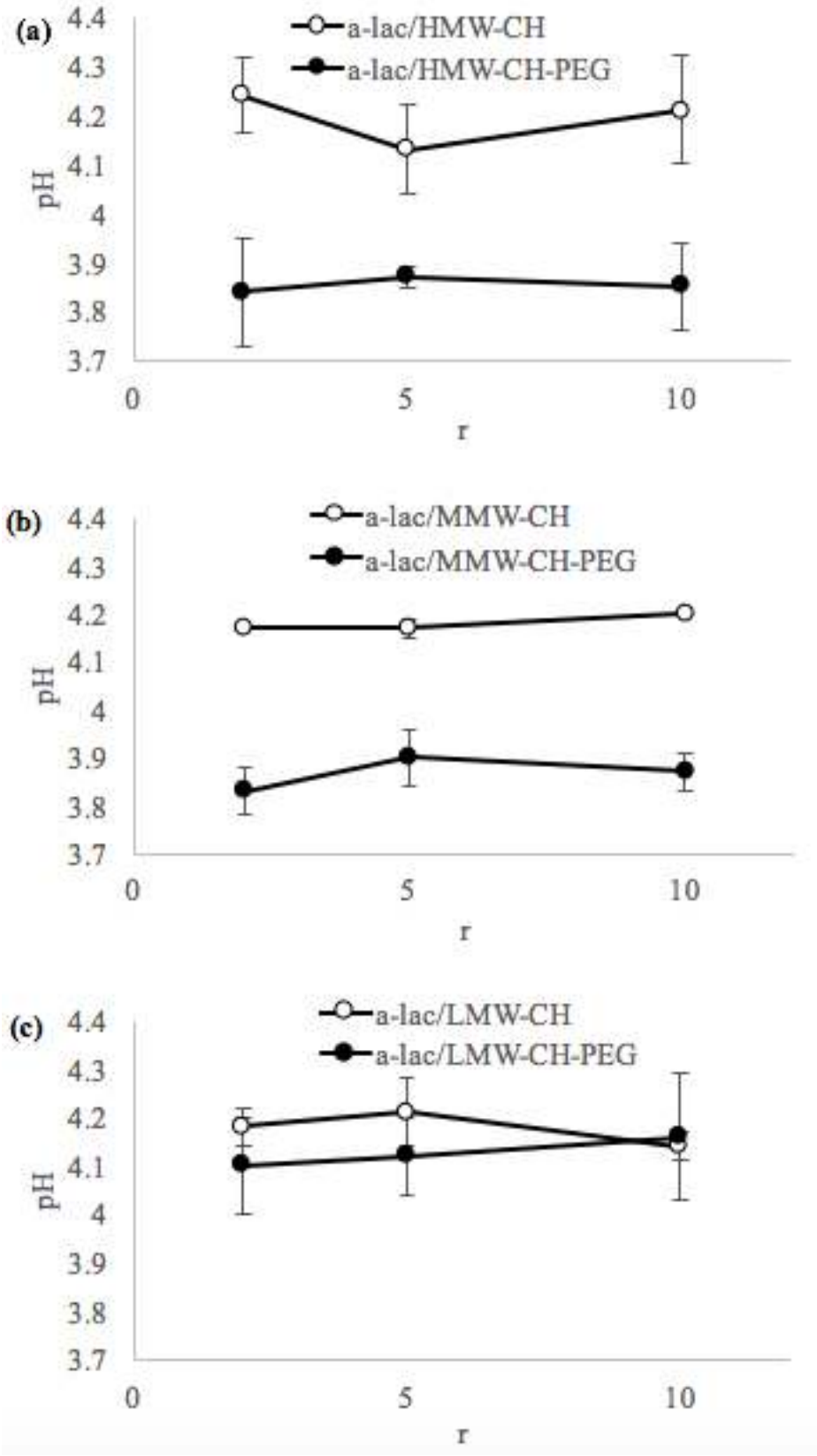

Fig. 3.4. pHc of complexes formed by α-lac and (a) HMWCH/HMWCH-PEG (b) MMWCH/MMWCH-PEG (c) LMWCH/LMWCH-PEG as a function of r

Fig 3.4 (a) shows the differences of the detected colloidal charges among α-lac and CH or CH-PEG of different molecular weight. With increasing pH, the α-lac charge became less positive and eventually net-negative at pH values above 4.5, consistent with previous findings of the proteins isoelectric pH (REF). This demonstrated the increasing quantity of exposed anionic residues on α-lac with increased pH, facilitating the possibility of electrostatic interaction with the positively-charged CH or CH-PEG samples.

Figures 3.4(b) and (c) describe the colloidal charge of mixtures of α-lac and HMWCH/HMWCH-PEG. Detected colloidal charge was less in magnitude than the polysaccharides, alone (Fig. 3.5a), but PEGylation did not significantly reduce the surface charge. For HMWCH-PEG at $r = 10$, sample surface charge was significantly diminished at higher pH, which might due to the saturation of protein to interact with CH-PEG. Mixtures of α-lac and MMWCH/MMWCH-PEG (Figure 3.5d, e) were insensitive to r with the exception of $r = 20$ for MMWCH-PEG in the region of pH 3.5-4.5. At this low pH range at $r = 20$, the colloidal charge resembled that of the original protein, likely reflecting that the high r allowed the charged of un-complexed protein to dominate the electrophoretic mobility signal during the measurement. With increasing pH, the colloidal charge of the mixture in Figure 3.5e became similar to MMWCH-PEG as the α-lac became associated within the copolymer complex. Reduced colloidal charge was also noted for LMWCH samples at $r = 10$ (Figure 3.5f) although this was not observed at the same ratio among mixtures with LMWCH-PEG (Figure 3.5g). In all cases, the significant positive charge of mixtures up to pH 7 (or pH 6 for HMWCH-PEG at $r = 10$) was a strong indication that complex formation indeed took place, as the interacting chitosan or chitosan-PEG chains would provide the necessary charges to not only interact with α-lac but also provide additional charges on the exterior of the colloidal assembly.

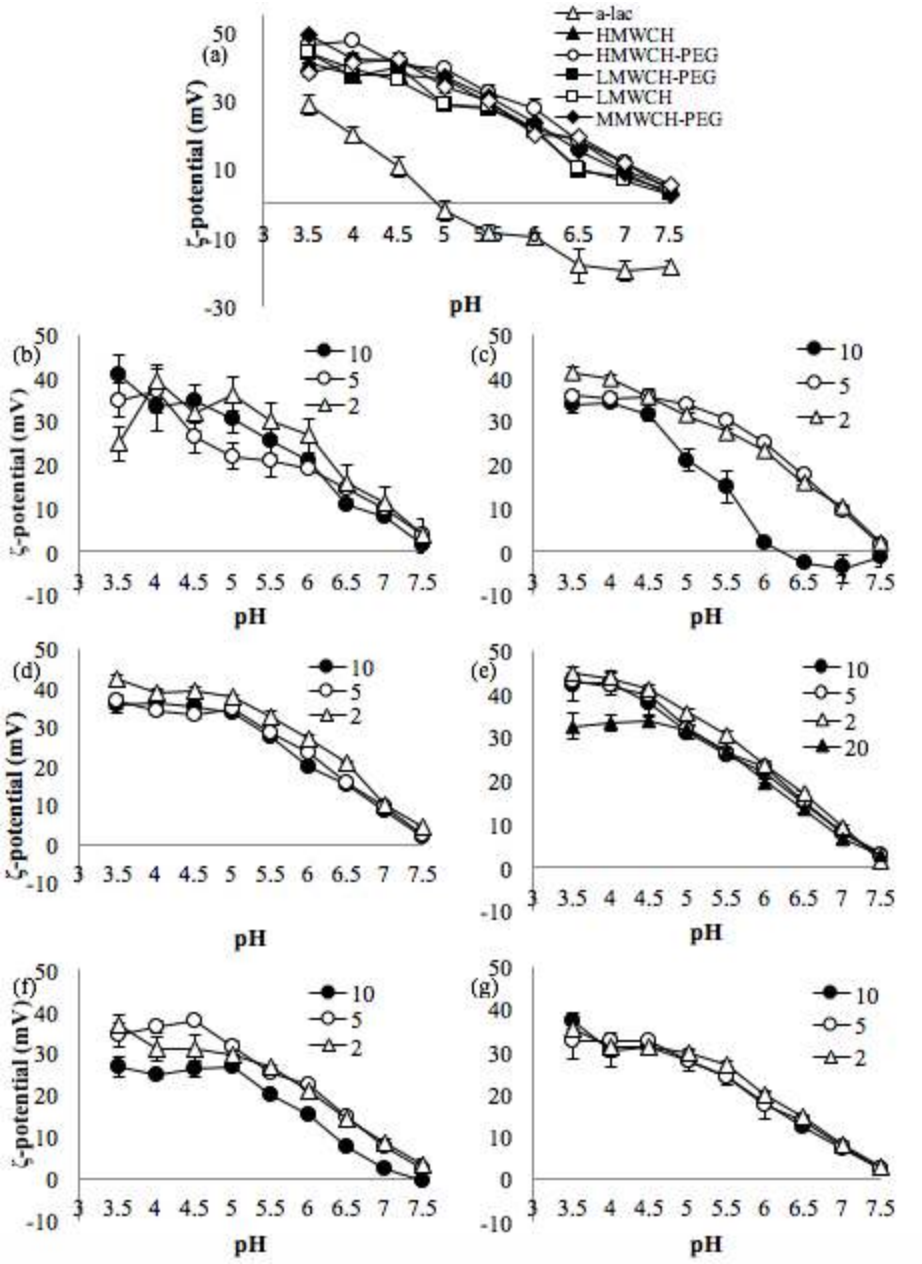

Fig. 3.5. ζ-potential as a function of solution pH of (a) individual polymers, complexes formed at different R-values by (b) α-lac and HMW-CH (c) α-lac and HMW-CH-PEG(d) α-lac and MMW-CH (e) α-lac and MMW-CH-PEG (f) α-lac and LMW-CH (g) α-lac and LMW-CH-PEG in 6mM Imidazole 3mM acetate buffer

3.4.2 Influence of Protein-Polysaccharide ratio on complex coacervation

Fig. 3.6 shows turbidity of complexes formed by different copolymer at different r, Turbidity of complexes formed by either HMWCH or HMWCH-PEG are not different from each other (Figure 3.6a), while the turbidity of complexes involving MMWCH and LMWCH was significantly reduced following PEGylation (Figure 3.6b,c). This showed that with the attached PEG, the chitosan-protein complexes are either smaller in diameter, reduced in number, or significantly less dense (reduced average refractive index). Smaller diameter in the samples which were PEGylated could be due to smaller complexes, or less clustering/aggregation of the complexes in suspension.

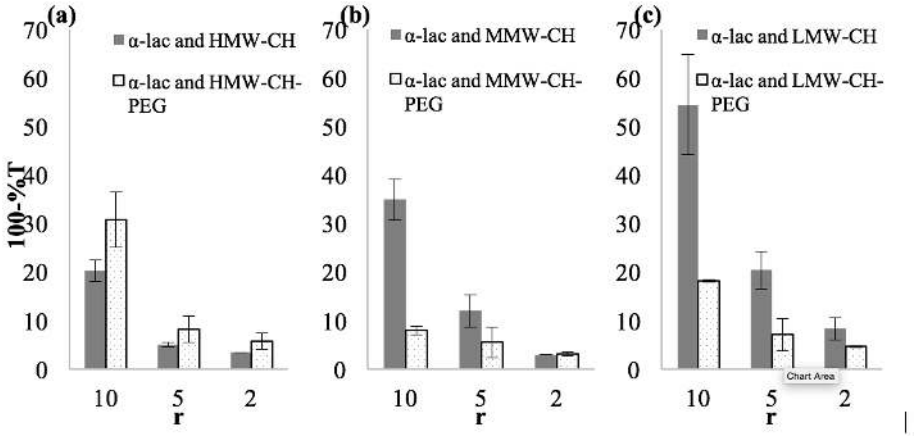

Fig. 3.6. Turbidity as a function of r value of complexes formed by (a) α-lac and HMWCH/HMWCH-PEG, (b) α-lac and MMWCH/MMWCH-PEG, (c) LMWCH/HMWCH-PEG of different r values at pH of 5.8

3.4.3 Complex hydrodynamic radius

Similar to the complexes formed by α-lac and CMD/CMD-b-PEG, there are three peaks detected by dynamic light scattering: the fast mode with size under 10nm, slow mode with size between 10-100nm, and slower mode with size higher than 100nm, and these peaks are presented in Fig. 3.7. The smallest peaks is smaller probably unreacted protein or polysaccharide that did not contribute to the formation of com-

plex, while the large dominating peak, even though it occupies a large percentage in the figure, but it is not the majority of the particle since these figures are unweighted. Also, if the large peak is the major particles, we should not be able to detect any slow and fast mode particles. In Fig. 3.7 (b) we did find the particles larger than 100nm, but their structure is more similar to the aggregate of copolymer rather than complexes. For these reasons, we are focused more on the middle peak, which is the formation of complexes by α-lac and MMWCH/MMWCH-PEG.

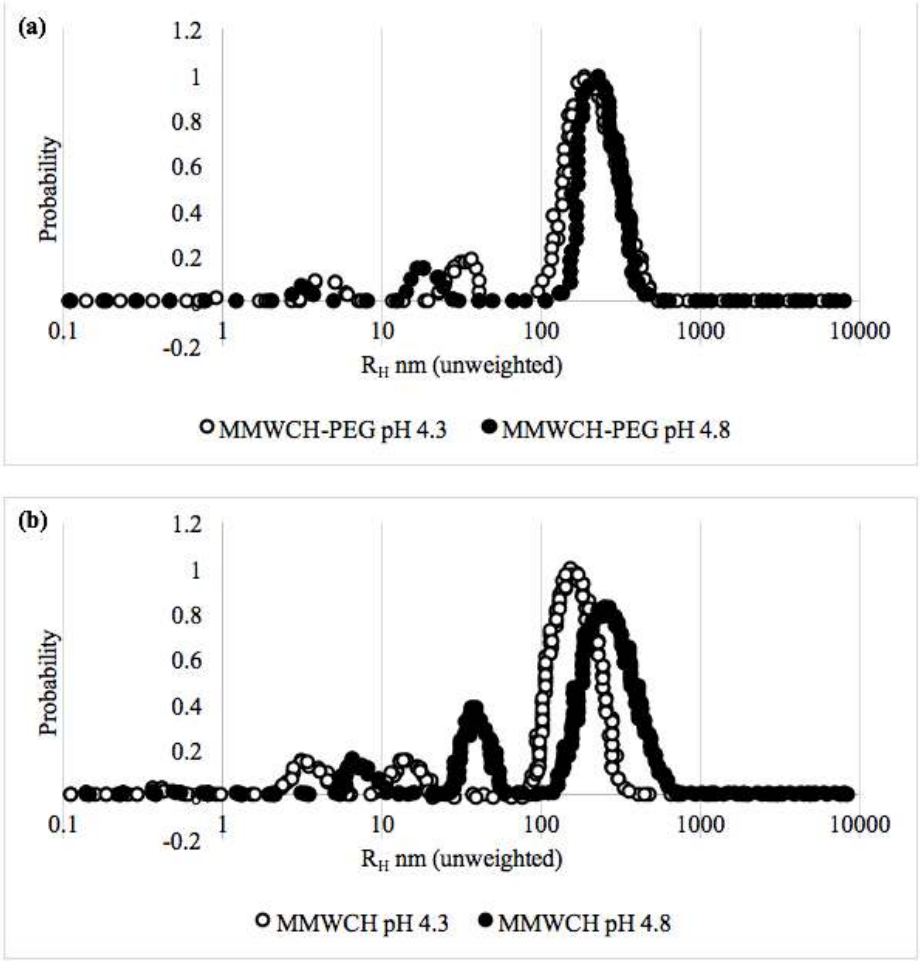

Fig. 3.7. Particle Size Distribution on hydrodynamic radius of complexes involving (a) MMWCH and (b) MMWCH-PEG at r=2, pH 4.3, 4.8

Figure 3.7 describes the determined influence of pH and rs on slow mode hydrodynamic radius (R_H) of the complexes formed by α-lac and MMWCH/MMWCH-PEG. From pH 3.8 to pH 5.8, there was no significant linear relationship of RH with pH. For α-lac complexes with MMWCH at $r = 10$, RH is significantly higher than the other samples (Figure 3.8a), which might due to the higher concentration of protein in the system. However, complexes of with MMWCH-PEG at $r = 10$ were not significantly larger (Figure 3.7b). It is possible that the covalently-attached PEG reduced the size of complexes at higher r by the PEG chains presenting themselves on the exterior of the complex, providing repulsive interactions to limit further growth into larger assemblies. However, more studies would be needed to confirm.

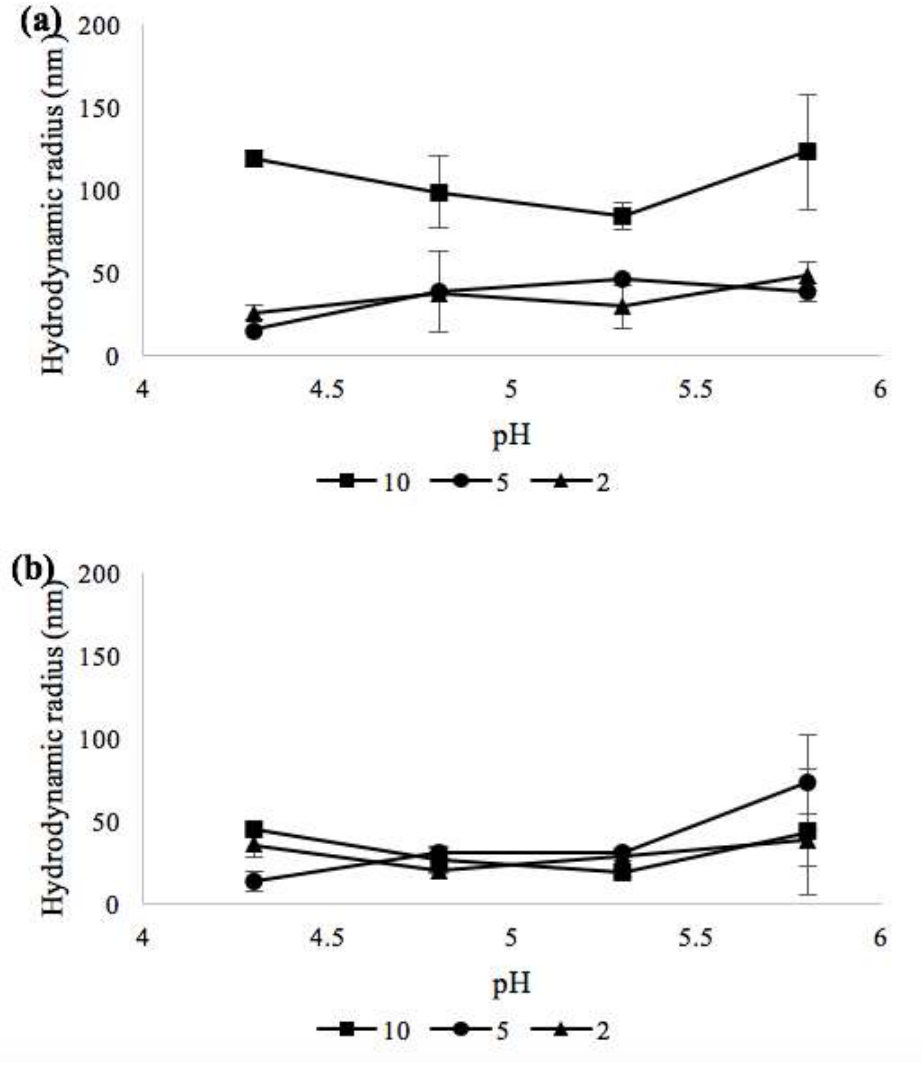

Fig. 3.8. Effect of pH on radius of complexes involving (a) MMWCH and (b) MMWCH-PEG with varying r

Figure 3.9 illustrates the effect of MW on the formation of complexes at a fixed r value of 2. There was a slight tendency for the hydrodynamic complexes with HMWCH-PEG to increase with increasing pH (Figure 3.9a). However, these values were not significantly different from determined sizes of complexes with MMWCH-PEG at pH 5.8 (Figure 3.8b), indicating that there was unexplained variability in the measurements taken at higher pH. No differences were observed between complexes

with MMWCH-PEG or LMWCH-PEG in these conditions. Differences were also not observed in the determined hydrodynamic radii of any of the complexes with non-pegylated chitosan of differing molecular weight for $r = 2$ (Figure 3.9b).

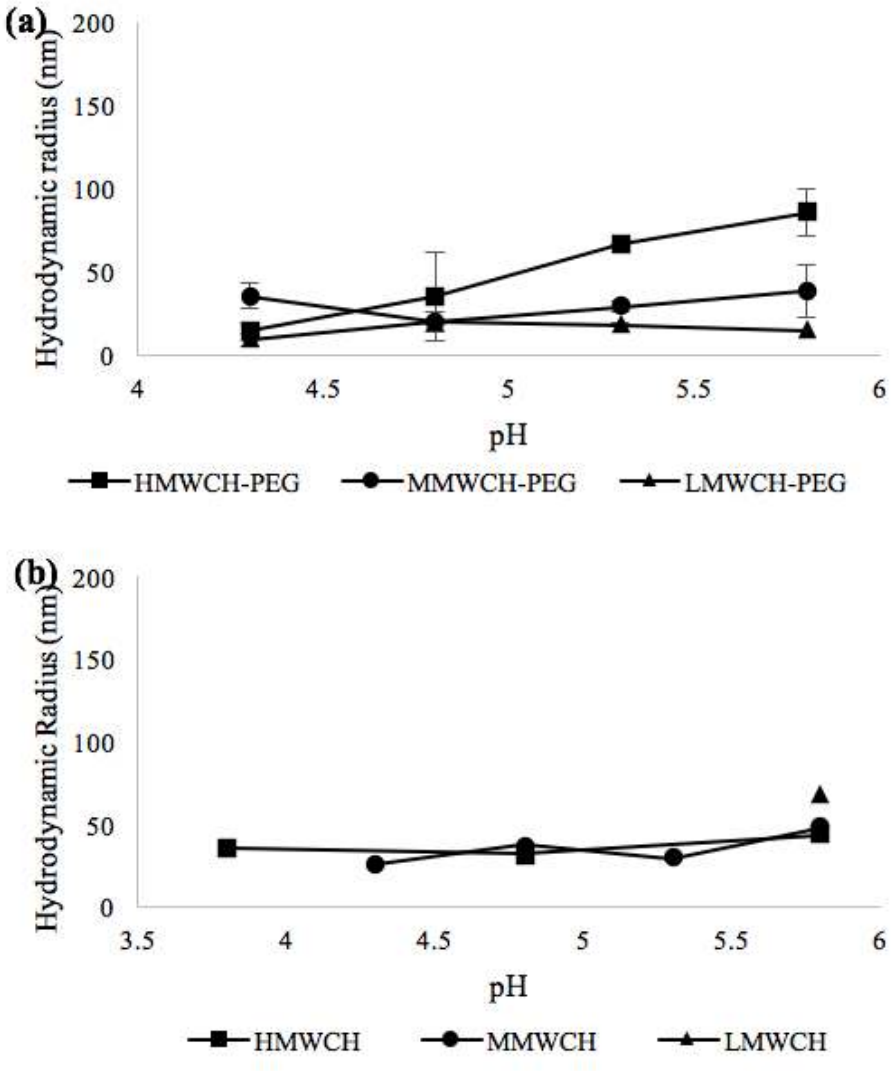

Fig. 3.9. Effect of pH on radius of complexes involving PEGylated chitosan at different molecular weight ($r = 2$)

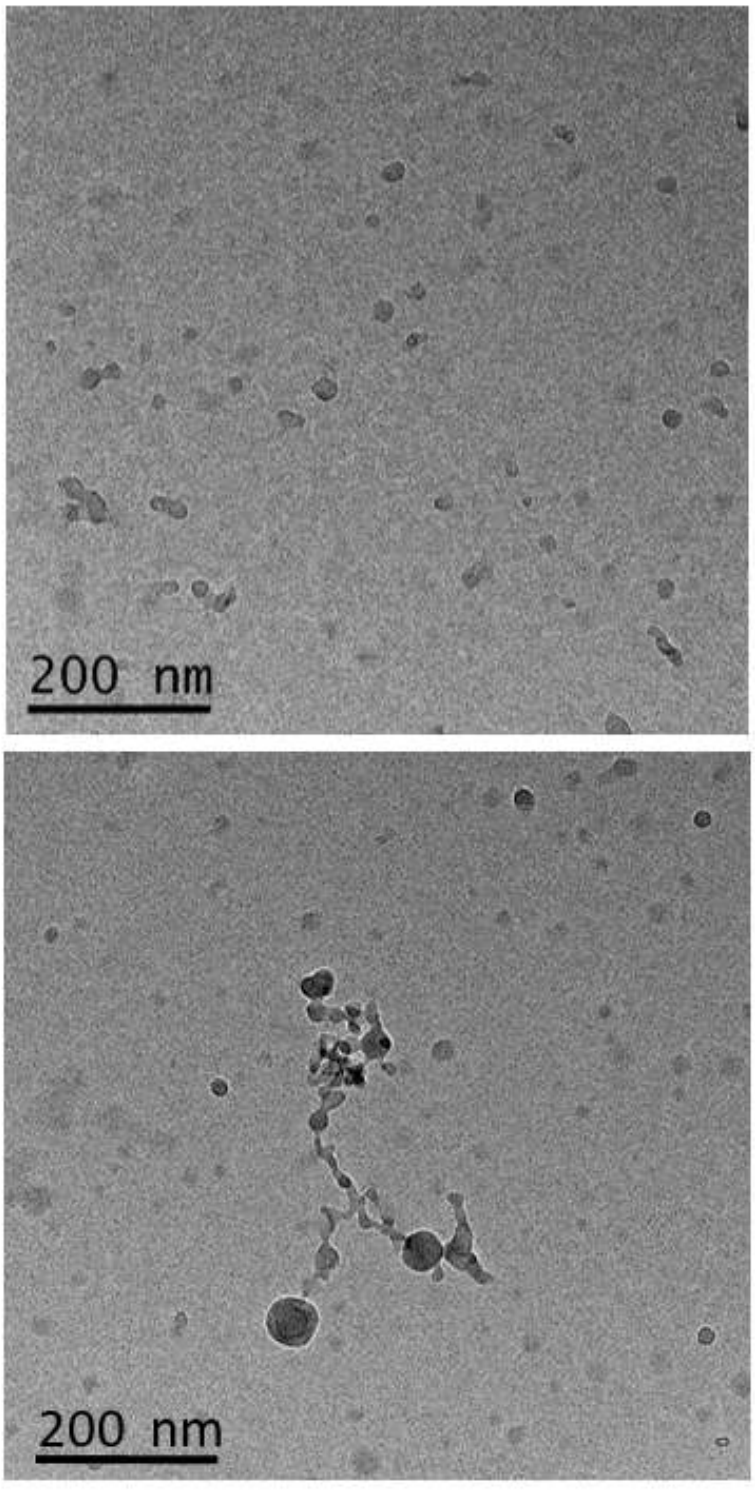

Fig. 3.10. Cryo-transmission electron micrograph of α-lac and MMW-CH-PEG($r = 2$)pH4.3

3.4.4 Visual Characterization of Complexess

The Cryo-TEM images in Fig. 3.10 show the morphology of complexes between α-lac and MMWCH-PEG at $r = 2$ and pH 4.3. The apparent diameter of complexes in the images are around 10-20nm, which is slightly smaller than the hydrodynamic diameters determined by DLS (Figures 3.8 & 3.9). The differences between Cryo-TEM and DLS results might due to the scattering of non-spherical structure in DLS or the inability to resolve individual chains of PEG on the periphery of the complexes due to inherent limitations of Cryo-TEM. Some big assemblies were also observed (Figure 3.10b) that appeared to be a clustering of the complexes attached together by a fibrous substance. It was speculated that the fibrous substance was excess CH-PEG that was acting to bridge separate complex assemblies together. These large assemblies were also observed among α-lac complexes with carboxy-methyldextran-PEG (Chapter 2).

3.4.5 Conclusions

Interactions between α-lac, chitosan and CH-PEG were confirmed by a shift in the electrophoretic mobility of the protein to less negative values as the pH was increased above its isoelectric pH. Light scattering intensity verified that complex formation for α-lac/CH and α-lac/LMWCH-PEG occurred at pH values of 4.1-4.2, while α-lac/HMWCH-PEG and α-lac/MMWCH-PEG occurs at pH values around 3.8. Above pH 5.0, turbidity significantly increased for both complexes, indicating a phase-separation at a similar pH range, yet the turbidity of α-lac/CH-PEG samples were significantly less than α-lac/CH samples. Turbidity of MMW and LMW complexes was significantly reduced by PEGylation at three different r values. Hydrodynamic radii of α-lac/MMWCH-PEG complexes ranged from 10 to 40 nanometers with additional peaks demonstrating the presence of larger assemblies of several hundred nanometers. Despite larger hydrodynamic radii of α-lac/HMWCH-PEG complexes, there was little indication that ratios of protein-polysaccharide, molecular weight, or

even presence of PEG has a significant impact on the size of complexes with protein at the studied pH values. However, the reduced turbidity of complexes with covalent attachment of the PEG chain implied that there is a reduction in number or internal density of the complexes. This phenomenon needs to be verified in further experiments with these complexes, as well as other similar complex structures. Furthermore, techniques need to be envisioned to prepare these complexes without formation of larger clusters, which appear to form due to bridging interactions between complexes by excess copolymer.

3.5 Appendices

Appendix A Chromatographs of Chitosan with High, Middle and Low Molecular Weights

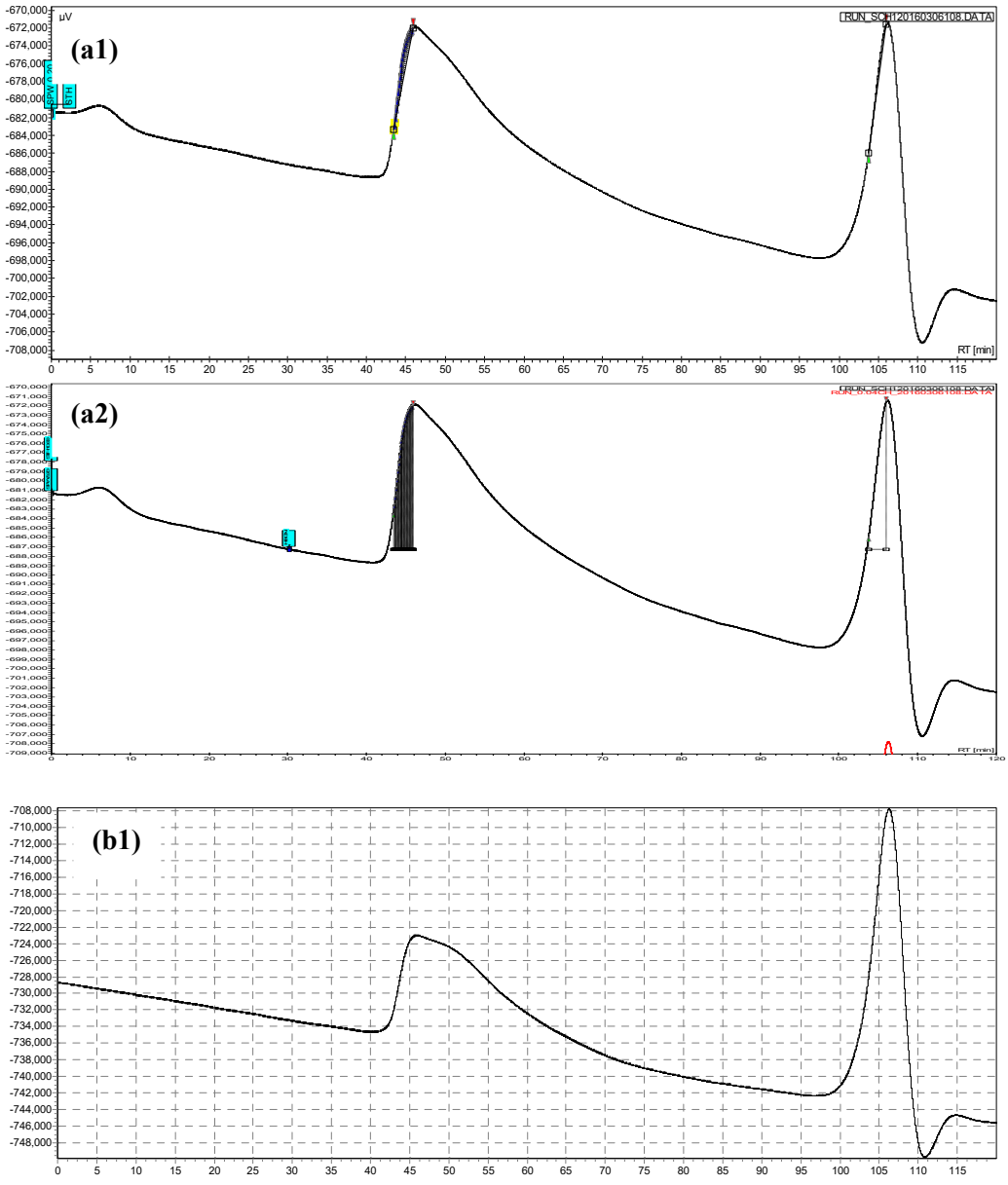

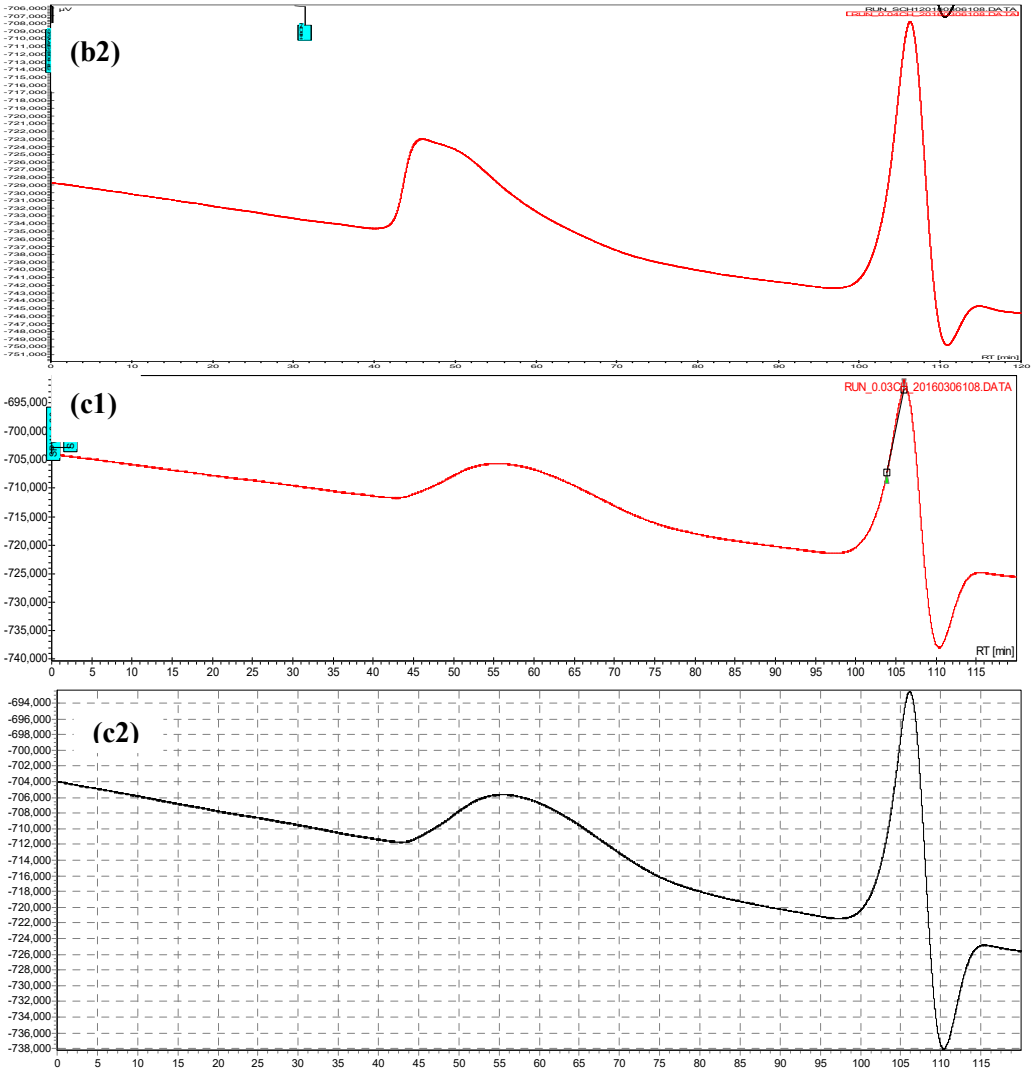

Figure 1. SEC graphs of HMWCH (a1, a2), MMWCH (b1, b2), LMWCH (c1, c2) refractive Index as a function of retention time (min) in duplicate

Appendix B ^{1}H NMR spectra of (a)HMWCH, (b)MMWCH, and (c)LMWCH after heating to 70°C then cooled to room temperature in duplicate or triplicates

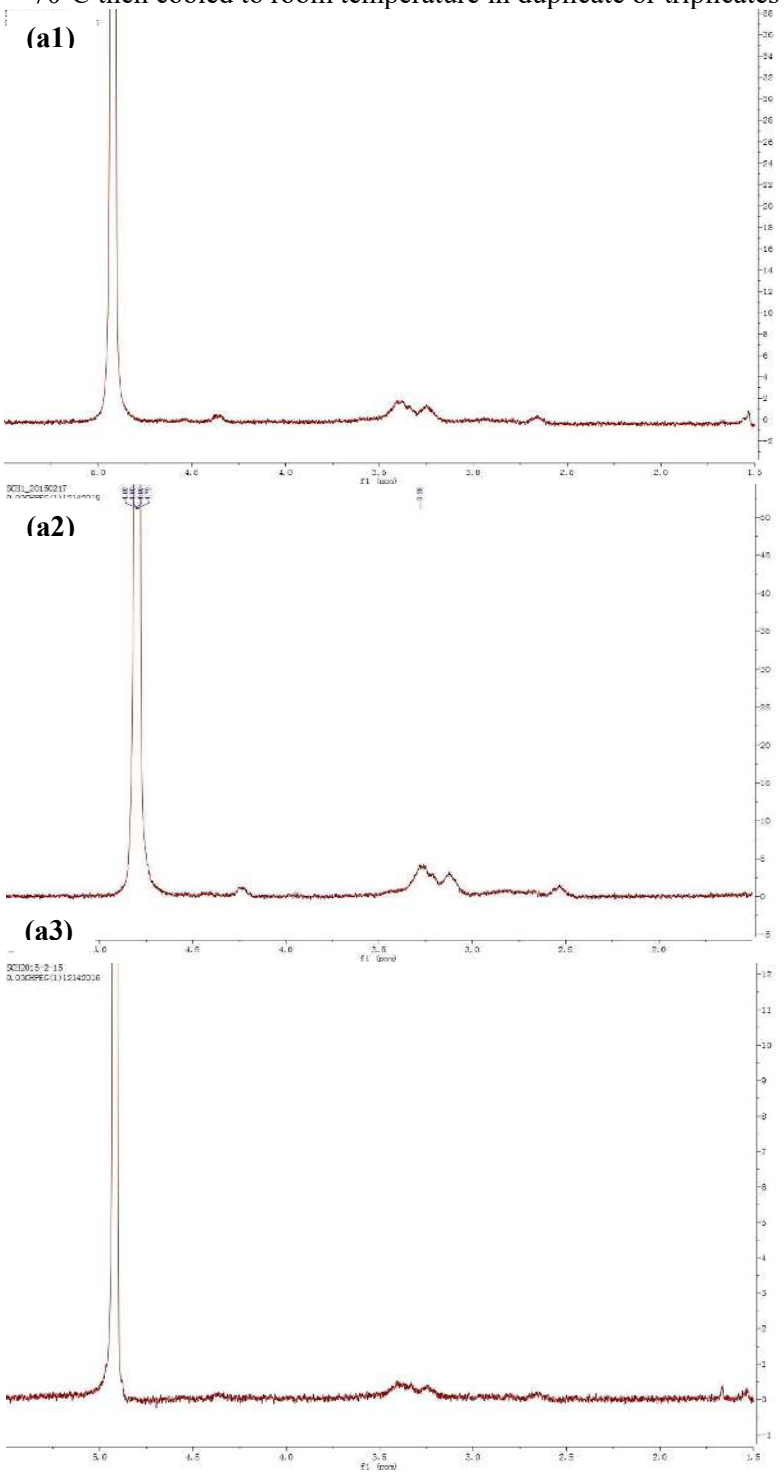

(b1)

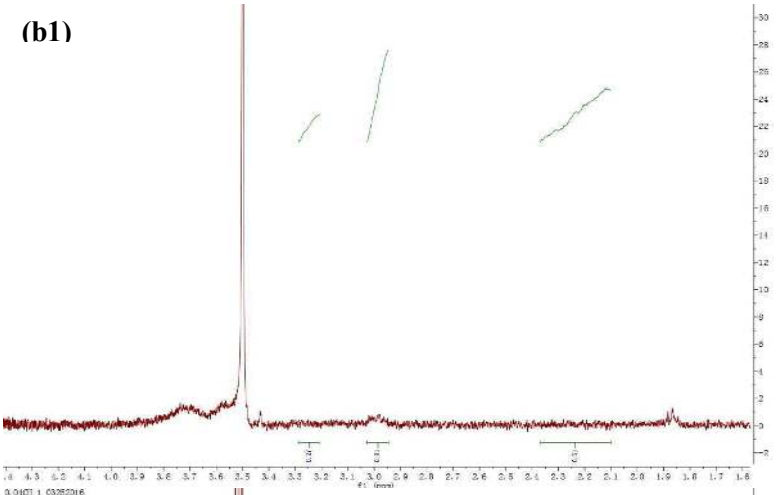

(b2)

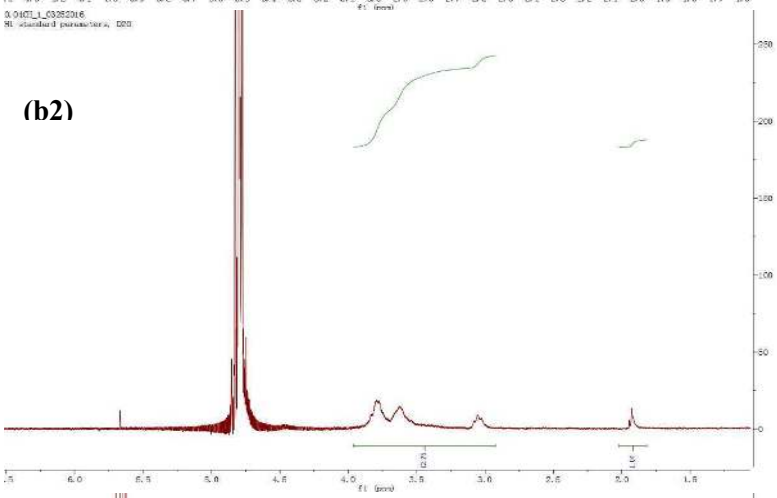

(b3)

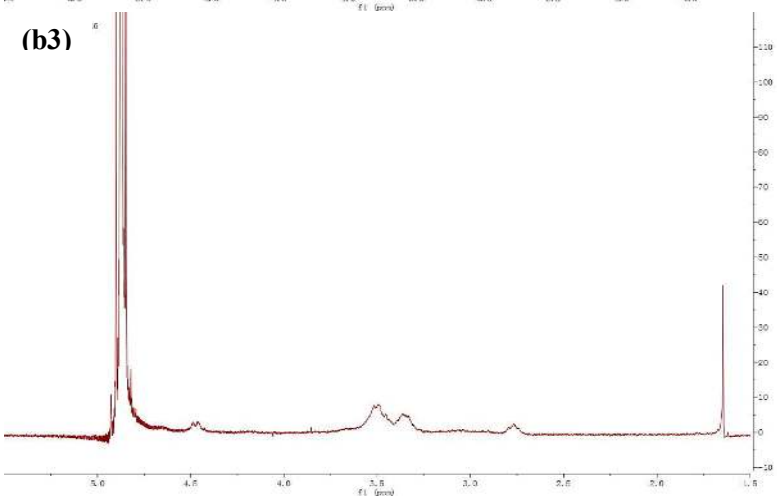

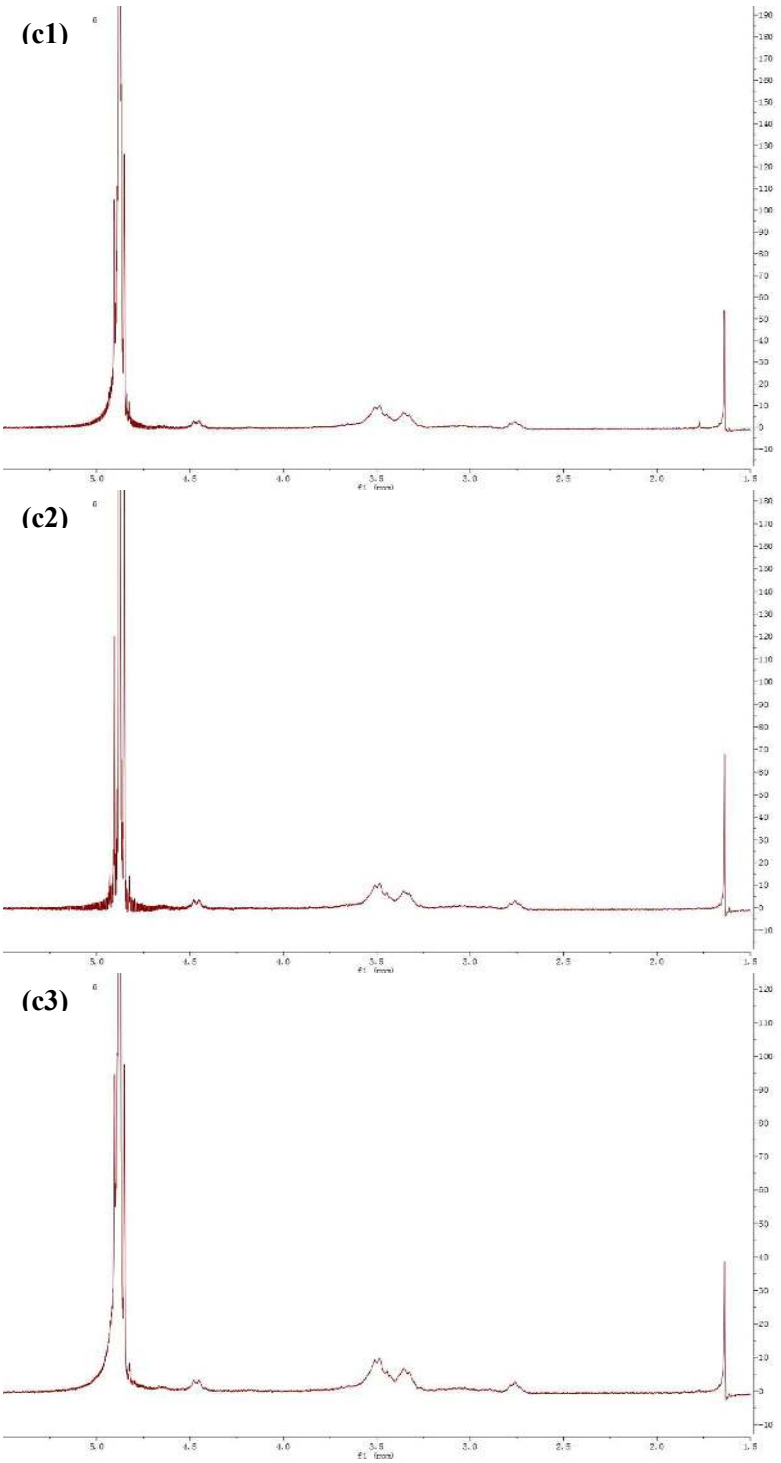

Figure 2. ^{1}H NMR spectra of (a1, a2, a3) HMWCH, (b1, b2, b3) MMWCH, and (c1, c2, c3) LMWCH after heating to 70 ^{o}C then cooled to room temperature.

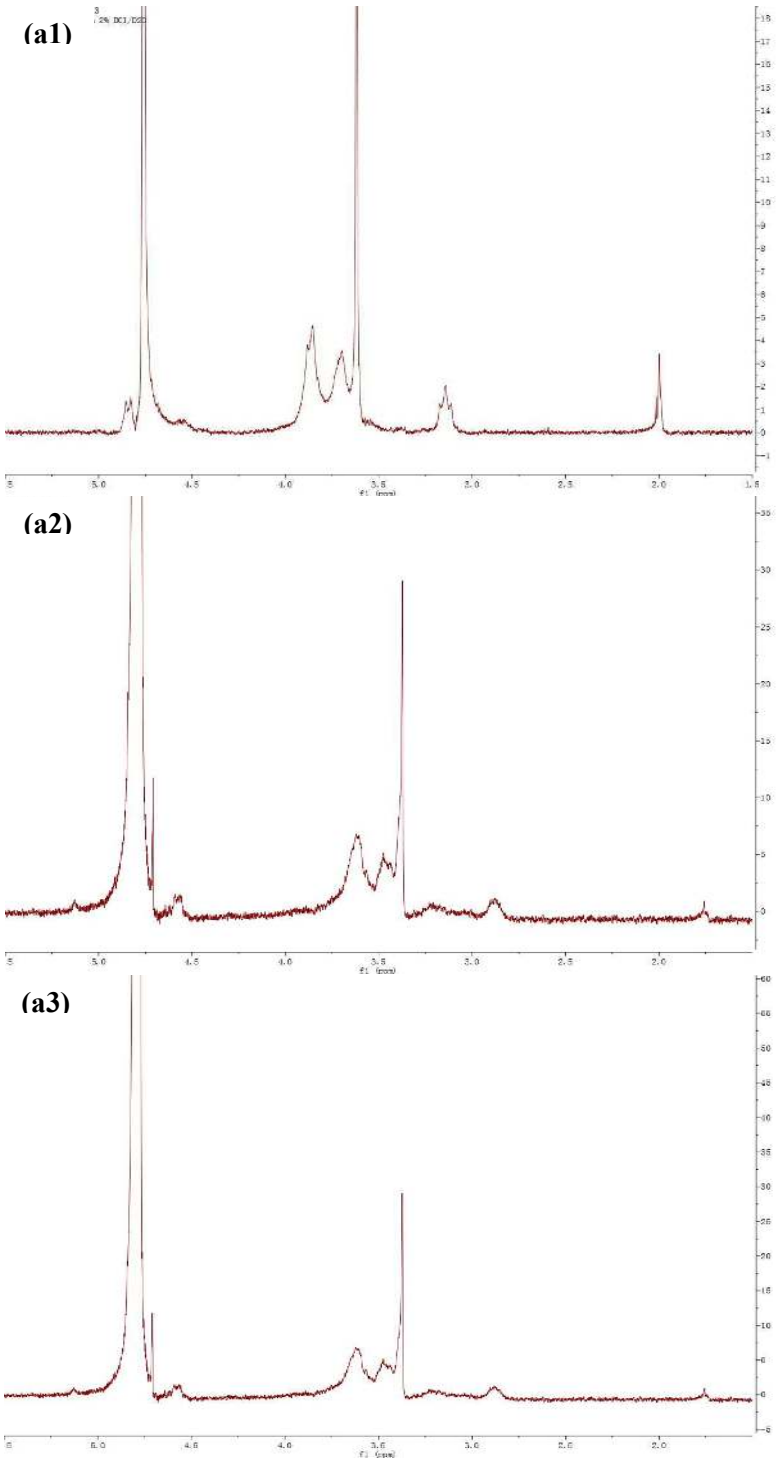
(a1)
(a2)
(a3)

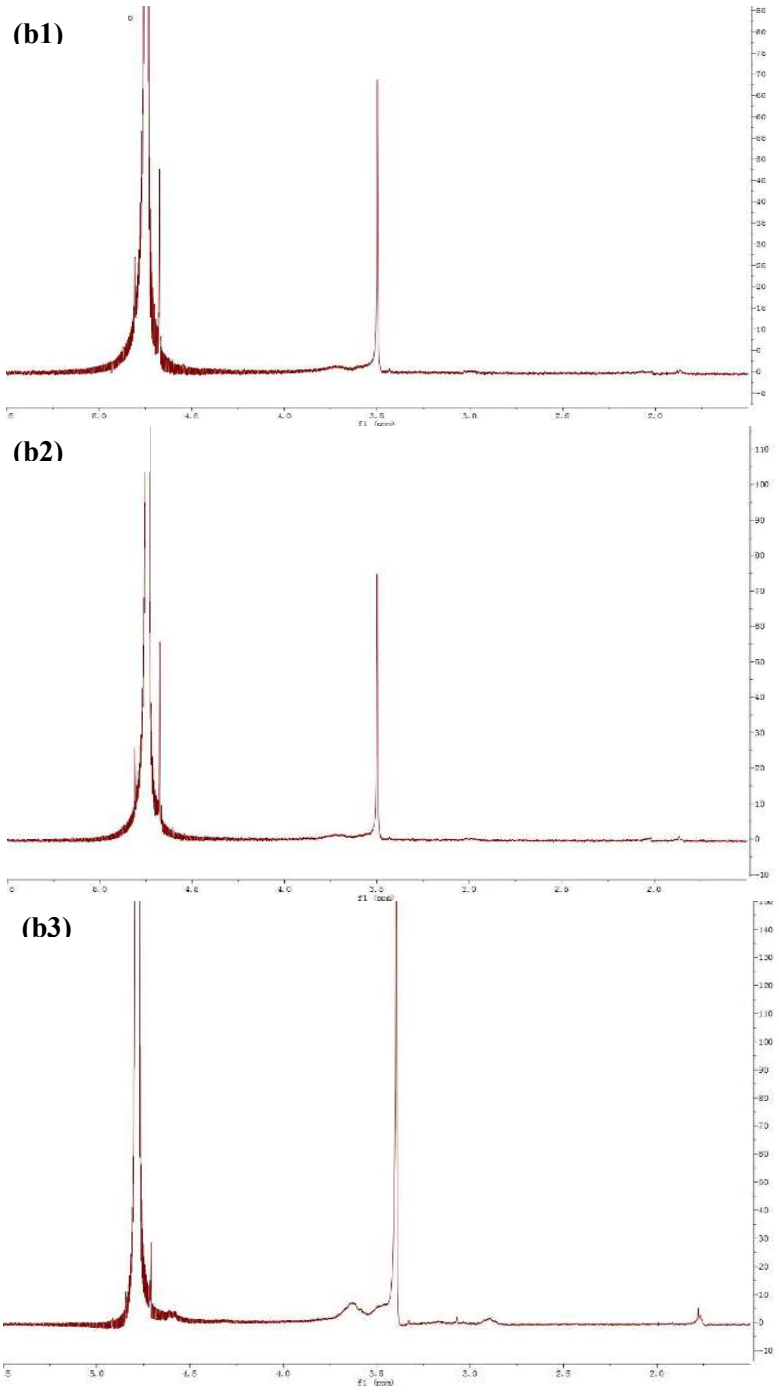
(b1)
(b2)
(b3)

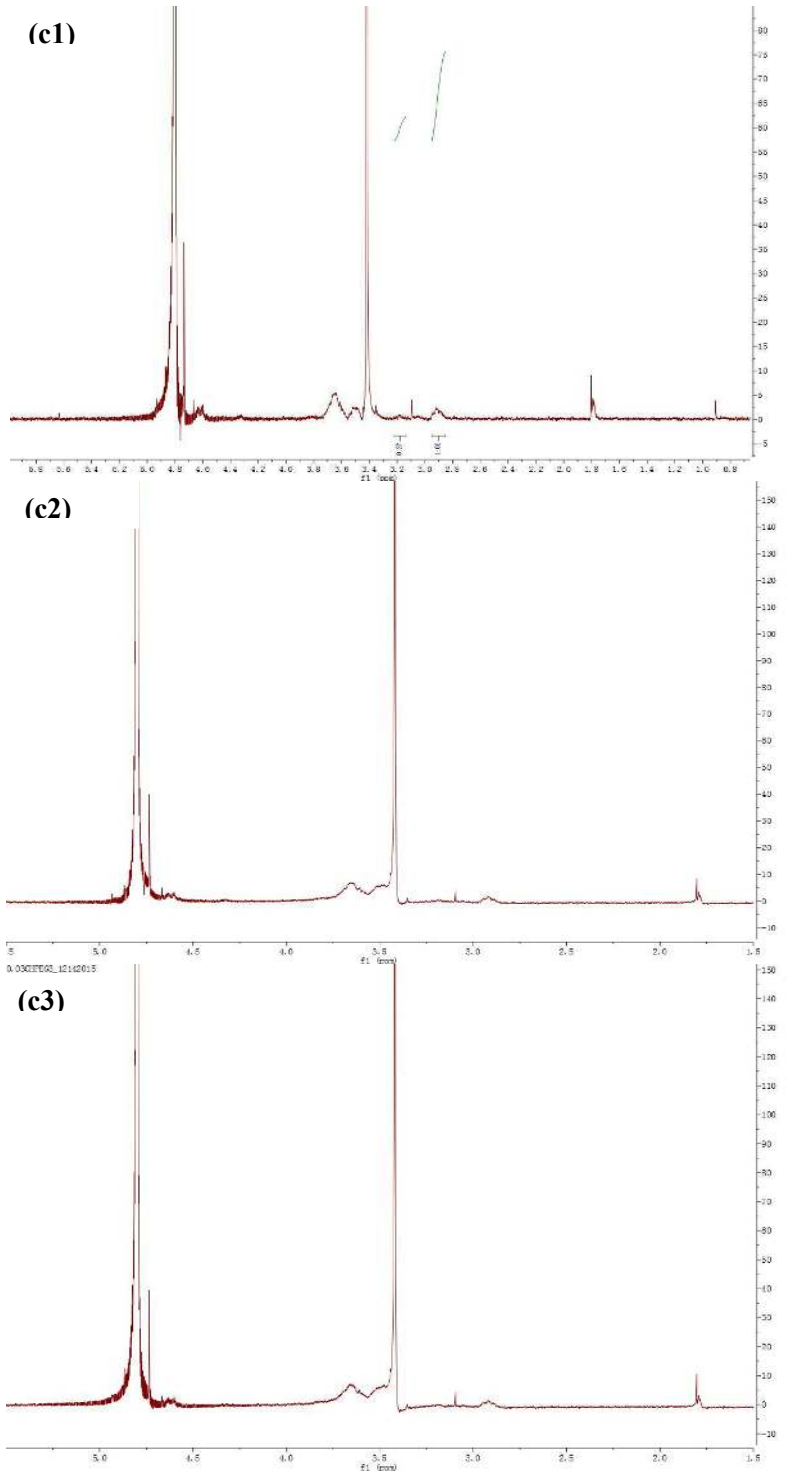

Figure 3. ^{1}H NMR spectra of (a1, a2, a3) HMWCH-PEG, (b1, b2, b3) MMWCH-PEG, and (c1, c2, c3) LMWCH-PEG after heating to 70 ^{o}C then cooled to room temperature.

Appendix C Complex formation pH (pHc) and phasing separation pH (pHϕ) determination

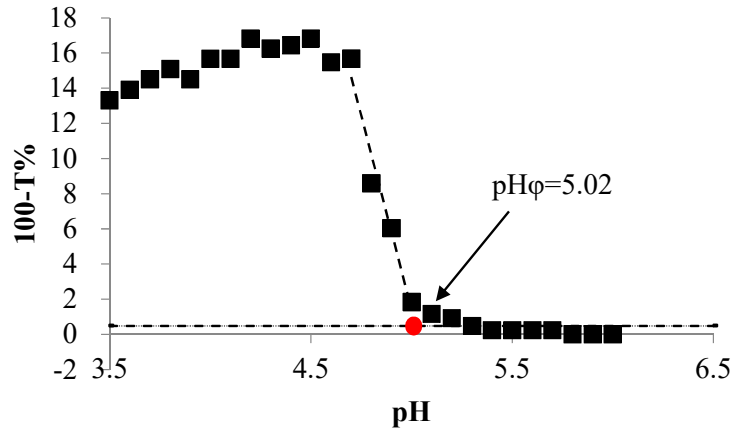

(a)

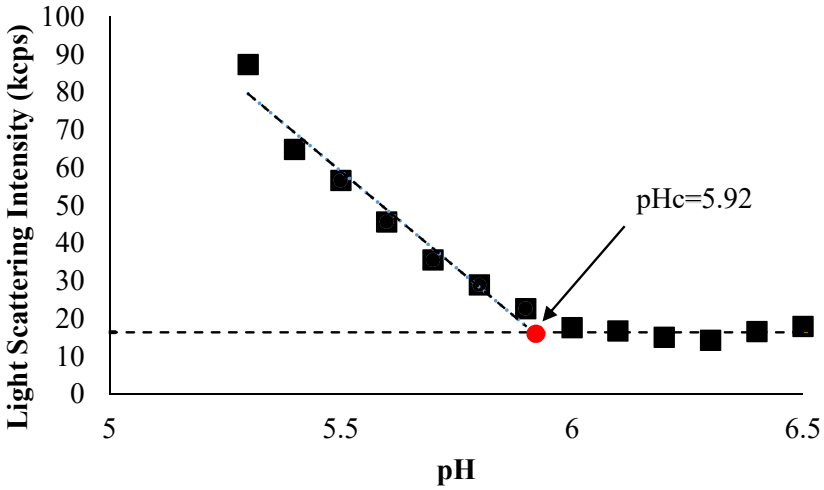

(b)

Figure 4. (a) Turbidity (100-T%) vs pH and (b) Light scattering intensity vs pH as example for pHc and pHϕ determination of complexes formed by α-lac and CMD-*b*-PEG (*r*=5)

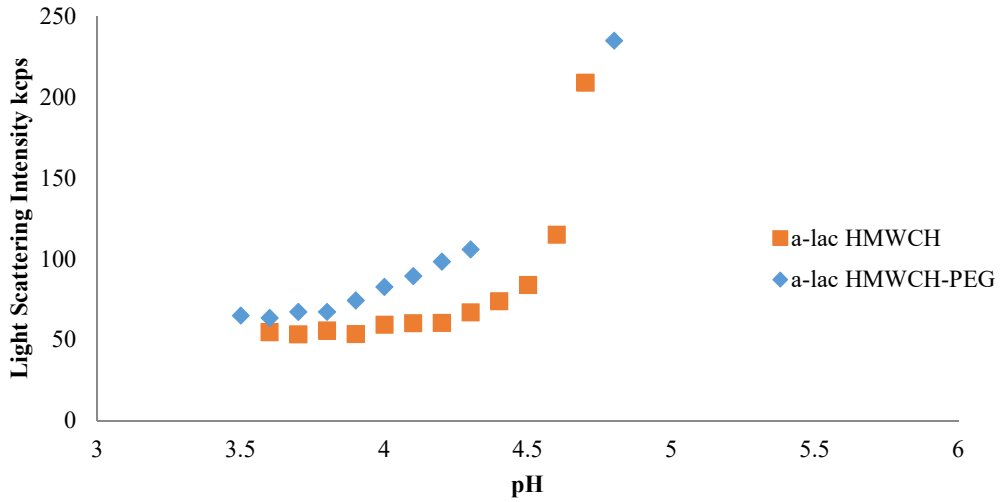

Figure 5. Light scattering intensity as a function of pH of complexes formed by α-lac and HMWCH/HMWCH-PEG (*r*=10)

4. PHYSICAL PROPERTIES OF HEAT-INDUCED AGGREGATES FROM α-LACTALBUMIN WITH CHITOSAN OR CHITOSAN COPOLYMER

4.1 Abstract

Hypothesis

α-Lactalbumin (α-lac) and polysaccharide chitosan (CH) or chitosan-grafted-poly (ethylene glycol) (CH-PEG) are able to form complexes at pH above 4.3. Based upon previous findings, heat treatment of proteins near their isoelectric pH yields nanometer-scale spherical aggregates if the protein is interacting with a charged polysaccharide (Jones et al., 2009). It is hypothesized that the presence of a PEG chain attached to the polysaccharide can stabilize complexes of α-lac/CH-PEG during heating, influencing the structure of the resulting aggregates. Similarly, CH molecular weight (MW) is proposed to impact the size and structures of aggregates formed by α-lac and CH/CH-PEG.

Experiments

Solutions of protein and CH or CH-PEG were mixed with different protein to polysaccharide ratios (r-value) and polysaccharide molecular weight. Complexes formed by base titration of mixed solutions and samples were collected at pH 3.8, 4.3, 4.8, 5.3. Complexes were then heated for 20 min at temperature of 70 ^{o}C to form aggregates, referred to as "microgels" based upon earlier findings on the internal structure of the small spherical aggregates (Murphy et al., 2015). Characterization of microgel samples using light scattering (DLS), electrophoretic mobility, turbidimetry, and atomic force morphology (AFM) were included in this study.

Findings

Microgel formation among α-lac, chitosan or CH-PEG was confirmed by increased turbidity, AFM morphology, and DLS. Reduction in turbidity of PEGylated samples was observed among samples with higher r- and pH-values when compared to those made from non-pegylated samples, indicating these microgels were either smaller in size, lower in amount, or less in density. However, no significant influence of chitosan molecular weight or r-value on hydrodynamic radius of microgels was observed, indicating that PEG chains likely impacted only the number of formed microgels. This result may relate to a stabilizing effect of the PEG chain, preventing some of the aggregation during formation of microgels.

4.2 Introduction

As mentioned in chapter 3, complexation between biopolymer α-lac and CH or CH-PEG was verified and characterized as the pH of the solution was increased. And the physicochemical properties of these complexes can be altered through pH, molecular weight of CH/CH-PEG, and protein/polysaccharide ratios (r-value). A previous study proved that complex coacervates formed by α-lac and chitosan has denaturation temperature higher than α-lac itself, which shows a stabilization effect of complexation with the polysaccharide (Lee and Hong, 2009). Aggregates formed by -lactoglobulin and chitosan was also studied by Hong and McClements (2007), with confirmation that the resulting aggregate particles can be formed by heating the mixture of -lactoglobulin and chitosan under controlled condition. Based on the studies in chapter 3 and the distinguished pH regions reviewed by Jones and McClements (2010); Weinbreck et al. (2002), when α-lac is mixed with chitosan in low pH condition (¡3.8), no complex is formed. With slow titration with alkali solution, the initial formation of soluble complexes will start, followed by coacervation, then precipitation at high pH as the polysaccharide becomes insoluble. Previous studies of -lactoglobulin (b-lac) shows that heating treatment above the denaturation tem-

perature of protein will release the unfolding of proteins in to the surrounding with exposure of hydrophobic residues, and therefore promote the cross-linking between particles composed of proteins and polysaccharides through hydrophobic attraction, (Bellogque and Smith, 1998; Jones and McClements, 2011), resulting in stable complexes. A-lac has similar physicochemical properties as whey protein will promote formation of stable complexes. The purpose of this study is to understand the influence of thermal treatment on complexes composed of α-lac with either CH or CH-PEG as a function of pH, polysaccharide molecular weight, and r-value. Aggregates formed after heat treatment were characterized for their surface charge, particle size, morphology, and turbidity in aqueous suspensions.

4.3 Materials and Methods

4.3.1 Materials

High purity chitosan which was directly used as high molecular weight chitosan (HMWCH) with a determined molecular weight of 113 kDa (see Chapter 3). Depolymerized chitosan was obtained by nitrite-induced hydrolysis of HMWCH to achieve a medium (MMWCH) and low (LMWCH) molecular weight chitosan material with mean molecular weights of 76kDa and 8.9kDa, respectively. Poly(ethylene glycol) (PEG) was then covalently attached to each chitosan sample in order to obtain HMWCH-PEG, MMWCH-PEG, and LMWCH-PEG (see Chapter 3). A-lac was kindly donated by Davisco Food International from Le Sueur, MN. a-Lac was further purified for removal of minerals, with details mentioned in chapter 2. Chemicals including acetic acid, sodium hydroxide, sodium acetate, imidazole, hydrochloride acid, were purchased from Sigma-Aldrich (St. Louis, MO). Physical data, including molecular weight of each sample and degree of deacetylation of the chitosan may be found in Table 3.1 of Chapter 3.

4.3.2 Solution Preparation

Buffer solution was prepared with 6mM acetate and 3mM imidazole at pH 3.5. Solution of α-lac was prepared by dissolving lyophilized protein powder in buffer for 4 hours at ambient temperature. Solutions of CH or CH-PEG samples were prepared by dissolving lyophilized powders in buffer for 12 hours at ambient temperature. Mixtures of α-lac and either CH or CH-PEG were prepared from stock solutions and buffer to achieve desired concentrations and r-values, which are outlined in Table 3.2 (see Chapter 3). The complexes were formed by base titration method using 1N and 0.1 N NaOH solutions dropwise by 1-200 L Eppendorf pipette. Solution were collected at pH 3.8, 4.3, 4.8, 5.3 with 1 mL aliquots taken and placed in a glass culture tube. Tubes were heated in a circulating water bath (Grant, Cambridge, U.K.) for 20 min at temperature of 70 ^{o}C. After heating, samples were submerged in cold water and stored under refrigeration until their characterization.

4.3.3 Colloidal Sample Characterization

ζ-Potential of α-lac, CH (HMWCH, MMWCH, LMWCH), CH-PEG (HMWCH-PEG, MMWCH-PEG, LMWCH-PEG), or solutions of protein and polysaccharide complexes after heating at pH 4.3, 4.8, 5.3, 5.8 were determined through electrophoretic mobility at ambient temperature (Malvern Zetasizer Nano ZS, Malvern Instruments, Worcestershire, U.K.).

Turbidity of α-lac and mixtures as a function of pH was also measured by a UV-Vis spectrophotometer (DU 730 Beckman Coulter, CA) at wavelength of 450 nm (Hirt et al., 2014; Du et al., 2016). The results of turbidity were presented as 100-T%, where T is the light transmitted through the sample in cuvette. Buffer of 6mM acetate, 3mM imidazole was used as blank reference. hydrodynamic radii (RH) of complexes formed by protein and polysaccharide mixture were determined by dynamic light scattering with an ALV-CGS3 light-scattering goniometer (ALV, Langen, Germany) at an angle of 90 degrees. RH reported in the figures were calculated from the z-

average diffusion coefficients using the StokesEinstein equation. RH of heated α-lac and CH/CH-PEG solutions were determined using the CONTIN algorithm within the instrument software (ALV, Langen, Germany). All samples were diluted in buffer until concentration dependence was no longer observed in order to eliminate multiple scattering effects. The details of this method was published by our previous study (Burchard, 1983; Du et al., 2016).

Complex morphology of selected samples were characterized by on an MDP-3D AFM (Asylum Research, Santa Barbara, CA). Each sample with 50 L fresh complex solution were deposited directly onto cleaved mica, then the sample was dried by filtered air with a membrane filter (0.45 m pore size), then stored in a desiccator for at least overnight. Intermittent contact mode was used and images were obtained by using Asylum Research software (Murphy et al., 2015).

4.3.4 Statistical Treatment

The results were presented as the average of duplicate or triplicate. Statistical significance was conducted by means of the student's t-test. Displayed error bars represent the standard deviation from independent sample measurements.

4.4 Results and Discussion

4.4.1 State of the complex prior to heat-treatment: Influence of pH on complex charge

Figure 4.1 shows the colloidal charge of α-lac and α-lac complexes with either CH or CH-PEG with varying molecular weight. With increasing pH, the positive charge of α-lac decreases until becoming dominantly-negative above pH 4.5. Colloidal charge of α-lac complexes with CH or CH-PEG was positive for all molecular weights over the pH region of 3.5 to 7.5, indicating that the polysaccharide interacted with the negative charges of α-lac and conferred an excess of positive charge to the assembly,

which is in agreement of literature values of the pKa = 6.5 of chitosan (Liu et al., 2005). At neutral pH, the charge of complexes approached zero, which could reflect either the increasing dominance of negative-charge from α-lac at pH values well above its isoelectric pH or the decreasing charge of the CH or CH-PEG, itself .

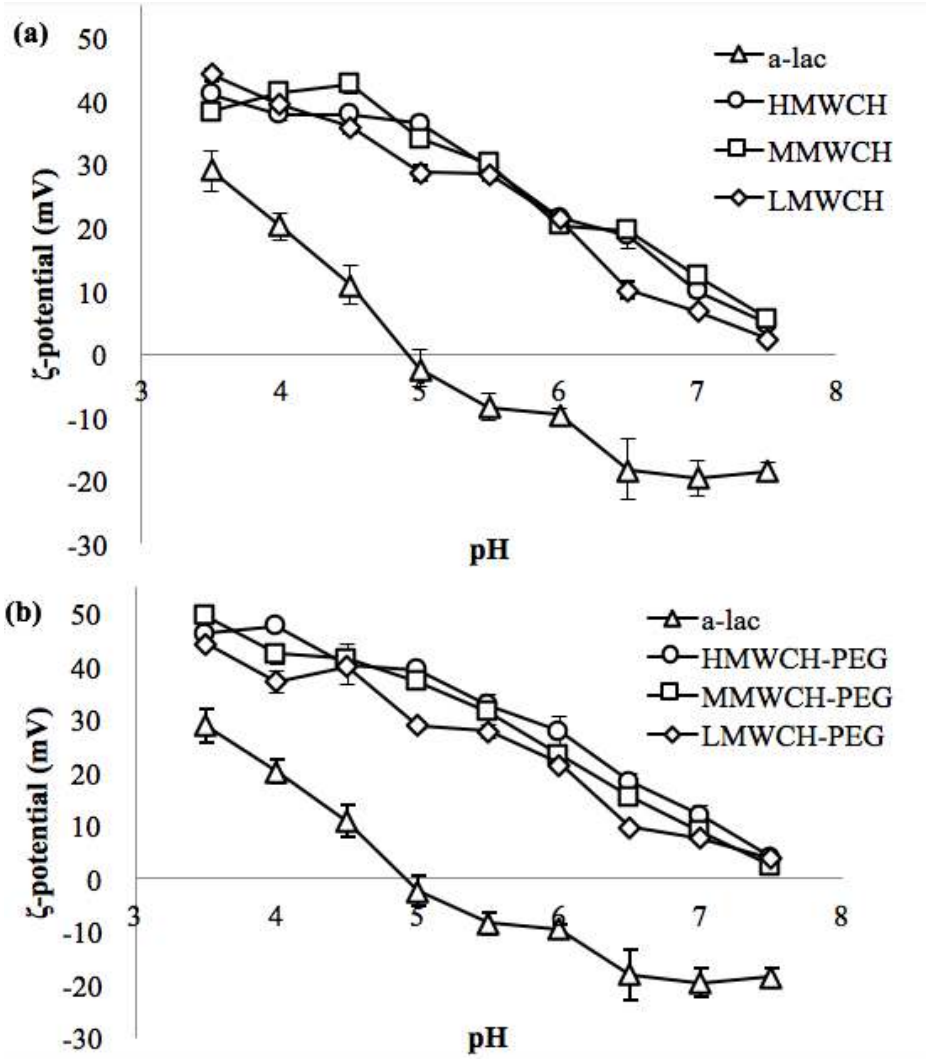

Fig. 4.1. ζ-potential as a function of solution pH of (a) 0.1% α-lac, 0.012% HMWCH, 0.012% MMWCH, 0.012% LMWCH (b) 0.1% α-lac, 0.012% HMWCH-PEG, 0.012% MMWCH-PEG, 0.012% LMWCH-PEG

4.4.2 Influence of PEGylation on turbidity of heated protein polysaccharide complex

Following thermal treatment of α-lac complexes, the turbidity of the resulting suspension was characterized to determine general physical properties of formed aggregates, with results from samples with MMWCH or MMWCH-PEG shown in Figure 4.2. A general feature of all samples was the very low turbidity after heat treatment at pH 4.3, which may indicate that few aggregates were formed or that the aggregates formed were very small in diameter. Turbidity values of samples containing PEG were significantly less than samples without PEG, particularly at higher pH values of 5.3 or 5.8 and with r = 10 or 5. Reduced turbidity with PEG was attributed to the formation of aggregates with either smaller size, lower in amount, or less in density. For aggregates formed at r=2, there was minimal difference in the turbidity between samples with or without PEG, which might be caused by excessive amount of polysaccharide acting to prevent association of α-lac during thermal treatment. The PEG chain then had less influence in relation to the impact of the CH, itself.

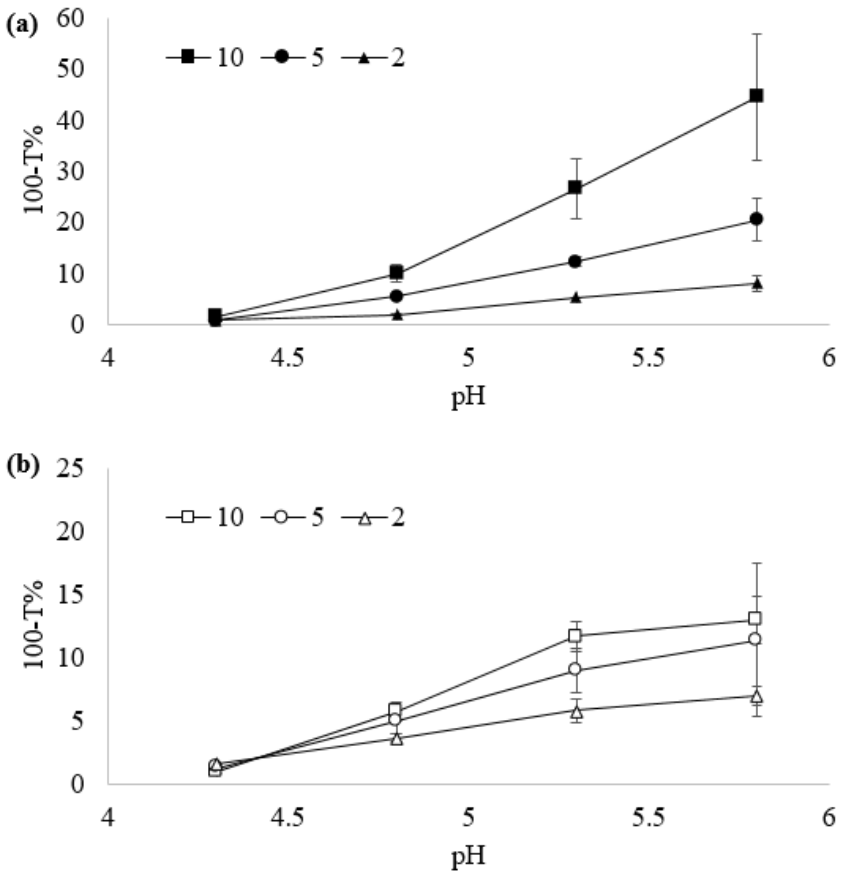

Fig. 4.2. Effect of pH on turbidity of heated (a) α-lac and MMWCH (b) α-lac and MMWCH-PEG with changing r-value

4.4.3 Effect of Chitosan Molecular Weight on Turbidity of Heated Protein Polysaccharide Complex

Fig. 4.3 shows turbidity as a function of pH for mixtures of α-lac with either CH or CH-PEG (r = 2) of differing molecular weight after heating. In all heated complexes there was an increase in turbidity with increasing pH. Samples of α-lac and LMWCH were significantly more turbid than all others, which might due to the

reduced ability of LMWCH to restrict α-lac aggregation due to its relatively short chain length (8.9kDa). Turbidity of aggregates formed from α-lac and LMWCH-PEG was not significantly different from samples with MMWCH-PEG or HMWCH-PEG. This indicated that attachment of the PEG chain confers greater resistance of α-lac to aggregation during thermal treatment. No difference was shown between PEGylated and non-PEGylated complexes at higher MW. This was attributed to the improved ability of higher molecular weight CH to interact with and protect α-lac.

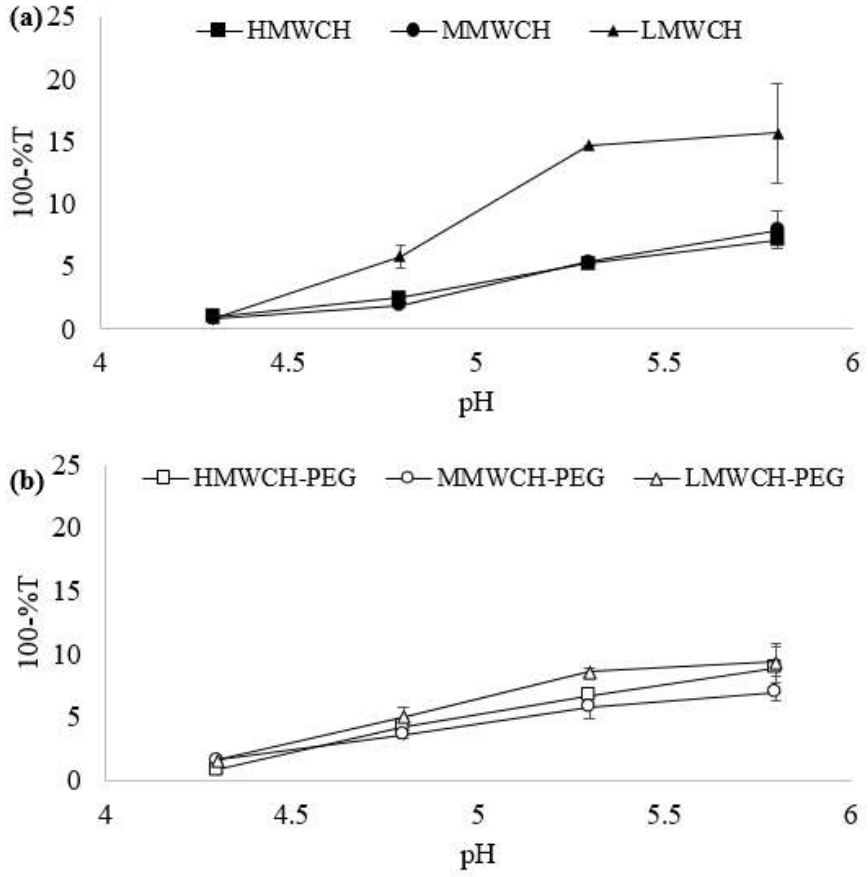

Fig. 4.3. Effect of CH molecular weight on turbidity of heated (a) α-lac and CH (b) α-lac and CH-PEG (r = 2) at different heating pH

4.4.4 Colloidal charge of aggregates formed from protein polysaccharide complexes

Figure 4.4 and 4.5 shows the results of surface charge after heating, emphasizing the role of r-value and molecular weight, respectively. In each of the figures, there were no consistent statistical differences in charge between aggregates formed with CH versus CH-PEG, indicating that the PEG chain did not alter the presentation of exposed surface charges after thermal treatment. Samples prepared from complexes with r=2 possessed significantly greater positive charge (Figure 4.4), which could be attributed to the greater amount of positively-charged CH or CH-PEG present in the samples. Colloidal charge was largely not impacted by the molecular weight of the CH or CH-PEG, except for samples containing LMWCH, which had lower surface charge (Figure 4.5). These results are in agreement with turbidity observed in these samples, with greater or less charge coinciding with lesser or greater turbidity, respectively (Figure 4.3). Since the MW of LMWCH (8.9kDa) is smaller than α-lac (14kDa), α-lac might be easy to exposed to the surface of the complex, and therefore reduced the net charge on complex surface.

It should be noted that the values of surface charges measured after heating was not significant different from the samples before heating (Fig 3.4), which indicated that the surface structures of complexes were not changed significantly after heat treatment. The reason for this phenomena is either the lacking of protein to associate to the complexes, or unfolded protein are located in the core of the coacervates or microgel, or a combination of both.

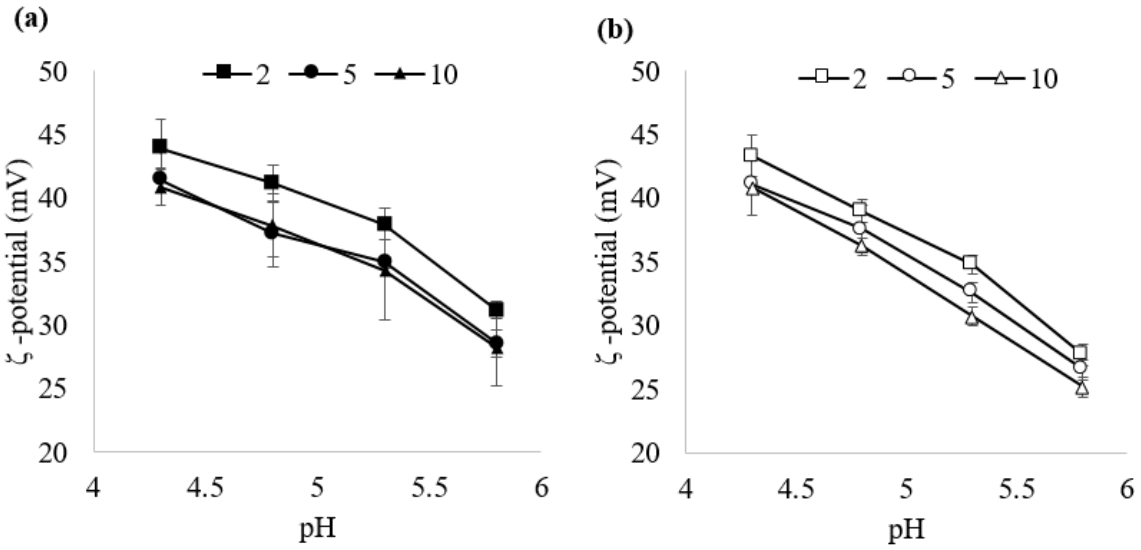

Fig. 4.4. Effect of r- value on ζ-potential of heated (a) α-lac and MMWCH (b) α-lac and MMWCH-PEG at different heating pH

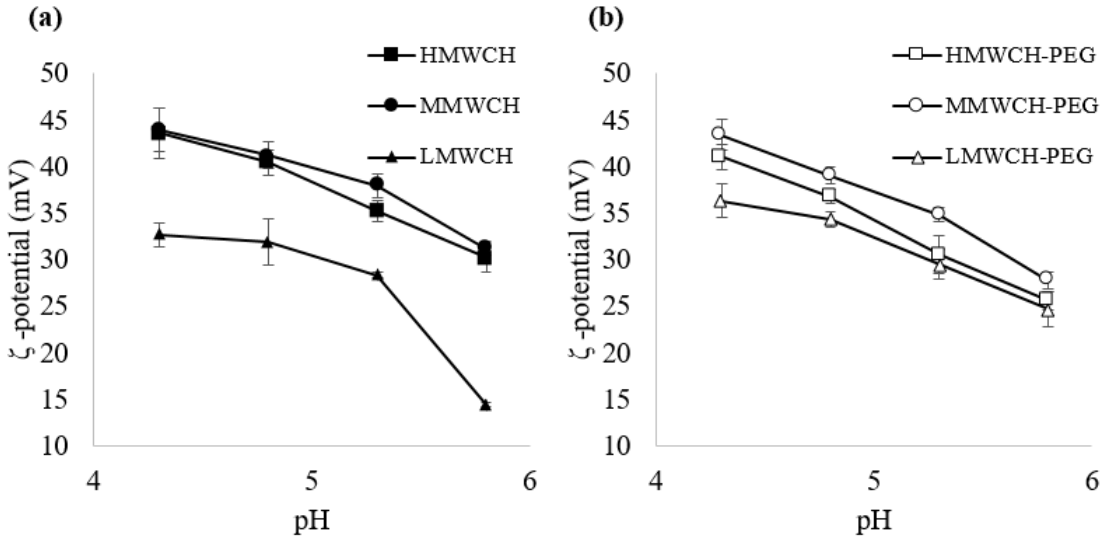

Fig. 4.5. Effect of CH molecular weight on ζ-potential of heated (a) α-lac and CH (b) α-lac and CH-PEG with changing r-value

4.4.5 Microgel hydrodynamic radius

Fig. 4.6 and 4.7 shows RH of protein-polysaccharide complexes after heating, emphasizing the role of r-value and polysaccharide molecular weight, respectively. In all cases, sizes observed at pH 4.3 were significantly larger than at higher pH values, indicating minimal protection of α-lac against aggregation at the lower pH. With increasing pH, aggregate radii were typically around 100 nm, and there was no significant difference between aggregates with or without PEG chains. Fig. 4.7 shows that there was also no significant differences in the RH of aggregates in samples with differing molecular weight of the polysaccharide component. Micogels, sometimes refers as nanogels, are a semi-permanent colloidal particle with gel-like internal structure, and size ranges from approximately 100-10,000 nm (Oh and Park, 2009). The increase of turbidity with the trending of pH, and the structure of internal polymer network, the RH range of the aggregates detected by DLS, and similar morphology indicates the aggregates formed by α-lac and CH/CH-PEG are similar to the microgels formed by b-lac and pectin at low salt concentration (Hirt et al., 2014; Murphy et al., 2015).

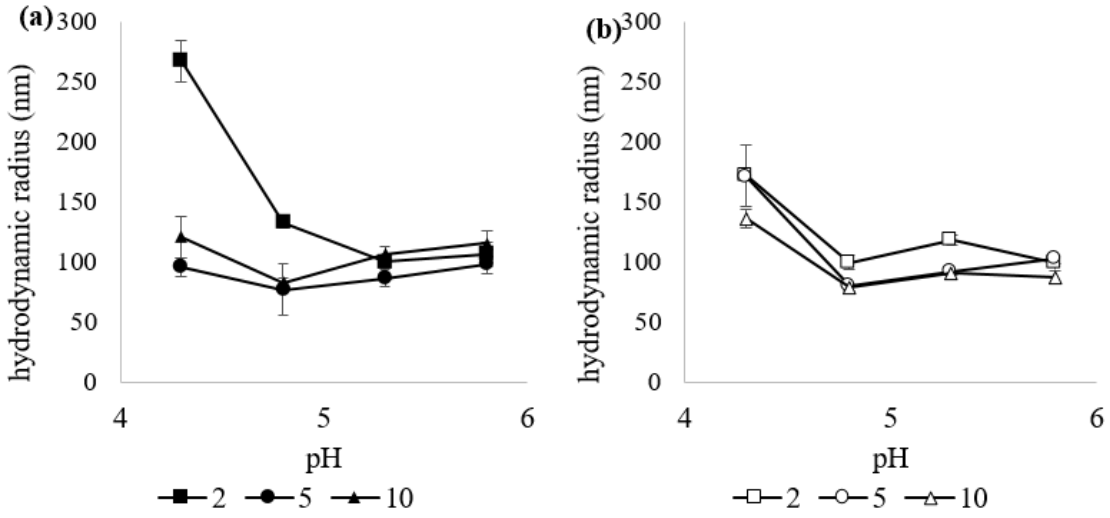

Fig. 4.6. Effect of pH on hydrogel radius of complexes involving (a) α-lac and MMWCH (b) α-lac and MMWCH-PEG with varying r-value

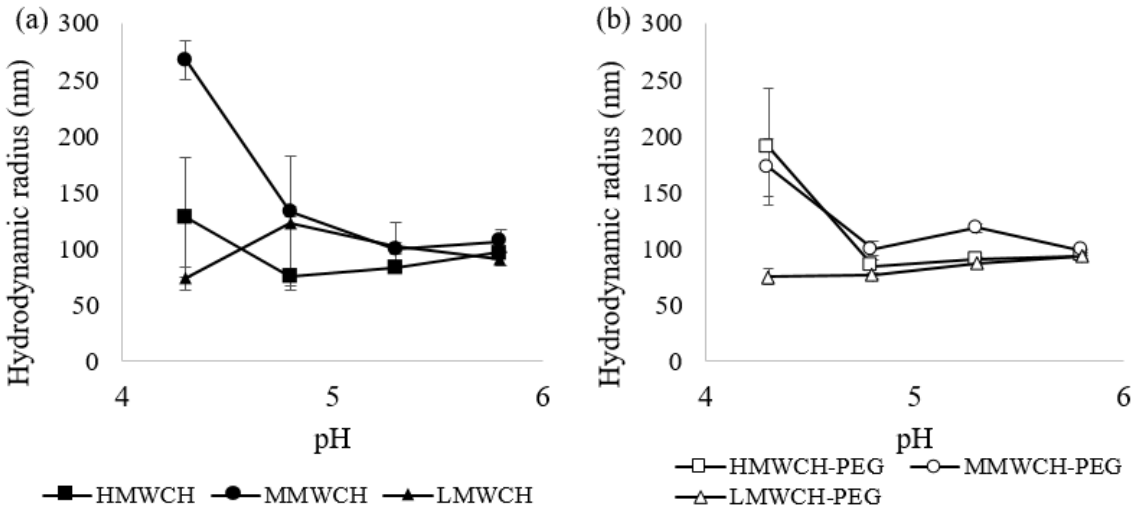

Fig. 4.7. Effect of pH on hydrogel radius of complexes involving (a) α-lac and CH (b) α-lac and CH-PEG with CH molecular weight

4.4.6 Visual Characterization of Complexes

The AFM images in Fig. 4.8 demonstrate the morphology of microgels formed by α-lac/MMWCH or α-lac/MMWCH-PEG at pH 4.8 and r=2. Based on the spherical morphology of the aggregates, it was confirmed that microgels are formed by the method and materials used. Approximate diameter of the samples in AFM images were around 100nm, which are smaller than the RH results obtained from DLS. The reduced of size in AFM might due to the shrinking during drying or the absence of water layers compared to microgels in solution. Differences of microgel size between α-lac/HMWCH to α-lac/HMWCH-PEG could be observed by AFM, which is also in agreement with DLS results. Further increase of r-value among α-lac and CH/CH-PEG samples is needed to confirm the effect of PEGylation on microgel sizes.

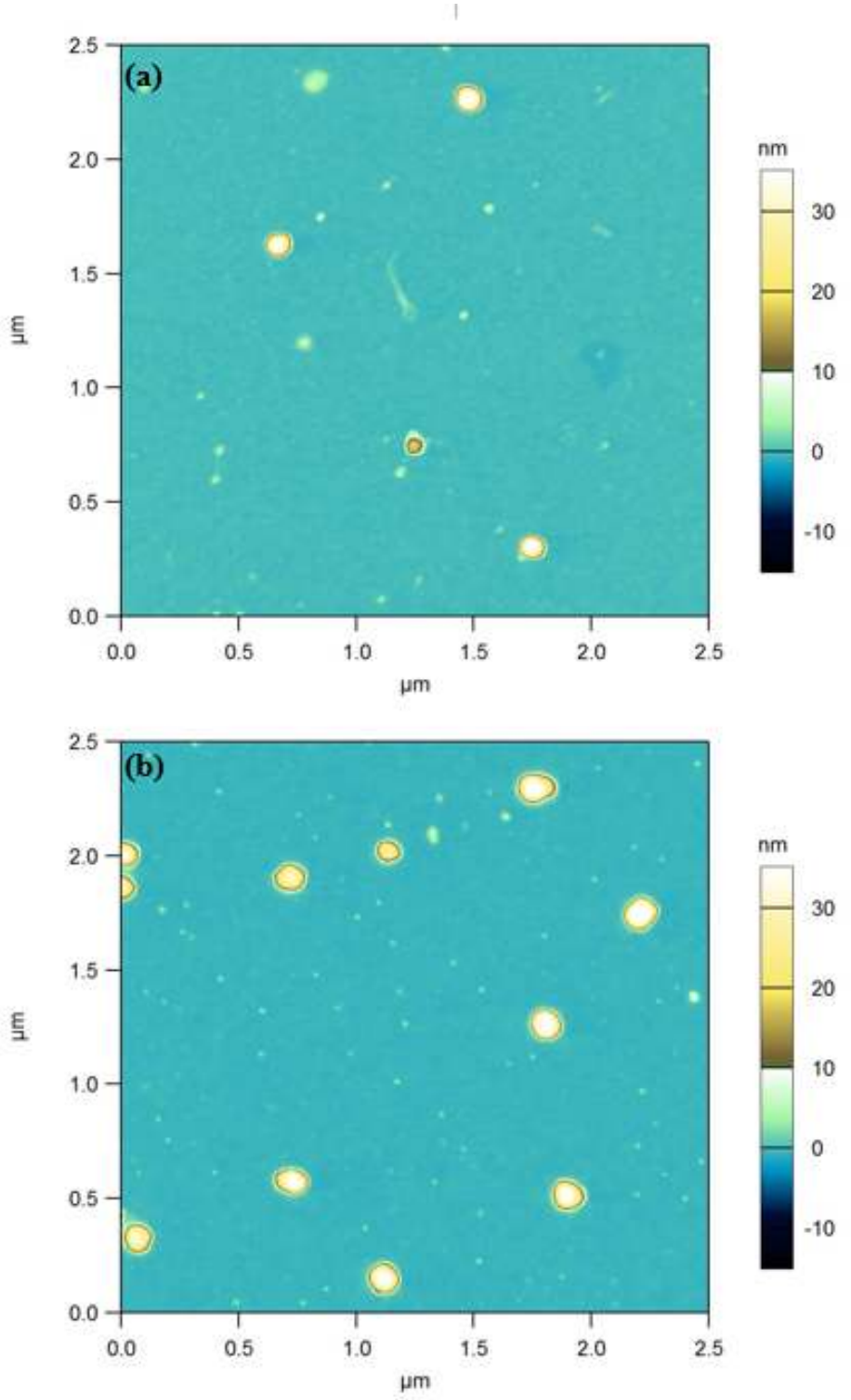

Fig. 4.8. Topographical images of (a) microgels of α-lac and HMWCH, r = 2, pH 4.8 (b) microgels of α-lac and HMWCH-PEG, r = 2, pH 4.8 after heating

4.5 Conclusions

The shift to less negative values of α-lac electrophoretic mobility over increase of pH indicates the potential of microgel formation by α-lac and CH/CH-PEG with all MW. Microgel formation among α-lac, CH or CH-PEG were confirmed by increased turbidity, AFM morphology, and DLS. Reduction in turbidity of PEGylated samples is observed among samples with higher r and pH values, indicating these microgels are formed either smaller in size, lower in amount, or less in density. The result also indicates the stabilizing effect of PEG chain due to the function of repulsion of the neutral charged PEG chain, and therefore prevent the further association of protein and polysaccharides to form microgel. Under the materials and methods used in this chapter, no significant influence of different CH molecular weight, ratios of protein to polysaccharide on hydrodynamic radius of microgel was observed. Further studies are needed to explain the impact of polymer ratio, or molecular weight of CH on microgel formation, such as higher ratios of protein to polysaccharide, and anther molecular weight of CH.

5. CONCLUSIONS

Interactions between α-lac and CMD-*b*-PEG were verified by a negative-shift in the electrophoretic mobility when compared to pure α-lac, as well as significant increases in light scattering and turbidity at pH 5.9 and 5, respectively. Neither complex formation at pH 5.9 nor phase separation at pH 5 was influenced by the α-lac to CMD-*b*-PEG ratio (r). Complex formation also occurred at a higher pH value between α-lac/CMD-*b*-PEG when compared to α-lac/CMD. This insensitivity of phase separation to r and the increased pH of complex formation implied that addition of the PEG chain to CMD increased the favorability of forming complexes with α-lac in a manner that was insensitive to the quantity of added CMD-*b*-PEG, at least in the concentration regimes tested here. It was proposed that α-lac/CMD-*b*-PEG formed a C3M structure that was energetically favored at pH 5.9, and that at pH 5 the C3M, surrounded by the non-ionic PEG chains, flocculated and separated from the continuous phase. However, the internal structure of the complex needs to be further characterized to verify this hypothesis, which may be done by small angle scattering in future studies.

Interactions between α-lac, chitosan and CH-PEG were confirmed by a shift in the electrophoretic mobility of the protein to less negative values as the pH was increased above its isoelectric pH. Light scattering intensity verified that complex formation for α-lac/CH and α-lac/LMWCH-PEG occurred at pH values of 4.1-4.2, while α-lac/HMWCH-PEG and α-lac/MMWCH-PEG occurs at pH values around 3.8. Above pH 5.0, turbidity significantly increased for both complexes, indicating a phase-separation at a similar pH range, yet the turbidity of α-lac/CH-PEG samples were significantly less than α-lac/CH samples. Turbidity of MMW and LMW complexes was significantly reduced by PEGylation at three different r values. Hydrodynamic radii of α-lac/MMWCH-PEG complexes ranged from 10 to 40 nanometers with

additional peaks demonstrating the presence of larger assemblies of several hundred nanometers. Despite larger hydrodynamic radii of α-lac/HMWCH-PEG complexes, there was little indication that the r-value, molecular weight, or even presence of PEG has a significant impact on the size of complexes with protein at the studied pH values. However, the reduced turbidity of complexes with covalent attachment of the PEG chain implied that there is a reduction in number or internal density of the complexes. This phenomenon needs to be verified in further experiments with these complexes, as well as other similar complex structures.

The shift to less negative values of α-lac electrophoretic mobility over increase of pH indicates the potential of microgel formation by α-lac and CH/CH-PEG with all MW. Microgel formation among α-lac, CH or CH-PEG were confirmed by increased turbidity, AFM morphology, and DLS. Reduction in turbidity of PEGylated samples is observed among samples with higher r and pH values, indicating these microgels are formed either smaller in size, lower in amount, or less in density. The result also indicates the stabilizing effect of PEG chain due to the function of repulsion of the neutral charged PEG chain, and therefore prevent the further association of protein and polysaccharides to form microgel. Under the materials and methods used in this chapter, no significant influence of different CH molecular weight, ratios of protein to polysaccharide on hydrodynamic radius of microgel was observed.

In the further studies, understand of if greater lengths of the PEG chain will confer increased stability of the complexes to lower pH values is needed. Furthermore, techniques need to be envisioned to prepare these complexes without formation of larger clusters, which appear to form due to bridging interactions between complexes by excess copolymer. Further research are also needed to explain the impact of polymer ratio, or molecular weight of CH on microgel formation, such as higher ratios of protein to polysaccharide, and anther molecular weight of CH.

LIST OF REFERENCES

LIST OF REFERENCES

[1] H. Bohidar, “Coacervates: a novel state of soft matter: an overview," J Surf Sci Technol, vol. 24, pp. 105-124, 2008.

[2] J. T. G. Overbeek and M. Voorn, “Phase separation in polyelectrolyte solutions. theory of complex coacervation," Journal of Cellular and Comparative Physiology, vol. 49, no. S1, pp. 7-26, 1957.

[3] O. G. Jones and D. J. McClements, “Functional biopolymer particles: design, fabrication, and applications," Comprehensive Reviews in Food Science and Food Safety, vol. 9, no. 4, pp. 374-397, 2010.

[4] M. Girard, S. L. Turgeon, and S. F. Gauthier, “Thermodynamic parameters of α-lactoglobulin-pectin complexes assessed by isothermal titration calorimetry," Journal of Agricultural and Food Chemistry, vol. 51, no. 15, pp. 4450-4455, 2003.

[5] M. Girard, S. L. Turgeon, and S. F. Gauthier, “Interbiopolymer complexing between α-lactoglobulin and low-and high-methylated pectin measured by potentiometric titration and ultrafiltration," Food Hydrocolloids, vol. 16, no. 6, pp. 585-591, 2002.

[6] M. Girard, S. Turgeon, and P. Paquin, “Emulsifying properties of whey protein-carboxymethylcellulose complexes," Journal of Food Science, vol. 67, no. 1, pp. 113-119, 2002.

[7] M. Girard, S. L. Turgeon, and S. F. Gauthier, “Quantification of the interactions between β-lactoglobulin and pectin through capillary electrophoresis analysis," Journal of Agricultural and Food Chemistry, vol. 51, no. 20, pp. 6043-6049, 2003.

[8] M. Girard, C. Sanchez, S. I. Laneuville, S. L. Turgeon, and S. F. Gauthier, “Associative phase separation of β-lactoglobulin/pectin solutions: a kinetic study by small angle static light scattering," Colloids and Surfaces B: Biointerfaces, vol. 35, no. 1, pp. 15-22, 2004.

[9] F. Weinbreck, H. Nieuwenhuijse, G. W. Robijn, and C. G. de Kruif, “Complexation of whey proteins with carrageenan," Journal of Agricultural and Food Chemistry, vol. 52, no. 11, pp. 3550-3555, 2004.

[10] F. Weinbreck, H. Nieuwenhuijse, G. W. Robijn, and C. G. de Kruif, “Complex formation of whey proteins: exocellular polysaccharide eps b40," Langmuir, vol. 19, no. 22, pp. 9404-9410, 2003.

[11] F. Weinbreck, H. S. Rollema, R. H. Tromp, and C. G. de Kruif, “Diffusivity of whey protein and gum arabic in their coacervates," Langmuir, vol. 20, no. 15, pp. 6389-6395, 2004.

[12] F. Weinbreck, R. Tromp, and C. De Kruif, “Composition and structure of whey protein/gum arabic coacervates," Biomacromolecules, vol. 5, no. 4, pp. 1437-1445, 2004.

[13] F. Weinbreck, R. H. Wientjes, H. Nieuwenhuijse, G. W. Robijn, and C. G. de Kruif, “Rheological properties of whey protein/gum arabic coacervates," Journal of Rheology, vol. 48, no. 6, pp. 1215-1228, 2004.

[14] M. Vikelouda and V. Kiosseoglou, “The use of carboxymethylcellulose to recover potato proteins and control their functional properties," Food hydrocolloids, vol. 18, no. 1, pp. 21-27, 2004.

[15] D. Burgess and J. Carless, “Microelectrophoretic studies of gelatin and acacia for the prediction of complex coacervation," Journal of Colloid and interface Science, vol. 98, no. 1, pp. 1-8, 1984.

[16] D. Burgess, K. Kwok, and P. Megremis, “Characterization of albumin-acacia complex coacervation," Journal of pharmacy and pharmacology, vol. 43, no. 4, pp. 232-236, 1991.

[17] D. Burgess and O. Singh, “Spontaneous formation of small sized albumin/acacia coacervate particles," Journal of pharmacy and pharmacology, vol. 45, no. 7, pp. 586-591, 1993.

[18] N. A. Elgindy and M. A. Elegakey, “Carbopol-gelatin coacervation: influence op some variables," Drug Development and Industrial Pharmacy, vol. 7, no. 5, pp. 587-603, 1981.

[19] P. Gilsenan, R. Richardson, and E. Morris, “Associative and segregative interactions between gelatin and low-methoxy pectin: Part 1. associative interactions in the absence of Ca^{2+}," Food Hydrocolloids, vol. 17, no. 6, pp. 723-737, 2003.

[20] C.-Y. Lii, S. Liaw, V.-F. Lai, and P. Tomasik, “Xanthan gum-gelatin complexes," European Polymer Journal, vol. 38, no. 7, pp. 1377-1381, 2002.

[21] H. Peters, E. Van Bommel, and J. Fokkens, “Effect of gelatin properties in complex coacervation processes," Drug development and industrial pharmacy, vol. 18, no. 1, pp. 123-134, 1992.

[22] M. Kazmierski, L. Wicker, and M. Corredig, “Interactions of β-lactoglobulin and high-methoxyl pectins in acidified systems," Journal of food science, vol. 68, no. 5, pp. 1673-1679, 2003.

[23] S. Laneuville, P. Paquin, and S. Turgeon, “Effect of preparation conditions on the characteristics of whey proteinxanthan gum complexes," Food Hydrocolloids, vol. 14, no. 4, pp. 305-314, 2000.

[24] C. Sanchez, S. Despond, C. Schmitt, and J. Hardy, “Effect of heat and shear on b-lactoglobulin-acacia gum complex coacervation," Food colloids: fundamentals of formulation, Royal Society of Chemistry, Cambridge, UK, pp. 332-343, 2001.

[25] C. Sanchez, G. Mekhloufi, C. Schmitt, D. Renard, P. Robert, C.-M. Lehr, A. Lamprecht, and J. Hardy, “Self-assembly of β-lactoglobulin and acacia gum in aqueous solvent: Structure and phase-ordering kinetics," Langmuir, vol. 18, no. 26, pp. 10323-10 333, 2002.

[26] C. Sanchez and D. Renard, “Stability and structure of protein-polysaccharide coacervates in the presence of protein aggregates," International journal of pharmaceutics, vol. 242, no. 1, pp. 319-324, 2002.

[27] C. Schmitt, C. Sanchez, S. Despond, D. Renard, F. Thomas, and J. Hardy, “Effect of protein aggregates on the complex coacervation between β-lactoglobulin and acacia gum at ph 4.2," Food Hydrocolloids, vol. 14, no. 4, pp. 403-413, 2000.

[28] C. S. C. Sanchez, S. Despond, D. Renard, P. Robert, and J. Hardy, “Structural modification of β-lactoglobulin as induced by complex coacervation with acacia gum," Food colloids: Fundamentals of formulation, vol. 258, p. 323, 2001.

[29] C. Schmitt, C. Sanchez, A. Lamprecht, D. Renard, C.-M. Lehr, C. G. de Kruif, and J. Hardy, “Study of β-lactoglobulin/acacia gum complex coacervation by dffusing-wave spectroscopy and confocal scanning laser microscopy," Colloids and Surfaces B: Biointerfaces, vol. 20, no. 3, pp. 267-280, 2001.

[30] C. Schmitt, C. Sanchez, F. Thomas, and J. Hardy, “Complex coacervation between β-lactoglobulin and acacia gum in aqueous medium," Food Hydrocolloids, vol. 13, no. 6, pp. 483-496, 1999.

[31] S. Girod, M. Boissière, K. Longchambon, S. Begu, C. Tourne-Petheil, and J. Devoisselle, “Polyelectrolyte complex formation between iota-carrageenan and poly(l-lysine) in dilute aqueous solutions: a spectroscopic and conformational study," Carbohydrate Polymers, vol. 55, no. 1, pp. 37-45, 2004.

[32] I. Plashchina, T. Mrachkovskaya, A. Danilenko, G. Kozhevnikov, N. Y. Starodubrovskaya, E. Braudo, and K. Schwenke, “Complex formation of faba bean legumin with chitosan: surface activity and emulsion properties of complexes," Food colloids, fundamentals of formulation. Cambridge: Royal Society of Chemistry, pp. 293-303, 2001.

[33] X. Yan, E. Khor, and L. Lim, “PEC films prepared from chitosan-alginate coacervates." Chemical and pharmaceutical bulletin, vol. 48, no. 7, pp. 941-946, 2000.

[34] X. Yan, E. Khor, and L.Y. Lim, “Chitosan-alginate films prepared with chitosans of dfferent molecular weights," Journal of biomedical materials research, vol. 58, no. 4, pp. 358-365, 2001.

[35] E. Shumilina and Y. A. Shchipunov, “Chitosan-carrageenan gels," Colloid Journal, vol. 64, no. 3, pp. 372-378, 2002.

[36] Y. A. Antonov and M. Gonçalves calves, “Phase separation in aqueous gelatin-k-carrageenan systems," Food Hydrocolloids, vol. 13, no. 6, pp. 517-524, 1999.

[37] V. Galazka, D. Smith, D. Ledward, and E. Dickinson, “Complexes of bovine serum albumin with sulphated polysaccharides: effects of pH, ionic strength and high pressure treatment," Food Chemistry, vol. 64, no. 3, pp. 303-310, 1999.

[38] A. Gurov, N. Gurova, A. Leontiev, and V. Tolstoguzov, “Equilibrium and non-equilibrium complexes between bovine serum albumin and dextran sulfatei. complexing conditions and composition of non-equilibrium complexes," Food Hydrocolloids, vol. 2, no. 4, pp. 267-283, 1988.

[39] H. Georg et al., “Encapsulation process by complex coacervation using inorganic polyphosphates and organic hydrophilic polymeric material," Oct. 10 1972, US Patent 3,697,437.

[40] I. Haug, M. A. Williams, L. Lundin, O. Smidsrød, and K. I. Draget, “Molecular interactions in, and rheological properties of, a mixed biopolymer system undergoing order/disorder transitions," Food hydrocolloids, vol. 17, no. 4, pp. 439-444, 2003.

[41] R. Thimma and S. Tammishetti, “Study of complex coacervation of gelatin with sodium carboxymethyl guar gum: microencapsulation of clove oil and sulphamethoxazole," Journal of microencapsulation, vol. 20, no. 2, pp. 203-210, 2003.

[42] C. Schmitt, C. Sanchez, S. Desobry-Banon, and J. Hardy, “Structure and technofunctional properties of protein-polysaccharide complexes: a review," Critical Reviews in Food Science and Nutrition, vol. 38, no. 8, pp. 689-753, 1998.

[43] C. Schmitt and S. L. Turgeon, “Protein/polysaccharide complexes and coacervates in food systems," Advances in colloid and interface science, vol. 167, no. 1, pp. 63-70, 2011.

[44] Y.-H. Hong and D. J. McClements, “Formation of hydrogel particles by thermal treatment of β-lactoglobulin-chitosan complexes," Journal of agricultural and food chemistry, vol. 55, no. 14, pp. 5653-5660, 2007.

[45] R. Murphy, Y.-H. Cho, B. Farkas, and O. G. Jones, “Control of thermal fabrication and size of β-lactoglobulin-based microgels and their potential applications," Journal of colloid and interface science, vol. 447, pp. 182-190, 2015.

[46] J. Belloque and G. M. Smith, “Thermal denaturation of β-lactoglobulin. A 1H NMR study," Journal of Agricultural and Food Chemistry, vol. 46, no. 5, pp. 1805-1813, 1998.

[47] R. Carrotta, R. Bauer, R. Waninge, and C. Rischel, “Conformational characterization of oligomeric intermediates and aggregates in β-lactoglobulin heat aggregation," Protein Science, vol. 10, no. 7, pp. 1312-1318, 2001.

[48] A. M. Donald, “Aggregation in β-lactoglobulin," Soft Matter, vol. 4, no. 6, pp. 1147-1150, 2008.

[49] S. Iametti, B. Gregori, G. Vecchio, and F. Bonomi, “Modifications occur at different structural levels during the heat denaturation of β-lactoglobulin," European Journal of Biochemistry, vol. 237, no. 1, pp. 106-112, 1996.

[50] O. G. Jones and D. J. McClements, “Recent progress in biopolymer nanoparticle and microparticle formation by heat-treating electrostatic protein-polysaccharide complexes," Advances in Colloid and Interface Science, vol. 167, no. 1, pp. 49-62, 2011.

[51] W. Liu, S. Sun, Z. Cao, X. Zhang, K. Yao, W. W. Lu, and K. Luk, “An investigation on the physicochemical properties of chitosan/dna polyelectrolyte complexes," Biomaterials, vol. 26, no. 15, pp. 2705-2711, 2005.

[52] J. K. Oh, D. I. Lee, and J. M. Park, “Biopolymer-based microgels/nanogels for drug delivery applications," Progress in Polymer Science, vol. 34, no. 12, pp. 1261-1282, 2009.

[53] K. Avgoustakis, “Pegylated poly (lactide) and poly (lactide-co-glycolide) nanoparticles: preparation, properties and possible applications in drug delivery," Current drug delivery, vol. 1, no. 4, pp. 321-333, 2004.

[54] P. K. Dutta, J. Dutta, and V. Tripathi, “Chitin and chitosan: Chemistry, properties and applications," Journal of scientific and industrial research, vol. 63, no. 1, pp. 20-31, 2004.

[55] W. J. Lin and W. Y. Hsu, “Pegylation effect of chitosan based polyplex on DNA transfection," Carbohydrate polymers, vol. 120, pp. 7-14, 2015.

[56] H. K. No, N. Y. Park, S. H. Lee, and S. P. Meyers, “Antibacterial activity of chitosans and chitosan oligomers with different molecular weights," International journal of food microbiology, vol. 74, no. 1, pp. 65-72, 2002.

[57] P. Fox, “Milk proteins: general and historical aspects," in Advanced Dairy Chemistry 1 Proteins. Springer, 2003, pp. 1-48.

[58] C. Barbana, M. Pérez, L. Sánchez, M. Dalgalarrondo, J. Chobert, T. Haertlé, and M. Calvo, “Interaction of bovine β-lactalbumin with fatty acids as determined by partition equilibrium and uorescence spectroscopy," International dairy journal, vol. 16, no. 1, pp. 18-25, 2006.

[59] A.-C. Lee and Y.-H. Hong, “Coacervate formation of β-lactalbumin-chitosan and β-lactoglobulin-chitosan complexes," Food Research International, vol. 42, no. 5, pp. 733-738, 2009.

[60] R. Zhang, M. Tang, A. Bowyer, R. Eisenthal, and J. Hubble, “A novel pH and ionic-strength-sensitive carboxy methyl dextran hydrogel," Biomaterials, vol. 26, no. 22, pp. 4677-4683, 2005.

[61] C. G. de Kruif, R. Tuinier, “Polysaccharide protein interactions," Food hydrocolloids, vol. 15, no. 4, pp. 555-563, 2001.

[62] IUPAC compendium of Chemical Technology 1997.

[63] H.G. Bungenberg de Jong, H.R. Kruyt, “Coacervation (partial miscibility in colloid systems),” Proceedings of the Koninklijke Nederlandse Akademie van Wetenschappen, vol. 32, pp. 849–856, 1929.

[64] F.W.Z. Tiebackx, “Gleichzeitige Ausflockung zweier Kolloide” Chem. Ind. Kolloide, vol. 8, no. 4, pp. 198–201, 1911.

[65] “Reprint from Current Opinion in Colloid & Interface Science, Vol. 9, De Kruif, C. G., Weinbreck, F., & de Vries, R. Complex coacervation of proteins and anionic polysaccharides., pp 340-349, Copyright (2004), with permission from Elsevier.”

[66] "Reprint from Food Chemistry, Vol. 196, Du, J., Reuhs, B. L., & Jones, O. G, Influence of PEGylation on the ability of carboxymethyl-dextran to form complexes with α-lactalbumin, pp 853-859, Copyright (2016), with permission from Elsevier."

VITA

VITA

Juan Du was born in Tonghua, a beautiful city of northern China. She finished his Bachelor degree at Purdue University in 2009. Later she received the degree of Master at University of Wisconsin-Madison in 2012. Juan Du joined the PhD program in Food Science at Purdue University in 2013 and received the PhD degree in December 2016.